Distributed Optimal Control of Cyber-Physical Systems: Controller Synthesis, Architecture Design and System Identification

Thesis by

Nikolai Matni

In Partial Fulfillment of the Requirements

for the Degree of

Doctor of Philosophy

Caltech

California Institute of Technology

Pasadena, California

2016

(Defended December 2, 2015)

To my family

Acknowledgments

I want to thank my advisor, John Doyle, for his generous support & encouragement during these years. He has been an incredible mentor and role model, constantly challenging me to grow as a researcher and providing me with opportunities rarely given to graduate students. He has changed the way that I view science, engineering and research, and for this I am eternally grateful. I also want to thank my unofficial co-advisor, Venkat Chandrasekaran. Venkat brings a rare elegance and sophistication to his work, and I am incredibly fortunate to have been able to collaborate with and learn from him these past few years.

I would also like to express my thanks to the remaining members of my thesis committee, Adam Wierman and Richard M. Murray, as well as to Steven Low, Joel Tropp, Babak Hassibi, Anders Rantzer and Joel Burdick. Be it through teaching, informal discussions, or collaborations, all of these amazing professors have played an instrumental role in making my time at Caltech intellectually stimulating and enjoyable. I would also like to thank Andrew Lamperski for his mentorship early in my graduate student career: without his guidance and support, this thesis would most certainly look very different. I must also thank my master's advisor, Meeko Oishi, for introducing me to the field of control theory, and for giving me my first shot at research.

I would be remiss not to acknowledge my CDS and CMS colleagues: the inhabitants of Steele and Annenberg have made my time at Caltech a rich and rewarding experience. I must also thank my friends (you know who you are) for making sure that I took at least some time off from work to have some fun – I cannot express how much your friendship has meant to me over the years, and cannot imagine having

survived my time here without you.

Of course, I never would have made it to or through Caltech without the unwavering love and support of my mother Nadia, father Nick, and sister Natasha – I dedicate this thesis to them as a small token of my gratitude for all that they have done for me. Above all, I thank my favorite collaborator, best friend and partner Vanessa: you are my inspiration, my motivation, and my joy.

Contents

Acknowledgments **iv**

Abstract **xv**

1 Introduction **1**

1.1 Non-Classical Information Sharing Constraints 2

1.2 Thesis Contribution and Outline 5

2 Distributed Control subject to Delays Satisfying an $\mathcal{H}_\infty$ Norm Bound **8**

2.1 Introduction 8

2.2 Problem Formulation 10

2.2.1 Notation and Operator Theoretic Preliminaries 11

2.2.2 The model-matching problem subject to delay 12

2.3 A Review of "1984" $\mathcal{H}_\infty$ Control 15

2.3.1 $\mathcal{T}_3 = I$ Case 15

2.3.2 General $\mathcal{T}_3$ 19

2.4 Distributed $\mathcal{H}_\infty$ Control Subject to Delays 20

2.4.1 $\mathcal{T}_3 = I$ Case 21

2.4.2 General $\mathcal{T}_3$ 26

2.5 Example 28

2.6 Conclusion 29

2.7 Factorization Formulas 30

2.7.1 Inner-Outer Factorizations 30

2.7.2 Bi-stable Spectral Factorizations 30

2.7.3 Stable Approximations 31

3 Optimal Two Player LQR State Feedback with Varying Delay 33

3.1 Introduction 33

3.2 Problem Formulation 35

3.2.1 The two-player problem 35

3.3 Main Result 38

3.3.1 Effective delay 38

3.3.2 Partial Nestedness 39

3.3.3 Information Graph and Controller Coordinates 40

3.4 Controller Derivation 42

3.4.1 Controller States and Decoupled Dynamics 42

3.4.2 Finite Horizon Dynamic Programming Solution 45

3.4.3 Infinite Horizon Solution 48

3.5 Conclusion 49

3.6 Proofs of Intermediate Lemmas 49

4 Regularization for Design 54

4.1 Introduction 54

4.2 Preliminaries & Notation 58

4.3 RFD as Structured Approximation 59

4.3.1 Convex Model Matching 60

4.3.2 Architecture Design through Structured Solutions 62

4.4 RFD Cost Functions and Regularizers 67

4.4.1 Convex Cost Functions 67

4.4.2 The $\mathcal{H}_2$ RFD Problem with an Atomic Norm Penalty 70

4.4.3 Further Connections with Structured Inference 75

4.5 The RFD Procedure 77

4.5.1 The Two-Step Algorithm 77

4.5.2 Simultaneous Actuator, Sensor and Communication RFD . . . 78

4.6 Recovery of Optimal Actuation Structure 80

4.6.1 Identifiability Conditions in Control 85
4.6.2 Sufficient Conditions for Recovery 88
4.7 A RFD Signal to Noise Ratio 90
4.8 Case Study 93
4.9 Future Work 97
4.10 Proofs 97

5 Communication Delay Co-design in $\mathcal{H}_2$ Distributed Control Using Atomic Norm Minimization 100

5.1 Introduction 100
5.2 Preliminaries 103
5.2.1 Operator Theoretic Preliminaries 103
5.2.2 Notation 104
5.3 Communication Architecture Co-Design 105
5.3.1 Distributed $\mathcal{H}_2$ Optimal Control subject to Delays 105
5.3.2 Communication Delay Co-Design via Convex Optimization . . 109
5.4 Communication Graphs and Quadratically Invariant Subspaces 110
5.4.1 Generating Subspaces from Communication Graphs 111
5.4.2 Quadratically Invariant Communication Graphs 114
5.5 The Communication Graph Co-Design Algorithm 120
5.5.1 The Communication Link Norm 121
5.5.2 Co-Design Algorithm and Solution Properties 125
5.6 Computational Examples 127
5.7 Discussion 131

6 Low-Rank and Low-Order Decompositions for Local System Identification 134

6.1 Introduction 134
6.2 Problem Formulation 136
6.2.1 Notation 136
6.2.2 Distributed systems with sparse interconnections 138

6.2.3 Local and interconnection observations 138
6.2.4 Local system identification 139
6.3 Full interconnection measurements 140
6.3.1 A robust variant 142
6.4 Hidden interconnection measurements 143
6.5 Numerical Experiments 146
6.6 Conclusion 148

7 Conclusions and Future Work **150**
7.1 Future Work: A theory of dynamics, control and optimization in layered architectures 150
7.1.1 Software Defined Networking 152
7.2 Concluding Remarks 153

Bibliography **154**

List of Figures

1.1 A schematic diagram of norm-optimal control. The objective is to design a feedback controller that minimizes the size (as measured by an appropriate signal-to-signal norm) of the system's closed-loop response to the environment. 1

1.2 Schematics of centralized, decentralized and distributed control architectures. 3

1.3 A schematic of Witsenhausen's counterexample [courtesy of wikipedia], a control problem subject to non-classical information sharing constraints for which nonlinear control can arbitrarily outperform linear control. . 4

2.1 The graph depicts the communication structure of the three-player chain problem. Edge weights (not shown) indicate the delay required to transmit information between nodes. 13

3.1 The distributed plant considered in (3.6), shown here for $D = 4$. Dummy nodes δ_t^i, $i = 1, \ldots, D-1$, as defined by (3.5), are introduced to make explicit the propagation delay of D between plants. 36

3.2 The information graph $\mathcal{G} = (\mathcal{V}, \mathcal{E})$, and label sets $\{\mathcal{L}_t^s\}_{s\in\mathcal{V}}$, for system (3.6), shown here for $D = 4$, and $e_t = (3, 2)$. Notice that: (i) for each $(r, s) \in \mathcal{E}$, with $|r| < D + 1$, we have that $|s| = |r| + 1$, (ii) that $|s|$ corresponds exactly to how delayed the information in the label set is, and (iii) that $\mathcal{L}_t^V$ contains all of the information at nodes s.t. $|s| > e_t^i$, $s \ni i$. We also see that the graph is naturally divided into two branches, with each branch corresponding to information pertaining to a specific plant. 37

4.1 A diagram of the generalized plant defined in (4.2). 60

4.2 Examples of QI sparsity patterns generated via a) actuator, b) sensor, and c) actuator/sensor RFD procedures without any distributed constraints, and d) actuator RFD subject to nested information constraints. 66

4.3 Three player chain system 73

4.4 Topology of system considered for RFD example. Solid lines indicate both physical interconnections and existing communication links between controllers. Dashed lines correspond to possible additional edges to be added. 79

4.5 A small degradation in closed loop performance allows for a significant decrease in architectural complexity. 81

4.6 Resulting architecture for $\lambda = 500$: despite only using eight actuators (orange squares), eight sensors (blue triangles) and five additional communication links (green arrows), the performance only degraded by 0.71% relative to the distributed controller using all eleven actuators, eleven sensors and seven communication links. 81

4.7 A diagram of the Stable Unidirectional Chain System case study. . . . 93

4.8 Behavior of identifiability parameters $\gamma^{\leq t,v}$ and $\beta^{\leq t,v}$. 94

5.1 A diagram of the generalized plant defined in (5.2). 105

5.2 Three subsystem chain example 113

5.3 The closed loop norms achieved by distributed optimal controllers implemented on communication graphs constructed by adding $k = 1, \ldots, |\mathscr{E}|$ links to the base QI communication graph $\Gamma_{\text{6-chain}}$ are plotted as circles. The solid line denotes the performance achieved by distributed optimal controllers implemented on the communication graphs identified by the co-design procedure described in Algorithm 1. The dotted/dashed lines indicate the closed loop norm achieved by the distributed optimal controllers implemented on the base and maximal QI communication graphs, respectively. 129

5.4 The solid line denotes the performance achieved by distributed optimal controllers implemented on the communication graphs identified by the co-design procedure described in Algorithm 1. The dotted and dashed lines indicate the closed loop norm achieved by the distributed optimal controllers implemented on the base and maximal QI communication graphs, respectively. 131

6.1 Illustrated in Figures 6.1 (a) and (b) are the full and hidden interconnection measurement cases, respectively. Dashed green lines correspond to low-order signals, and dotted/solid black/red lines correspond to measured/hidden high-order interconnection signals. In the full measurement case, the high order dynamics of the large scale system are isolated from the local measurements, as the interconnection signals can simply be treated as inputs to the system. In the hidden interconnection measurement setting, high order global signals "leak" into our local measurements via the hidden interconnection signal (solid red), but do so through a low-rank transfer function. 136

6.2 The graph depicts the physical interconnection structure of the three-subsystem chain. 146

6.3 By examining how the values of the singular values of $\mathcal{H}(\hat{S}^i)$ vary across different values of δ and δ_h, the order of the local subsystem is correctly identified as three. 149

7.1 A functional schematic of the layered architecture derived in [1]. 150

List of Tables

4.1 A dictionary relating various SLIP methods in structured inference and Actuator RFD problems. 76

4.2 Interpretation of parameters in Structured Controller Design and Structured Inference. 82

4.3 Summary of relevant values for the controller U_2 with actuators at nodes 1 and 5. 95

Abstract

The centralized paradigm of a single controller and a single plant upon which modern control theory is built is no longer applicable to modern cyber-physical systems of interest, such as the power-grid, software defined networks or automated highways systems, as these are all large-scale and spatially distributed. Both the scale and the distributed nature of these systems has motivated the decentralization of control schemes into local sub-controllers that measure, exchange and act on locally available subsets of the globally available system information. This decentralization of control logic leads to different decision makers acting on asymmetric information sets, introduces the need for coordination between them, and perhaps not surprisingly makes the resulting optimal control problem much harder to solve. In fact, shortly after such questions were posed, it was realized that seemingly simple decentralized optimal control problems are computationally intractable to solve, with the Wistenhausen counterexample being a famous instance of this phenomenon. Spurred on by this perhaps discouraging result, a concerted 40 year effort to identify tractable classes of distributed optimal control problems culminated in the notion of quadratic invariance, which loosely states that if sub-controllers can exchange information with each other at least as quickly as the effect of their control actions propagates through the plant, then the resulting distributed optimal control problem admits a convex formulation.

The identification of quadratic invariance as an appropriate means of "convexifying" distributed optimal control problems led to a renewed enthusiasm in the controller synthesis community, resulting in a rich set of results over the past decade. The contributions of this thesis can be seen as being a part of this broader family of results,

with a particular focus on closing the gap between theory and practice by relaxing or removing assumptions made in the traditional distributed optimal control framework. Our contributions are to the foundational theory of distributed optimal control, and fall under three broad categories, namely controller synthesis, architecture design and system identification.

We begin by providing two novel controller synthesis algorithms. The first is a solution to the distributed $\mathcal{H}_\infty$ optimal control problem subject to delay constraints, and provides the only known exact characterization of delay-constrained distributed controllers satisfying an $\mathcal{H}_\infty$ norm bound. The second is an explicit dynamic programming solution to a two player LQR state-feedback problem with varying delays. Accommodating varying delays represents an important first step in combining distributed optimal control theory with the area of Networked Control Systems that considers lossy channels in the feedback loop. Our next set of results are concerned with controller architecture design. When designing controllers for large-scale systems, the architectural aspects of the controller such as the placement of actuators, sensors, and the communication links between them can no longer be taken as given – indeed the task of designing this architecture is now as important as the design of the control laws themselves. To address this task, we formulate the Regularization for Design (RFD) framework, which is a unifying computationally tractable approach, based on the model matching framework and atomic norm regularization, for the simultaneous co-design of a structured optimal controller and the architecture needed to implement it. Our final result is a contribution to distributed system identification. Traditional system identification techniques such as subspace identification are not computationally scalable, and destroy rather than leverage any a priori information about the system's interconnection structure. We argue that in the context of system identification, an essential building block of any scalable algorithm is the ability to estimate local dynamics within a large interconnected system. To that end we propose a promising heuristic for identifying the dynamics of a subsystem that is still connected to a large system. We exploit the fact that the transfer function of the local dynamics is low-order, but full-rank, while the transfer function of the global

dynamics is high-order, but low-rank, to formulate this separation task as a nuclear norm minimization problem. Finally, we conclude with a brief discussion of future research directions, with a particular emphasis on how to incorporate the results of this thesis, and those of optimal control theory in general, into a broader theory of dynamics, control and optimization in layered architectures.

Chapter 1

Introduction

Robust and optimal control theory [2, 3] have been active areas of research since the 1970s: they aim to provide rigorous mathematical methods for analyzing and designing complex cyber-physical systems that are composed of a physical plant coupled in feedback with a controller. The need for control theory, and robust control theory in particular, arises from the inherent uncertainty present in any model of a complex physical system – this uncertainty captures un-modeled dynamics, measurement errors, and exogenous disturbances from the environment. Indeed even if we could obtain a perfect model of a given physical system and its environment, it would be too complex (i.e., high-dimensional and nonlinear) to be amenable to any kind of useful analysis. The role of feedback control is thus to mitigate and minimize undesirable behavior in a system despite our inability to exactly model the world.

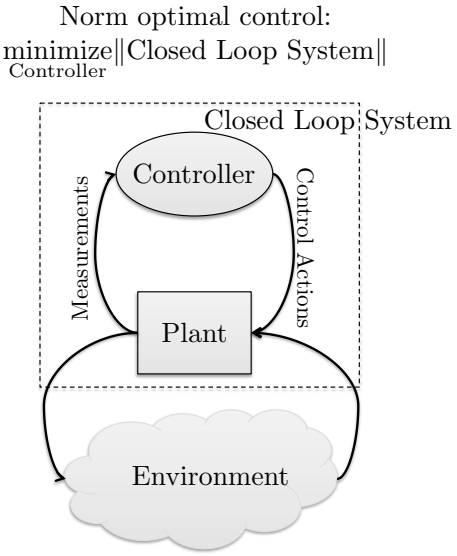

Figure 1.1: A schematic diagram of norm-optimal control. The objective is to design a feedback controller that minimizes the size (as measured by an appropriate signal-to-signal norm) of the system's closed-loop response to the environment.

Minimizing the undesirable behavior of a system due to uncertainty has been formalized via the concept of norm optimal control, in which one seeks to compute

a feedback controller that minimizes the size (as capture by an appropriate signal-to-signal norm) of the system's closed-loop response to the environment (this may include model-uncertainty, exogenous disturbances or measurement errors) – see Fig. 1.1 for an illustration. When dealing with linear systems, as we do in this thesis, this formulation establishes a natural connection to mathematical optimization theory, and to convex analysis and optimization in particular. This connection will be a cornerstone of our results, and play a determining role when we move to extend classical centralized results to distributed settings.

1.1 Non-Classical Information Sharing Constraints

Robust and optimal control theory were originally formulated in the context of *centralized* control: that is to say a single physical system coupled in feedback with a single control unit (cf. Fig 1.2a) – this was indeed a reasonable paradigm for the dominant applications of the time such as aerospace and chemical process control. However, modern cyber-physical systems such as the smart-grid, software defined networks and automated highway systems are large-scale and spatially *distributed* – this shift has motivated the study of decentralized and distributed control problems. In such problems, the plant is modeled as being composed of a collection of *subsystems* interacting according to some physical topology, and each subsystem is equipped with a *sub-controller*. These sub-controllers acquire and exchange local measurements according to a communication topology, and take actions based on their locally available subsets of the global plant information. In this thesis we use the term decentralized (cf. Fig 1.2b) to refer to control schemes in which local sub-controllers exchange *no information* with other sub-controllers, and distributed (cf. Fig 1.2c) to refer to control schemes in which local sub-controllers exchange information. We use the blanket term *non-classical information sharing* to refer to a setting in which the control scheme is not centralized.

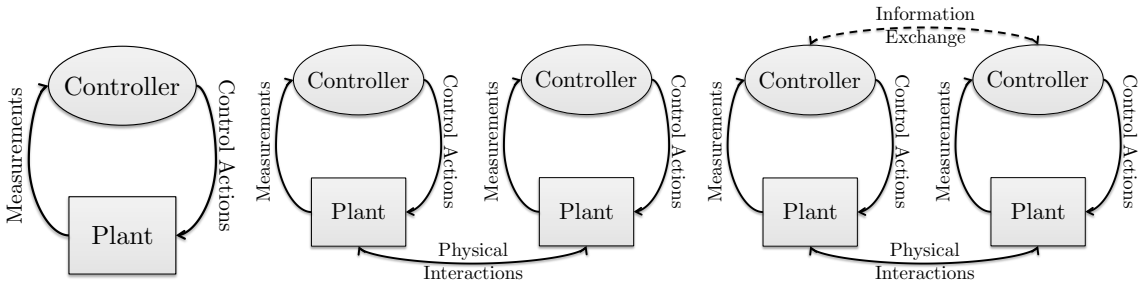

(a) Centralized control.

(b) Decentralized control for a system composed of two subsystems.

(c) Distributed control for a system composed of two subsystems.

Figure 1.2: Schematics of centralized, decentralized and distributed control architectures.

We now provide a brief overview of the relevant aspects of the rich literature on norm optimal control subject to non-classical information sharing, and refer the interested reader to the excellent review paper [4] and the references therein for a more exhaustive and in depth exploration of these ideas. Non-classical information sharing leads to an asymmetry in the information available to each sub-controller – it was realized early on that this asymmetry can make seemingly simple optimal control problems (e.g., those with linear dynamics, Gaussian disturbances and quadratic costs) have extremely complex solutions. The canonical example of such a "hard simple" problem is the Witsenhausen counterexample [5], illustrated in Fig. 1.3 – this well studied problem (cf. [6, 7] and references therein) is one for which a nonlinear control policy can perform arbitrarily better than a linear control policy. Informally, Witsenhausen's counterexample is a difficult control problem because it involves an implicit *communication problem*: controller C_1 must attempt to communicate the value x_0 (via $x_1 = x_0 + u_1$) to controller C_2 through a channel corrupted by the Gaussian noise z, all while minimizing control effort. It is this mixing of communication and control that can be viewed as leading to the computational difficulties of the problem.

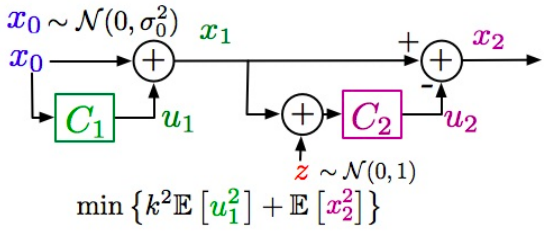

Figure 1.3: A schematic of Witsenhausen's counterexample [courtesy of wikipedia], a control problem subject to non-classical information sharing constraints for which nonlinear control can arbitrarily outperform linear control.

This observation led to a concerted effort in the control community to identify *computationally tractable* control problems subject to non-classical information sharing. An early and important result in this direction was the work by Ho and Chu on *partial nestedness* [8] which stated that an LQG control problem subject to non-classical information sharing constraints admits a unique optimal control policy that is *linear* in the information of each sub-controller *if* information is shared quickly enough between sub-controllers. We defer a formal discussion of partial nestedness to Chapter 3, and instead provide here some intuition behind the result. In [8], the authors show that optimal control policies are unique and linear if sub-controllers can exchange information at least as quickly as their control actions propagate through the plant. In this way, any incentive for sub-controllers to attempt to *signal* to each other through the plant (as in the Witsenhausen counterexample) is removed, thus re-establishing a separation between communication and control and yielding a tractable problem. Indeed this intuition of removing the incentive for sub-controllers to signal to each other through the plant is a common theme in the subsequent generalizations of partial nestedness upon which much of modern distributed optimal control theory is built. These efforts to identify tractable classes of distributed optimal control problems culminated with the notion of *quadratic invariance* [9, 10], which is a simple algebraic condition that ensures that *model-matching problems* subject to non-classical information sharing constraints admit a convex reformulation via the Youla parameterization. As our later work builds on these results, we introduce and discuss relevant concepts from model matching and quadratic invariance theory as needed in

Chapters 2, 4 and 5.

It is important to note however, that convexity is often necessary but not immediately sufficient to guarantee the computational tractability of an optimal control problem. This is because in general, even if a distributed optimal control problem admits a convex formulation, the resulting convex optimization problem may still be infinite dimensional. Indeed, it was a great triumph of centralized modern control theory to reduce the solution of infinite dimensional robust and optimal control problems to solving two finite dimensional Algebraic Riccati Equations (AREs) [11]. Likewise, a renewed enthusiasm in the controller synthesis community has led to a bevy of results that show how certain distributed optimal control problems can be reduced to solving a finite dimensional optimization problem or set of equations (e.g., [2,12–17]).

1.2 Thesis Contribution and Outline

The contributions of this thesis are to the foundational theory of distributed optimal control, and can be divided into three categories: synthesis, architecture design and system identification. Our contributions to distributed optimal controller synthesis can be found in

- **Chapter 2**, where we provide a characterization of distributed controllers subject to delay constraints induced by a strongly connected communication graph that achieve a prescribed closed loop $\mathcal{H}_\infty$ norm. Inspired by the solution to the $\mathcal{H}_2$ problem subject to delays, we exploit the fact that the communication graph is strongly connected to decompose the controller into a local finite impulse response component and a global but delayed infinite impulse response component. This allows us to reduce the control synthesis problem to a linear matrix inequality feasibility test. The results of this chapter have been published in [17].

- **Chapter 3**, where we present an explicit solution to a two player distributed LQR problem in which communication between controllers occurs across a communication link with varying delay. We extend known dynamic programming methods to

accommodate this varying delay, and show that under suitable assumptions, the optimal control actions are linear in their information, and that the resulting controller has piecewise linear dynamics dictated by the current effective delay regime. The results of this chapter have been published in [18, 19].

The results of Chapter 3 should be viewed as part of a broader agenda of removing or relaxing the unrealistic assumptions that are made in the distributed optimal control framework. In Chapter 3, by no longer assuming that delays are fixed, we allow for a more realistic model of communication channels in which packet drop-outs, coding, noise, and congestion are captured by the varying end-to-end delay. The rest of the contributions of this thesis are in line with the overall aim of relaxing unrealistic assumptions in the existing distributed optimal control literature so as to help close the gap between theory and practice.

The next assumption that we tackle is that of a preexisting controller architecture, that is to say a preexisting set of sensors, actuators and communication links connecting them. Indeed, for large-scale cyber-physical systems, the architectural aspects of the controller can no longer be taken as given, and the task of designing this architecture is now as important as the design of the control laws themselves. To that end, in

- **Chapter 4** we introduce the Regularization for Design (RFD) framework, which is a unified computationally tractable approach, built around the model matching framework and atomic norm minimization [20], for the simultaneous co-design of a structured optimal controller and the actuation, sensing and communication architecture required to implement it. Further, we show that problems formulated in this framework are natural control-theoretic analogs of prominent approaches such as the Lasso, the Group Lasso, the Elastic Net, and others that are employed in structured inference. In analogy to that literature, we show that our approach identifies optimally structured controllers under a suitable condition on a "signal-to-noise" type ratio. The results of this chapter have been published in [21, 22].

- **Chapter 5** we give an explicit construction for an atomic norm useful for the

design of communication topologies that are well suited to distributed optimal control. Using this atomic norm we then show that in the context of $\mathcal{H}_2$ distributed optimal control, the communication architecture/control law co-design task can be performed through the use of finite dimensional second order cone programming. The results of this chapter have been published in [23].

Finally, an underlying assumption in all of the previous results is that the state-space parameters specifying the model of the distributed system are given. Such state-space parameters are most often obtained through system identification techniques. However, traditional system identification methods developed for centralized systems, such as subspace identification or prediction error, are not computationally scalable and do not preserve or identify the structure of the underlying distributed system. To that end, in

- **Chapter 6** we argue that in the context of system identification, an essential building block of any scalable algorithm is the ability to estimate local dynamics within a large interconnected system. We show that in what we term the "full interconnection measurement" setting, this task is easily solved using existing system identification methods. We also propose a promising heuristic for the "hidden interconnection measurement" case, in which contributions to local measurements from both local and global dynamics need to be separated. Inspired by the machine learning literature, and in particular by convex approaches to rank minimization and matrix decomposition, we exploit the fact that the transfer function of the local dynamics is low-order, but full-rank, while the transfer function of the global dynamics is high-order, but low-rank, to formulate this separation task as a nuclear norm minimization. The results of this chapter are based on the preprint [24].

Finally, we end with concluding remarks and directions for future work in **Chapter 7**.

A note on chapter content: Due to the length of this thesis, we aim to make each chapter self-contained so as to allow for a modular reading of the document – in doing so, some redundancy had to be introduced across chapters.

Chapter 2

Distributed Control subject to Delays Satisfying an $\mathcal{H}_\infty$ Norm Bound

2.1 Introduction

The identification of Quadratic Invariance[1](QI) [9] as an appropriate condition for the convexification of structured model matching problems has brought a renewed enthusiasm and excitement to optimal controller synthesis. In the following discussion, we survey recent results in this area, and in particular comment on three classes of quadratically invariant constraints: (1) sparsity constraints, in which we assume no delay in information sharing, but rather a restriction of what measurements each controller has access to, (2) delay constraints, in which we assume that controllers communicate with each other subject to delays induced by a strongly connected communication graph, and hence eventually have access to global, but delayed, information, and (3) delay-sparsity constraints, in which we allow both restrictions on measurement access and communication delay between controllers.

Related work: Before proceeding into a more detailed review of QI based results, it is worth mentioning that novel approaches to distributed control, not based on the QI framework, have begun to appear in the literature. Representative examples include: sparsity inducing control [26, 27], convex relaxations of rank constrained problems [28, 29], the minimization of convex surrogates to traditional performance

[1]QI [9] is closely related to funnel causality [25], partial nestedness [8] and poset causality [14].

metrics [30, 31], spatial truncation [32, 33], positive systems [34, 35], and localized distributed control [36–38].

Returning to QI constraint sets, in the $\mathcal{H}_2$ case, explicit state-space solutions exist for fixed and varying delay constrained [19,39] , sparsity constrained [14,40] and delay-sparsity constrained [41] state-feedback problems. For the special case of the one-step delay information sharing pattern, the general $\mathcal{H}_2$ problem was solved in the 1970s using dynamic programming ([42–44]). When moving to the output feedback case, specific sparsity constrained problems have been solved explicitly, such as the state-space solution for the two-player problem [12] and for lower-triangular systems [45]. The delay-sparsity-constrained case has earned considerable attention, with solutions via vectorization [9] and semi-definite programming [46, 47] existing – we note that although computationally tractable, in contrast with the sparsity constrained setting, none of these methods claim to yield a controller of minimal order. In the case of delay constraints without sparsity, the aforementioned results are applicable, but an additional method based on quadratic programming and spectral factorization [16] also exists. It is worth noting that for specific systems, sufficient statistics and a generalized separation principle have been identified and successfully applied in work by [48]. Furthermore, recent work by [49, 50] provides dynamic programming decompositions for the general delayed sharing model.

The landscape of distributed $\mathcal{H}_\infty$ controller synthesis is comparably much sparser, so to speak. However, especially in the sparsity constrained case, there has recently been some progress. In particular, [13] provides a semi-definite programming solution for the structured optimal $\mathcal{H}_\infty$ output-feedback problem subject to nested sparsity constraints. In [51], an explicit state-space representation of the minimum-entropy solution to the two-player version of this problem is presented. A more general approach, applicable to all three classes of constraint types, is presented in [52]. It allows for a principled approximation of the problem via a semi-definite programming based solution that computes an optimal $\mathcal{H}_\infty$ controller within a fixed finite-dimensional subspace. By allowing this finite impulse response (FIR) approximation to be of large enough order, they are able to achieve near optimal performance in a computa-

tionally tractable manner.

Contributions: This chapter is based on [17], and aims to provide a solution to the sub-optimal distributed $\mathcal{H}_\infty$ control problem subject to delay constraints – in particular, we seek a delay constrained controller that achieves a prescribed closed loop norm. Inspired by the results in [16], we exploit the fact that the controller can be written as a direct sum of a local FIR filter and a delayed, but global, infinite impulse response (IIR) element, and show that the synthesis problem can be reduced to a linear matrix inequality (LMI) feasibility test.

A caveat is that our method is based on the so-called "1984" approach to $\mathcal{H}_\infty$ control, and as such, suffers from the same computational burden that the centralized solution is subject to. We do not claim that our solution is computationally scalable, but provide it rather as evidence that in the case of delay constrained $\mathcal{H}_\infty$ synthesis, the problem admits a finite-dimensional formulation. Our hope is that this result, much as was the case for its centralized analogue, will be a stepping stone to more computationally scalable and explicit results.

Chapter organization: This chapter is organized as follows: Section 2.2 establishes notation, and formalizes the distributed $\mathcal{H}_\infty$ model matching problem subject to delay constraints. In Section 2.3, we provide a refresher on the "1984" solution to the $\mathcal{H}_\infty$ problem, as described in [53]. Section 2.4 provides the main result of the chapter, and we demonstrate our algorithm on a three-player chain example in Section 2.5. We end with a discussion and conclusions in Section 2.6, and Section 2.7 contains useful formulae for computing the transfer matrix factorizations and approximations required by our method.

2.2 Problem Formulation

In all of the following, we work in discrete-time.

2.2.1 Notation and Operator Theoretic Preliminaries

Here we establish notation and remind the reader of some standard results from operator theory, taken from [53].

- $\mathcal{H}_2$ denotes the set of stable proper transfer matrices that are norm square integrable on the unit circle with vanishing negative Fourier coefficients; i.e. if $G \in \mathcal{H}_2$ then $H(z) = \sum_{i=0}^{\infty} H_i z^{-i}$ and $\|H\|_2^2 = \text{trace}\,(\sum_{i=0}^{\infty} H_i^* H_i)$.
- $\mathcal{H}_\infty$ denotes the set of stable proper transfer matrices. Note that $G \in \mathcal{H}_\infty$ implies $G \in \mathcal{H}_2$.
- $\mathcal{L}_\infty$ denotes the frequency domain Lesbesgue space of essentially bounded functions.
- The prefix $\mathcal{R}$ to a set $\mathcal{X}$ indicates the restriction to real-rational members of $\mathcal{X}$.
- $\|\cdot\|_\infty$ denotes the norm on $\mathcal{L}_\infty$.
- For $R \in \mathcal{L}_\infty$, let $\text{dist}\,(R, \mathcal{H}_\infty) := \inf\{\|R - X\|_\infty \,:\, X \in \mathcal{H}_\infty\}$.
- $\|\cdot\|$ denotes the spectral norm (maximum singular value).
- For a transfer matrix $G \in \mathcal{RL}_\infty$, $G^\sim$ denotes its conjugate, i.e. $G^\sim(z) = G^*(z^{-1})$.
- For a transfer matrix $G \in \mathcal{RL}_\infty$, $G^\dagger$ denotes its Moore-Penrose pseudo-inverse.
- $\oplus$, and $\perp$, denote the direct sum, and orthogonality, respectively, as defined with respect to the standard inner product on $\mathcal{H}_2$.
- Decompose $R \in \mathcal{RL}_\infty$ as $R = R_1^\sim + R_2$, with R_1, $R_2 \in \mathcal{RH}_\infty$, and R_1 strictly proper. We shall refer to (R_1, R_2) as an anti-stable/stable decomposition of R.
- Γ_F denotes the Hankel operator with symbol F, that is to say the Hankel mapping from $\mathcal{H}_2$ to $\mathcal{H}_2^\perp$. Note that if (F_1, F_2) is an anti-stable/stable decomposition of F, then $\Gamma_F = \Gamma_{F_1^\sim}$.

- $\tilde{\Gamma}_F$ denotes the adjoint Hankel operator with symbol F, that is to say the Hankel mapping from $\mathcal{H}_2^\perp$ to $\mathcal{H}_2$. The following useful fact then holds:

$$\|\Gamma_F\| = \|\Gamma_{F_1^\sim}\| = \|\tilde{\Gamma}_{F_1}\|. \tag{2.1}$$

- Δ_N denotes the N-delay operator, i.e. $\Delta_N G = \frac{1}{z^N} G$.

2.2.2 The model-matching problem subject to delay

We provide a brief overview of the distributed optimal control problem subject to delay, and refer the reader to [16] for a much more thorough and general exposition.

Let P be a stable discrete-time plant given by

$$P = \left[\begin{array}{c|cc} A & B_1 & B_2 \\ \hline C_1 & 0 & D_{12} \\ C_2 & D_{21} & 0 \end{array}\right] = \begin{bmatrix} P_{11} & P_{12} \\ P_{21} & P_{22} \end{bmatrix} \tag{2.2}$$

with inputs of dimension p_1, p_2 and outputs of dimension q_1, q_2. We restrict attention to stable plants for simplicity. These methods could also be applied to an unstable plant if a stable stabilizing nominal controller can be found, as in [9]. Future work will look to incorporate the results in [16], which are based on those in [54], into our procedure so as to have a general solution to the model matching problem.

Throughout, we assume that $D_{12}^T D_{12} > 0$, $D_{21} D_{21}^T > 0$, $C_1^T D_{12} = 0$, and $B_1 D_{21}^T = 0$, so as to ensure the existence of stabilizing solutions to the necessary discrete algebraic Riccati equations (DAREs).

For $N \geq 1$, define the space of $\mathcal{RH}_\infty$ FIR transfer matrices by $\mathcal{X}_N = \oplus_{i=0}^{N-1} \frac{1}{z^i} \mathbb{C}^{p_2 \times q_2}$.

In this paper, we are concerned with controller constraints described by delay patterns that are imposed by *strongly connected communication graphs*. As such, let $\mathcal{S} \subset \mathcal{RH}_\infty$ be a subspace of the form

$$\mathcal{S} = \mathcal{Y} \oplus \Delta_N \mathcal{RH}_\infty \tag{2.3}$$

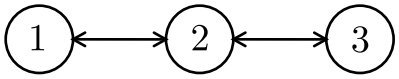

Figure 2.1: The graph depicts the communication structure of the three-player chain problem. Edge weights (not shown) indicate the delay required to transmit information between nodes.

where

$$\mathcal{Y} = \oplus_{i=0}^{N-1} \frac{1}{z^i} \mathcal{Y}_i \subset \oplus_{i=0}^{N-1} \frac{1}{z^i} \mathbb{R}^{p_2 \times q_2} \subset \mathcal{X}_N. \tag{2.4}$$

Specifically, this implies that every decision-making agent has access to *all* measurements that are at least N time-steps old.

We can therefore partition the measured outputs y and control inputs u according to the dimension of the subsystems:

$$y = [\ y_1^T \ \ \cdots \ \ y_m^T]^T \quad u = [\ u_1^T \ \ \cdots \ \ u_n^T]^T$$

and then further partition each constraint set $\mathcal{Y}_i$ as

$$\mathcal{Y}_i = \begin{bmatrix} \mathcal{Y}_i^{11} & \cdots & \mathcal{Y}_i^{1m} \\ \vdots & \ddots & \vdots \\ \mathcal{Y}_i^{n1} & \cdots & \mathcal{Y}_i^{nm} \end{bmatrix}, \tag{2.5}$$

where

$$\mathcal{Y}_i^{jk} = \begin{cases} \mathbb{R}^{p_2^j \times q_2^k} & \text{if } u_j \text{ has access to } y_k \text{ at time } i \\ 0 & \text{otherwise} \end{cases} \tag{2.6}$$

and $\sum_{j=1}^{n} p_2^j = p_2$, $\sum_{k=1}^{m} q_2^k = q_2$.

Example 2.1 *Consider the three player chain problem as illustrated in Figure 2.1,*

with communication delay τ_c between nodes. Then

$$\begin{aligned} \mathcal{S} &= \begin{bmatrix} \mathcal{RH}_\infty & \frac{1}{z^{\tau_c}}\mathcal{RH}_\infty & \frac{1}{z^{2\tau_c}}\mathcal{RH}_\infty \\ \frac{1}{z^{\tau_c}}\mathcal{RH}_\infty & \mathcal{RH}_\infty & \frac{1}{z^{\tau_c}}\mathcal{RH}_\infty \\ \frac{1}{z^{2\tau_c}}\mathcal{RH}_\infty & \frac{1}{z^{\tau_c}}\mathcal{RH}_\infty & \mathcal{RH}_\infty \end{bmatrix} \\ &= \oplus_{i=0}^{2\tau_c-1} \frac{1}{z^i}\mathcal{Y}_i \oplus \Delta_{2\tau_c}\mathcal{RH}_\infty \end{aligned} \tag{2.7}$$

with

$$\mathcal{Y}_i = \begin{cases} \begin{bmatrix} * & 0 & 0 \\ 0 & * & 0 \\ 0 & 0 & * \end{bmatrix} & \text{for } 0 \le i < \tau_c \\ \begin{bmatrix} * & * & 0 \\ * & * & * \\ 0 & * & * \end{bmatrix} & \text{for } \tau_c \le i < 2\tau_c, \end{cases} \tag{2.8}$$

*where, for compactness, * is used to denote a space of appropriately sized real matrices. In this setting, every decision maker then has access to all measurements that are at least $2\tau_c$ time-steps old.*

The distributed control problem of interest is to design a controller $K \in \mathcal{S}$ so as to achieve a pre-defined closed loop $\mathcal{H}_\infty$ norm. Specifically, the problem is to find an internally stabilizing $K \in \mathcal{S}$ such that

$$||P_{11} + P_{12}K(I - P_{22}K)^{-1}P_{21}||_\infty \le \gamma \tag{2.9}$$

for some pre-defined $\gamma > \gamma_{\text{inf}}$, where γ_{inf} is the optimal achievable closed loop $\mathcal{H}_\infty$ norm.

In order to reformulate this problem as a *convex* model matching problem, we require the notion of QI.

Definition 2.1 *A set $\mathcal{S}$ is* quadratically invariant *under P_{22} if*

$$KP_{22}K \in \mathcal{S} \text{ for all } K \in \mathcal{S}$$

In [9], it was shown that if $\mathcal{S}$ is quadratically invariant under P_{22}, then $K \in \mathcal{S}$ if and only if $Q = K(I - P_{22}K)^{-1} \in \mathcal{S}$. In the case of delay-constraints imposed by a communication graph, intuitive and easily verifiable conditions for QI can be stated [10]. Essentially these conditions say that in order to have QI, controllers must be able to communicate with each other faster than their control actions propagate through the plant – this is closely related to funnel causality [25], partial nestedness [8] and poset causality [14].

Thus, if quadratic invariance holds, the feasibility problem (2.9) can be reduced, via the Youla parameterization, to the following equivalent model matching problem:

Problem 2.1 *Find $Q \in \mathcal{S} \bigcap \mathcal{RH}_\infty$ such that*

$$||\mathcal{T}_1 - \mathcal{T}_2 Q \mathcal{T}_3||_\infty \leq \gamma \tag{2.10}$$

for some $\gamma > \gamma_{\text{inf}}$, with $\mathcal{T}_1 = P_{11}$, $\mathcal{T}_2 = P_{12}$ and $\mathcal{T}_3 = P_{21}$.

2.3 A Review of "1984" $\mathcal{H}_\infty$ Control

As our solution is based on the so-called "1984" approach to $\mathcal{H}_\infty$ control, we review it in this section. The following is based on material found in chapter 8 of [53].

2.3.1 $\mathcal{T}_3 = I$ Case

We begin with the solution to the sub-optimal model matching problem with $\mathcal{T}_3 = I$ first, as the general case follows from a nearly identical derivation. Specifically, we consider the problem:

Problem 2.2 *Find $Q \in \mathcal{RH}_\infty$ such that $\|\mathcal{T}_1 - \mathcal{T}_2 Q\|_\infty \leq \gamma$ for some $\gamma > \gamma_{\inf} \geq 0$, where $\gamma_{\inf}$ is the optimal achievable closed loop $\mathcal{H}_\infty$ norm.*

In order to state the main result, we first define the following transfer matrices:

1. Let U_i, U_o be an inner-outer factorization of $\mathcal{T}_2$ such that $\mathcal{T}_2 = U_i U_o$, with $U_i^\sim U_i = I$, and U_i, U_o, $U_o^\dagger \in \mathcal{RH}_\infty$.

2. Let $Y := (I - U_i U_i^\sim)\mathcal{T}_1$.

3. For $\gamma > \|Y\|_\infty$, let Y_o be a bi-stable spectral factor of $\gamma^2 I - Y^\sim Y$ such that $\gamma^2 I - Y^\sim Y = Y_o^\sim Y_o$, with Y_o, $Y_o^{-1} \in \mathcal{RH}_\infty$.

4. Define the $\mathcal{RL}_\infty$ matrix $R := U_i^\sim \mathcal{T}_1 Y_o^{-1}$.

Theorem 2.1 *Let $\alpha := \inf\{\|\mathcal{T}_1 - \mathcal{T}_2 Q\|_\infty \ : \ Q \in \mathcal{RH}_\infty\}$. Then*

1. $\alpha = \inf\{\gamma \ : \ \|Y\|_\infty < \gamma, \ \mathrm{dist}\,(R, \mathcal{RH}_\infty) < 1\}$, and

2. For $\gamma > \alpha$ and Q, $X \in \mathcal{RH}_\infty$ such that

- *$\|R - X\|_\infty \leq 1$, and*
- *$X = U_o Q Y_o^{-1}$,*

we have that $\|\mathcal{T}_1 - \mathcal{T}_2 Q\|_\infty \leq \gamma$.

Before proving this result, we need the following two preliminary lemmas:

Lemma 2.1 *Let U be inner and $E \in \mathcal{RL}_\infty$ be given by*

$$E := \begin{bmatrix} U^\sim \\ I - UU^\sim \end{bmatrix}.$$

Then for all $G \in \mathcal{RL}_\infty$, we have that $\|EG\|_\infty = \|G\|_\infty$.

Lemma 2.2 *For F, $G \in \mathcal{RL}_\infty$ with the same number of columns, if*

$$\left\| \begin{bmatrix} F \\ G \end{bmatrix} \right\|_\infty < \gamma \tag{2.11}$$

then $\|G\|_\infty < \gamma$ and $\|FG_o^{-1}\|_\infty < 1$, where G_o is a bi-stable spectral factor of $\gamma^2 I - G^\sim G$.

Conversely, if $\|G\|_\infty < \gamma$ and $\|FG_o^{-1}\|_\infty \leq 1$, then (2.11) holds.

Lemma 2.3 (Nehari's Theorem) *For any $R \in \mathcal{RL}_\infty$, we have that*

$$\operatorname{dist}(R, \mathcal{RH}_\infty) = \operatorname{dist}(R, \mathcal{H}_\infty) = \|\Gamma_R\|,$$

and that there exists $X \in \mathcal{RH}_\infty$ such that $\|R - X\|_\infty = \operatorname{dist}(R, \mathcal{RH}_\infty)$.

We may now prove Theorem 2.1.

Proof:

1) Let $\gamma_{\inf} := \inf\{\gamma \ : \ \|Y\|_\infty < \gamma, \ \operatorname{dist}(R, \mathcal{RH}_\infty) < 1\}$.

Choose $\epsilon > 0$ such that $\alpha < \gamma < \alpha + \epsilon$, implying that there exists $Q \in \mathcal{RH}_\infty$ such that $\|\mathcal{T}_1 - \mathcal{T}_2 Q\|_\infty < \gamma$. Then, by Lemma 2.1, we have that

$$\left\| \begin{bmatrix} U_i^\sim \\ I - U_i U_i^\sim \end{bmatrix} (\mathcal{T}_1 - \mathcal{T}_2 Q) \right\|_\infty < \gamma. \tag{2.12}$$

Now, notice that

$$\begin{bmatrix} U_i^\sim \\ I - U_i U_i^\sim \end{bmatrix} \mathcal{T}_2 = \begin{bmatrix} U_o \\ 0 \end{bmatrix}, \tag{2.13}$$

making (2.12) equivalent to

$$\left\| \begin{bmatrix} U_i^\sim \mathcal{T}_1 - U_o Q \\ Y \end{bmatrix} \right\|_\infty < \gamma. \tag{2.14}$$

Applying Lemma 2.2, this then implies that

$$\|Y\|_\infty < \gamma, \tag{2.15}$$

and

$$\|U_i^{\sim} T_1 Y_o^{-1} - U_o Q Y_o^{-1}\|_\infty < 1 \tag{2.16}$$

By Lemma 2.3, this in turn implies that $\text{dist}\,(R, U_o(\mathcal{RH}_\infty)Y_o^{-1}) < 1$, which, noting that U_o is right invertible in $\mathcal{RH}_\infty$ and that Y_o is invertible in $\mathcal{RH}_\infty$, is equivalent to

$$\text{dist}\,(R, \mathcal{RH}_\infty) < 1 \tag{2.17}$$

Then, from (2.15) and (2.17), and the definition of γ_{inf} we conclude that $\gamma_{\text{inf}} \leq \gamma$, and thus that $\gamma < \alpha + \epsilon$. Since ϵ was arbitrary, we then have that $\gamma_{\text{inf}} \leq \alpha$.

To prove the reverse inequality, again choose $\epsilon > 0$ and γ such that $\gamma_{\text{inf}} < \gamma < \gamma_{\text{inf}} + \epsilon$. Then (2.15) and (2.17) hold, so (2.16) holds for some $Q \in \mathcal{RH}_\infty$. Applying the converse of Lemma 2.2, this in turn implies that

$$\left\| \begin{bmatrix} U_i^{\sim} \mathcal{T}_1 - U_o Q \\ Y \end{bmatrix} \right\|_\infty \leq \gamma. \tag{2.18}$$

Finally, reversing the above steps, this leads to $\|\mathcal{T}_1 - \mathcal{T}_2 Q\|_\infty \leq \gamma$. Thus $\alpha \leq \gamma < \gamma_{\text{inf}} + \epsilon$, and hence $\alpha \leq \gamma_{\text{inf}}$.

2) This follows immediately from the previous derivation. ∎

Thus, a high level outline for computing an $\mathcal{H}_\infty$ controller satisfying a γ bound in closed loop is

1. Compute Y and $\|Y\|_\infty$.
2. Select a trial value $\gamma > \|Y\|_\infty$.
3. Compute R and $\|\Gamma_R\|$. Then $\|\Gamma_R\| < 1$ if and only if $\alpha < \gamma$, so increase or decrease γ accordingly, and return to step 2 until a sufficiently accurate upper bound for α is obtained.

4. Find a matrix $X \in \mathcal{RH}_\infty$ such that $\|R - X\|_\infty \leq 1$.

5. Solve $X = U_o Q Y_o^{-1}$ for a $Q \in \mathcal{RH}_\infty$ satisfying $\|\mathcal{T}_1 - \mathcal{T}_2 Q\|_\infty \leq \gamma$.

2.3.2 General $\mathcal{T}_3$

We now state the result for general $\mathcal{T}_3$. First, define the following matrices

1. Let U_i, U_o be an inner-outer factorization of $\mathcal{T}_2$ such that $\mathcal{T}_2 = U_i U_o$, with $U_i^\sim U_i = I$, and U_i, U_o, $U_o^\dagger \in \mathcal{RH}_\infty$.

2. Let $Y := (I - U_i U_i^\sim)\mathcal{T}_1$.

3. For $\gamma > \|Y\|_\infty$, let Y_o be a bi-stable spectral factor of $\gamma^2 I - Y^\sim Y$ such that $\gamma^2 I - Y^\sim Y = Y_o^\sim Y_o$, with Y_o, $Y_o^{-1} \in \mathcal{RH}_\infty$.

4. Let V_{co}, V_{ci} be a co-inner-outer factorization of $\mathcal{T}_3 Y_o^{-1}$ such that $\mathcal{T}_3 Y_o^{-1} = V_{co} V_{ci}$ and V_{ci}, V_{co}, $V_{co}^\dagger \in \mathcal{RH}_\infty$.

5. Let $Z := U_i^\sim \mathcal{T}_1 Y_o^{-1} \left(I - V_{ci}^\sim V_{ci}\right)$.

6. If $\|Z\|_\infty < 1$, let Z_{co} be a bi-stable co-spectral factor of $I - ZZ^\sim$ such that $I - ZZ^\sim = Z_{co} Z_{co}^\sim$, with Z_{co}, $Z_{co}^{-1} \in \mathcal{RH}_\infty$.

7. Let $R := Z_{co}^{-1} U_i^\sim \mathcal{T}_1 Y_o^{-1} V_{ci}^\sim$.

Theorem 2.2 *Let* $\alpha := \inf\{\|\mathcal{T}_1 - \mathcal{T}_2 Q \mathcal{T}_3\|_\infty : Q \in \mathcal{RH}_\infty\}$. *Then*

1. $\alpha = \inf\{\gamma : \|Y\|_\infty < \gamma,\ \|Z\|_\infty < 1,\ \mathrm{dist}\,(R, \mathcal{RH}_\infty) < 1\}$, *and*

2. For $\gamma > \alpha$ *and* Q, $X \in \mathcal{RH}_\infty$ *such that*

- $\|R - X\|_\infty \leq 1$, *and*
- $X = Z_{co}^{-1} U_o Q V_{co}$,

we have that $\|\mathcal{T}_1 - \mathcal{T}_2 Q \mathcal{T}_3\|_\infty \leq \gamma$.

Proof: Analogous from that of Theorem 2.1, and therefore omitted. ∎

Similarly, we may outline a general high level algorithm for computing a controller using Theorem 2.2:

1. Compute Y and $\|Y\|_\infty$.
2. Select a trial value $\gamma > \|Y\|_\infty$.
3. Compute Z and $\|Z\|_\infty$.
4. If $\|Z\|_\infty < 1$, continue; if not, increase γ and return to step 3.
5. Compute R and $\|\Gamma_R\|$. Then $\|\Gamma_R\| < 1$ if and only if $\alpha < \gamma$, so increase or decrease γ accordingly, and return to step 3 until a sufficiently accurate upper bound for α is obtained.
6. Find a matrix $X \in \mathcal{RH}_\infty$ such that $\|R - X\|_\infty \leq 1$.
7. Solve $X = Z_{co}^{-1} U_o Q V_{co}$ for a $Q \in \mathcal{RH}_\infty$ satisfying $\|\mathcal{T}_1 - \mathcal{T}_2 Q \mathcal{T}_3\|_\infty \leq \gamma$.

2.4 Distributed $\mathcal{H}_\infty$ Control Subject to Delays

As in [16], we exploit the fact that the communication graph is strongly connected to decompose Q into a local distributed FIR filter $V \in \mathcal{Y}$ and a global, but delayed, IIR component $\Delta_N D \in \frac{1}{z^N}\mathcal{RH}_\infty$, where in particular, $D \in \mathcal{RH}_\infty$ is unconstrained:

$$Q = V + \Delta D \in \mathcal{S}, \text{ with } V \in \mathcal{Y},\ D \in \mathcal{RH}_\infty \tag{2.19}$$

We will show that when Q admits such a decomposition, the norm bound test of Theorem 2.1 reduces to verifying the existence of a FIR filter $V \in \mathcal{Y}$ such that $\|\Gamma_{\hat{R}(V)}\| < 1$, where $\hat{R}(V)$ is a transfer matrix to be defined that depends affinely on V. Further we will show that verifying the existence of such a V, and constructing it if it exists, can be done by solving a LMI.

2.4.1 $\mathcal{T}_3 = I$ Case

We begin with a solution to the $\mathcal{T}_3 = I$ case to simplify the exposition, as the general case, much as in the centralized problem, follows from an analogous argument.

Let

- $\hat{\mathcal{T}}_1(V) := \mathcal{T}_1 - \mathcal{T}_2 V$,
- $\hat{\mathcal{T}}_2 := \mathcal{T}_2 \Delta_N$,
- $\hat{U}_i := U_i \Delta_N$, $\hat{U}_o = U_o \in \mathcal{RH}_\infty$ be inner and outer, respectively, such that $\hat{\mathcal{T}}_2 = \hat{U}_i \hat{U}_o$, and $\hat{U}_o^{-1} \in \mathcal{RH}_\infty$.
- $\hat{R}(V) := \Delta_N^\sim R - \hat{U}_o(\Delta_N^\sim V) Y_o^{-1}$,

with Y_o^{-1} and R defined as in Section 2.3.1. We then have that

Theorem 2.3 *Let* $\alpha := \inf\{\|\hat{\mathcal{T}}_1(V) - \hat{\mathcal{T}}_2 D\|_\infty \ : \ D \in \mathcal{RH}_\infty, V \in \mathcal{Y}\}$. *Then*

1. $\alpha = \inf\{\gamma \ : \ \|Y\|_\infty < \gamma, \exists V \in \mathcal{Y}$ *s.t.* $\operatorname{dist}\left(\hat{R}(V), \mathcal{RH}_\infty\right) < 1\}$, *and*
2. *For* $\gamma > \alpha$ *and* D, $X \in \mathcal{RH}_\infty$ *such that*
   - $\|\hat{R}(V) - X\|_\infty \leq 1$, *and*
   - $X = \hat{U}_o D Y_o^{-1}$,

   we have that $\|\hat{\mathcal{T}}_1(V) - \hat{\mathcal{T}}_2 D\|_\infty \leq \gamma$.

Before proving this result, we will need the following lemma:

Lemma 2.4 *For* $\hat{Y}(V) := (I - \hat{U}_i \hat{U}_i^\sim)\hat{\mathcal{T}}_1(V)$, *we have that* $\hat{Y}(V) = Y$, *where* Y *is as defined in Section 2.3.1.*

Proof: Straightforward, and thus omitted. ∎

We may now prove Theorem 2.3.

Proof: 1) Choose $\epsilon > 0$ such that $\alpha < \gamma < \alpha + \epsilon$, implying that there exists $V \in \mathcal{Y}$ and $D \in \mathcal{RH}_\infty$ such that $\|\hat{\mathcal{T}}_1(V) - \hat{\mathcal{T}}_2 D\|_\infty < \gamma$.

We now proceed as in the proof of Theorem 2.1, and premultiply by

$$\begin{bmatrix} \hat{U}_i^{\sim} \\ (I - \hat{U}_i \hat{U}_i^{\sim}) \end{bmatrix}, \tag{2.20}$$

and apply Lemma 2.2 to obtain the equivalence between $\|\hat{\mathcal{T}}_1(V) - \hat{\mathcal{T}}_2 D\|_\infty \leq \gamma$ and

$$\left\| \begin{bmatrix} (\hat{U}_i^{\sim} \hat{\mathcal{T}}_1(V) - \hat{U}_o D) \\ \hat{Y}(V) \end{bmatrix} \right\|_\infty < \gamma. \tag{2.21}$$

By Lemma 2.2 and Lemma 2.4, (2.21) is equivalent to

$$\|Y\|_\infty < \gamma \tag{2.22}$$

and

$$\|\hat{U}_i^{\sim} \hat{\mathcal{T}}_1(V) Y_o^{-1} - \hat{U}_o D Y_o^{-1}\|_\infty < 1. \tag{2.23}$$

Noting that

$$\begin{aligned} \hat{U}_i^{\sim} \hat{\mathcal{T}}_1(V) Y_o^{-1} &= \hat{U}_i^{\sim} \mathcal{T}_1 Y_o^{-1} - \hat{U}_i^{\sim} (\mathcal{T}_2 \Delta_N) \Delta_N^{\sim} V Y_o^{-1} \\ &= \Delta_N^{\sim} R - \hat{U}_o \Delta_N^{\sim} V Y_o^{-1} \\ &= \hat{R}(V) \end{aligned} \tag{2.24}$$

this is then equivalent to

$$\|\hat{R}(V) - \hat{U}_o D Y_o^{-1}\|_\infty < 1, \tag{2.25}$$

which by the arguments of the proof of Theorem 2.1, is equivalent to $\|\Gamma_{\hat{R}(V)}\| < 1$.

The rest of the proof proceeds as that of Theorem 2.1. ∎

Thus, for a fixed γ, we have reduced the problem to a feasibility test: does there exist a FIR filter $V \in \mathcal{Y}$ such that $\|\Gamma_{\hat{R}(V)}\| < 1$. As per identity (2.1), this is equivalent to $\|\tilde{\Gamma}_{\hat{R}_1(V)}\| < 1$, with $(\hat{R}_1(V), \hat{R}_2(V))$ an anti-stable/stable decomposition of $\hat{R}(V)$.

Reduction to a LMI

Let R_1 and R_2 be an anti-stable/stable decomposition of $\Delta_N^{\sim} R$. Now, define $G(V) \in \mathcal{RH}_\infty$ as

$$\begin{aligned} G(V) &:= \hat{U}_o V Y_o^{-1} \\ &= \textstyle\sum_{i=0}^{\infty} \frac{1}{z^i} G_i(V). \end{aligned} \tag{2.26}$$

where the terms $G_i(V)$ are the impulse response elements of G. It is easily verified that these terms are *affine* in $\{V_i\}$, the impulse response elements of V (i.e. $V = \sum_{i=0}^{N-1} \frac{1}{z^i} V_i$). Note that $G(V) \in \mathcal{RH}_\infty$ follows from U_o, V, $Y_o^{-1} \in \mathcal{RH}_\infty$. As such, let

$$G(V) := \left[\begin{array}{c|c} A_G & B_G \\ \hline C_G & D_G \end{array}\right]$$

be a minimal stable realization of G.

We then have that

$$\begin{aligned} \hat{U}_o \Delta_N^{\sim} V Y_o^{-1} &= \Delta_N^{\sim} G \\ &= z^N \textstyle\sum_{i=0}^{\infty} \frac{1}{z^i} G_i(V) \\ &= \textstyle\sum_{k=1}^{N} z^k G_{N-k}(V) + \sum_{j=0}^{\infty} \frac{1}{z^j} G_{j+N}(V) \\ &=: q(V)^{\sim} + N_G(V). \end{aligned} \tag{2.27}$$

with $q(V) = \sum_{k=1}^{N} \frac{1}{z^k} G_{N-k}^{\top}(V) \in \mathcal{RH}_\infty$ and strictly proper.

Also note that $N_G(V)$ has the following state space representation

$$N_G(V) = \left[\begin{array}{c|c} A_G & B_G \\ \hline C_G A_G^N & C_G A_G^{N-1} B_G \end{array}\right], \tag{2.28}$$

and is therefore also clearly in $\mathcal{RH}_\infty$.

The following lemma is an immediate consequence of the previous discussion.

Lemma 2.5 *Let $\hat{R}(V)$ be as defined. Then an anti-stable/stable decomposition of*

$\hat{R}(V)$ is given by

$$\begin{aligned} \hat{R}_1(V) &= R_1 - q(V) \\ \hat{R}_2(V) &= R_2 - N_G(V) \end{aligned} \tag{2.29}$$

From our previous discussion, we have thus reduced the problem to finding an FIR filter V such that $\|\tilde{\Gamma}_{\hat{R}_1(V)}\| < 1$, for $\hat{R}_1(V)$ given as in (2.29).

We begin by deriving a state space representation for $\hat{R}_1(V)$, and then use this representation to formulate the Hankel norm bound test as a LMI.

First note that $q(V)$ is simply a strictly causal FIR filter, and thus has a state space representation given by

$$q(V) = \left[\begin{array}{c|c} A_q & B_q \\ \hline C_q(V) & 0 \end{array}\right], \tag{2.30}$$

where A_q is the down-shift operator (i.e. a block matrix with appropriately dimensioned Identity matrices along the first sub block diagonal, and zeros elsewhere), $B_q = [I, 0 \ldots, 0]^\top$, and $C_q(V) = [G_{N-1}(V)^\top, \ldots, G_0(V)^\top]$. Note that only $C_q(V)$ is a function of our design variable V.

Letting the strictly proper $R_1 \in \mathcal{RH}_\infty$ have a minimal stable realization

$$R_1 = \left[\begin{array}{c|c} A_r & B_r \\ \hline C_r & 0 \end{array}\right] \tag{2.31}$$

we then have the following realization for $\hat{R}_1(V) \in \mathcal{RH}_\infty$:

$$\hat{R}_1(V) = \left[\begin{array}{cc|c} A_r & 0 & B_r \\ 0 & A_q & B_q \\ \hline C_r & -C_q(V) & 0 \end{array}\right] =: \left[\begin{array}{c|c} A_R & B_R \\ \hline C_R(V) & 0 \end{array}\right]. \tag{2.32}$$

We emphasize again that our design variable V appears only in $C_R(V)$.

We now recall the variational formulation for the Hankel norm of a strictly proper transfer matrix $F \in \mathcal{RH}_\infty$.

Proposition 2.1 *For a system*

$$F = \left[\begin{array}{c|c} A & B \\ \hline C & 0 \end{array}\right] \in \mathcal{RH}_\infty,$$

we have that $\|\tilde{\Gamma}_F\| < 1$ *if and only if there exist matrices* $P, Q \geq 0$ *and scalar* $\lambda \geq 0$ *such that*

$$\begin{bmatrix} A^\top Q A - Q & C^\top \\ C & -\lambda I \end{bmatrix} \leq 0$$

$$\begin{bmatrix} -P & PB & PA \\ B^\top P & -I & 0 \\ A^\top P & 0 & -P \end{bmatrix} \leq 0 \tag{2.33}$$

$$P - Q \geq 0$$

$$\lambda < 1$$

Proof: This is the discrete-time analog of the variational formulation found in Section 6.3.1 of [55]. ∎

Substituting our realization (2.32) into (2.33), we see that this is an LMI in the variables $\{V_i\}_{i=0}^{N-1}$, P, Q, and λ, and is feasible if and only if there exists an FIR filter $V \in \mathcal{Y}$ such that $\|\tilde{\Gamma}_{\hat{R}_1(V)}\| < 1$.

Thus, a high level outline for computing a distributed controller satisfying an $\mathcal{H}_\infty$ norm bound of γ in closed loop is

1. Compute Y and $\|Y\|_\infty$.

2. Select a trial value $\gamma > \|Y\|_\infty$.

3. Construct $\hat{R}_1(V)$ and check if the LMI in variables $\{V_i\}_{i=0}^{N-1}$, Q, P and λ

$$\begin{aligned}
\begin{bmatrix} A_R^\top Q A_R - Q & C_R(V)^\top \\ C_R(V) & -\lambda I \end{bmatrix} &\leq 0 \\
\begin{bmatrix} -P & PB_R & PA_R \\ B_R^\top P & -I & 0 \\ A_R^\top P & 0 & -P \end{bmatrix} &\leq 0 \\
P - Q &\geq 0 \\
\lambda &< 1
\end{aligned} \tag{2.34}$$

   is feasible for $V = \sum_{i=0}^{N-1} \frac{1}{z^i} V_i \in \mathcal{Y}$. This LMI is feasible if and only if $\|\tilde{\Gamma}_{\hat{R}_1(V)}\| < 1$, which in turn occurs if and only if $\alpha < \gamma$, so increase or decrease γ accordingly. This feasibility test will additionally yield an FIR filter $V \in \mathcal{Y}$ that satisfies this bound.

4. Find a matrix $X \in \mathcal{RH}_\infty$, implicitly dependent on V, such that $\|\hat{R}(V) - X\|_\infty \leq 1$ (such a matrix is guaranteed to exist by the same arguments as those used in the centralized case).

5. Solve $X = \hat{U}_o D Y_o^{-1}$ for $D \in \mathcal{RH}_\infty$ satisfying $\|\hat{\mathcal{T}}_1(V) - \hat{\mathcal{T}}_2 D\|_\infty \leq \gamma$.

6. Set $Q = V + \Delta_N D \in \mathcal{S} \bigcap \mathcal{RH}_\infty$

2.4.2 General $\mathcal{T}_3$

Define the following transfer matrices

1. $\hat{Z} = \hat{U}_i^\sim \mathcal{T}_1 Y_o^{-1}(I - V_{ci} V_{ci}^\sim)$,

2. $\hat{R}(V) := \Delta_N^\sim R - Z_{co}^{-1} \hat{U}_o (\Delta_N^\sim V) V_{co}$,

and let Y_o^{-1}, R, V_{co} and Z_{co}^{-1} be as defined in Section 2.3.2, and $\hat{\mathcal{T}}_1(V)$, $\hat{\mathcal{T}}_2$, $\hat{U}_i$ and $\hat{U}_o$ be as defined in Section 2.4.1. We note that just as $\hat{Y}(V)$ was independent of V, so too would be the analogous $\hat{Z}(V)$ – as such we simply define $\hat{Z}$ and not $\hat{Z}(V)$.

Theorem 2.4 *Let* $\alpha := \inf\{\|\hat{\mathcal{T}}_1(V) - \hat{\mathcal{T}}_2 D \mathcal{T}_3\|_\infty : D \in \mathcal{RH}_\infty,\ V \in \mathcal{Y}\}$. *Then*

1. $\alpha = \inf\{\gamma\ :\ \|Y\|_\infty < \gamma,\ \|Z\|_\infty < 1, \exists V \in \mathcal{Y}$ *s.t.* $\text{dist}\left(\hat{R}(V), \mathcal{RH}_\infty\right) < 1\}$, *and*

2. *For* $\gamma > \alpha$ *and* D, $X \in \mathcal{RH}_\infty$ *such that*

   - $\|\hat{R}(V) - X\|_\infty \leq 1$, *and*
   - $X = Z_{co}^{-1} \hat{U}_o D V_{co}$,

   we have that $\|\hat{\mathcal{T}}_1(V) - \hat{\mathcal{T}}_2 D \mathcal{T}_3\|_\infty \leq \gamma$.

Proof: Analogous to that of Theorem 2.3, and therefore omitted. ∎

Just as in the $\mathcal{T}_3 = I$ case, this problem has now been reduced to finding an FIR filter $V \in \mathcal{Y}$ such that $\|\tilde{\Gamma}_{\hat{R}(V)}\| < 1$. The arguments of the preceding section apply nearly verbatim, with the exception of replacing equation (2.26) with

$$G(V) := Z_{co}^{-1} \hat{U}_o V V_{co} \tag{2.35}$$

Therefore, a high level outline for computing a distributed controller satisfying an $\mathcal{H}_\infty$ norm bound of γ in closed loop is

1. Compute Y and $\|Y\|_\infty$.

2. Select a trial value $\gamma > \|Y\|_\infty$.

3. Compute $\hat{Z}$ and $\|\hat{Z}\|_\infty$.

4. If $\|\hat{Z}\|_\infty < 1$, continue; if not, increase γ and return to step 3.

5. Construct $\hat{R}_1(V)$ according to (2.29), with $G(V)$ defined as in (2.35), and check if there exists $V \in \mathcal{Y}$ such that LMI (2.34) is feasible. This LMI is feasible if and only if $\|\tilde{\Gamma}_{\hat{R}_1(V)}\| < 1$, which in turn occurs if and only if $\alpha < \gamma$, so increase or decrease γ accordingly. This feasibility test will additionally yield an FIR filter $V \in \mathcal{Y}$ that satisfies this bound.

6. Find a matrix $X \in \mathcal{RH}_\infty$, implicilty dependent on V, such that $\|\hat{R}(V) - X\|_\infty \leq 1$.

7. Solve $X = Z_{co}^{-1}\hat{U}_o D V_{co}$ for $D \in \mathcal{RH}_\infty$ satisfying $\|\hat{\mathcal{T}}_1(V) - \hat{\mathcal{T}}_2 D \mathcal{T}_3\|_\infty \leq \gamma$.

8. Set $Q = V + \Delta_N D \in \mathcal{S} \bigcap \mathcal{RH}_\infty$

2.5 Example

For the convenience of the reader, we provide explicit state-space formulae for the factorizations and approximations required to implement our algorithm in Section 2.7.

We consider a three-player chain with communication delay of $\tau_c = 1$ – the sparsity constraint $\mathcal{Y}$ on the FIR filter is as given in equation (2.8). We first consider the simplified case of $P_{21} = I$ – the remaining dynamics of P_{11}, P_{12} and P_{22} are given by

$$\begin{aligned} A &= \begin{bmatrix} .5 & .2 & 0 \\ .2 & .5 & .2 \\ 0 & .2 & .5 \end{bmatrix}, \quad B_1 = [I_{3\times3}\ 0_{3\times3}] \qquad B_2 = I_{3\times3}, \\ C_1 &= \begin{bmatrix} I_{3\times3} \\ 0_{3\times3} \end{bmatrix}, \qquad D_{11} = 0_{6\times6}, \qquad D_{12} = \begin{bmatrix} 0_{3\times3} \\ I_{3\times3} \end{bmatrix} \\ C_2 &= I_{3\times3}, \qquad D_{21} = [0_{3\times3}\ I_{3\times3}], \quad D_{22} = 0_{3\times3}, \end{aligned} \tag{2.36}$$

Note that this is a suitably modified version of the output feedback problem considered in [16].

We first computed the optimal centralized norm of the system using classical results [2], and obtained a centralized closed loop norm of .9772. We note that this is the theoretical lower bound as given by $\|Y\|_\infty$ from the algorithms we described above. To verify the consistency of our algorithm, we used our LMI formulation to compute a centralized controller as well. This was done by allowing the elements of the FIR filter V_0 and V_1 to be unconstrained, and not suprisingly, we were also able to achieve a closed loop norm of .9772 in this manner. We then constrained V to lie in the subspace $\mathcal{Y}$ as given by (2.8), and surprisingly, we were still able to achieve a

closed loop norm of .9772. This is a significant improvement over the delayed system (i.e.V_0 and V_1 constrained to be zero), for which we were only able to achieve a closed loop norm of 1.6856.

We then considered the general output-feedback problem, with P_{21} given by the parameters in (2.36) as well. The centralized and LMI computed centralized closed loop norms were both found to be 1.502, with the best distributed norm found to be 1.515. Once again, we see near identical performance from the centralized and distributed solutions, whereas the delayed controller was only able to achieve a closed loop norm of 2.213.

2.6 Conclusion

This chapter presented an LMI based characterization of the sub-optimal delay-constrained distributed $\mathcal{H}_\infty$ control problem. By exploiting the strongly connected nature of the communication graph, we were able to reduce the problem to a feasibility test in terms of the Hankel norm of a certain transfer matrix that is a function of the localized FIR component of the controller. We note that much as in the $\mathcal{H}_2$ case, by reducing the control synthesis problem to one that is convex in the FIR filter, communication delay co-design [23,56] and augmentation [57] methods are applicable. However, although finite dimensional, this method is based on the "1984" approach to $\mathcal{H}_\infty$ control – as such, the computational burden is quite high, limiting the scalability of the approach.

Future work will therefore focus on the following three aspects: (1) adapting the parameterization used in [16] so as to relax the assumption of a stable plant, (2) formally integrating communication delay co-design methods into the controller synthesis procedure, and most pressingly (3) seeking more direct and computationally scalable means of identifying appropriate FIR filters.

2.7 Factorization Formulas

In all of the following, we assume that the conditions needed for the existence of the required stabilizing solution of the corresponding Discrete Algebraic Riccati Equations (DARE) are met – the reader is referred to [2] and [58] for more details. All "co-X" factorizations, where "X" may be either inner-outer or bi-stable spectral, can be obtained by transposing the "X" factorization of the transpose system.

2.7.1 Inner-Outer Factorizations

Let

$$G := \left[\begin{array}{c|c} A & B \\ \hline C & D \end{array}\right] \in \mathcal{RH}_\infty.$$

From [2], an inner-outer factorization $G = U_i U_o$ of G, with U_i inner and U_o outer, is given by

$$U_i = \left[\begin{array}{c|c} A+BF & BH^{-1} \\ \hline C+DF & DH^{-1} \end{array}\right] \tag{2.37}$$

$$U_o = \left[\begin{array}{c|c} A & B \\ \hline -HF & H \end{array}\right] \tag{2.38}$$

with $H = (D^\top D + B^\top X B)^{\frac{1}{2}}$, and X the stabilizing solution of the following DARE

$$\begin{array}{rcl} X & = & A^\top X A + C^\top C + A^\top X B F, \\ F & = & -(D^\top D + B^\top X B)^{-1} B^\top X A. \end{array} \tag{2.39}$$

2.7.2 Bi-stable Spectral Factorizations

Let $Y \in \mathcal{RH}_\infty$ be strictly proper, and let

$$G_Y = \left[\begin{array}{c|c} A_Y & B_Y \\ \hline C_Y & 0 \end{array}\right]$$

be a state-space realization of the strictly proper $\mathcal{RH}_\infty$ component of $Y^\sim Y$.

If A_Y is invertible, then it holds that

$$\gamma^2 I - Y^{\sim}Y = G_Y + G_Y^{\sim} + D_Y + D_Y^{\top}$$

where $D_Y = \frac{1}{2}\left(\gamma^2 I + B_Y^{\top} A_Y^{-\top} C_Y^{\top}\right)$.

A bi-stable spectral factorization $\gamma^2 I - Y^{\sim}Y = M^{\sim}M$, with M, $M^{-1} \in \mathcal{RH}_\infty$ is then given by

$$M = \left[\begin{array}{c|c} A_Y & B_Y \\ \hline H^{-1}(C_Y + B_Y^{\top} X A_Y) & H \end{array}\right] \tag{2.40}$$

with $H = (D_Y + D_Y^{\top} + B_Y^{\top} X B_Y)^{\frac{1}{2}}$, and X the stabilizing solution of the following DARE

$$\begin{aligned} X &= A_Y^{\top} X A_Y + (A_Y^{\top} X B_Y + C_Y^{\top})F, \\ F &= -(D_Y^{\top} + D_Y + B_Y^{\top} X B_Y)^{-1}(B_Y^{\top} X A_Y + C_Y). \end{aligned} \tag{2.41}$$

This result follows directly from standard results on spectral factors and positive real systems [2]

2.7.3 Stable Approximations

The following is taken from [58]. Let

$$G := \left[\begin{array}{c|c} A & B \\ \hline C & D \end{array}\right] \in \mathcal{RH}_\infty$$

be a minimal state-space representation, and assume that $\rho = \|\tilde{\Gamma}_G\| < \gamma$. Let X and Y be the controllability and observability Gramians of G, respectively.

Let $Q \in \mathcal{RH}_\infty$ have the state-space representation

$$Q := \left[\begin{array}{c|c} A_Q & B_Q \\ \hline C_Q & D_Q \end{array}\right]$$

with

$$A_Q = A - BC_Q, \;\; B_Q = AXC^\top + BE^\top,$$
$$C_Q = (E^\top C + B^\top Y A)N, \;\; D_Q = D^\top - E^\top,$$

where $N = (\gamma^2 I - XY)^{-1}$, and for any unitary matrix U,

$$E = -(I + CNXC^\top)^{-1} CNXA^\top YB + \gamma(I + CNXC^\top)^{-\frac{1}{2}} U (I + B^\top YNB)^{-\frac{1}{2}}.$$

Then $\|G - Q^\sim\|_\infty = \gamma$ and $(G - Q^\sim)^\sim (G - Q^\sim) = \gamma^2 I$.

Chapter 3

Optimal Two Player LQR State Feedback with Varying Delay

3.1 Introduction

As described in Section 2.1, quadratic invariance has spurred on a flurry of activity in distributed optimal control synthesis subject to sparsity and delay constraints. However, an underlying assumption in the aforementioned results is that information, albeit delayed, can be transmitted *perfectly* across a communication network with a *fixed* delay. A realistic communication network, however, is subject to data rate limits, quantization, noise and packet drops – all of these issues result in possibly varying delays (due to variable decoding times) and imperfect transmission (due to data rate limits/quantization). The assumption that these delays are fixed necessarily introduces a significant level of conservatism in the control design procedure. In particular, to ensure that the delays under which controllers exchange information do not vary, worst case delay times must be used for control design, sacrificing performance and robustness in the process.

Related work: These issues have been addressed by the networked control systems (NCS) community, leading to a plethora of results for channel-in-the loop type problems: see the recent survey by [59], and the references therein. Some of the more relevant results from this field include the work by [60] and [61], which address optimal LQG control of a single plant over a packet dropping channel. Very few

results exist, however, that seek to combine NCS and decentralized optimal control. A notable exception is the work by [62], in which an explicit state space solution to a sparsity constrained two-player decentralized LQG state-feedback problem over a TCP erasure channel is solved.

Chapter contributions: We take a different view from these results, and suppress the underlying details of the communication network, and instead assume that packet drops, noise, and congestion manifest themselves to the controllers as varying delays. Indeed, as shown in [63], delays play a dominant role in determining closed-loop performance relative to channel issues such as quantization. In particular, we seek to extend the distributed state-feedback results of [39, 64] and [15] to accommodate varying delays. In addition to allowing for communication channels to be more explicitly accounted for in the control design procedure, the ability to accommodate varying delays provides flexibility in the coding design aspect of this problem – we are currently exploring the application of deadline based coding schemes developed by [65], initially designed for real-time video streaming, to optimal decentralized control.

In this chapter, we focus on a two plant system in which communication between controllers occurs across a communication link with varying delay. We extend the dynamic programming methods in [39] and [15] to accommodate this varying delay, and show that under suitable assumptions, the optimal control actions are linear in their information, and that the resulting controller has piecewise linear dynamics dictated by the current effective delay regime. The results in this chapter were first presented in [18, 19].

Chapter organization: This chapter is structured as follows: in Section 3.2 we fix notation, and present the problem to be solved in the chapter. Section 3.3 introduces the concepts of effective delay, partial nestedness (c.f. [8]) and a system's information graph (c.f. [15, 39]) before presenting our main result. Section 3.4 derives the optimal control actions and controller, and Section 3.5 ends with conclusions and directions for future work. Proofs of all intermediary results can be found in Section 3.6.

3.2 Problem Formulation

We begin by describing the general problem of interest, and then specialize the formulation to the particular case to be addressed in this paper.

Notation

For a matrix partitioned into blocks

$$M = \begin{bmatrix} M_{11} & \cdots & M_{1N} \\ \vdots & \ddots & \vdots \\ M_{N1} & \cdots & M_{NN} \end{bmatrix}$$

and $s, v \subset \{1, \ldots, N\}$, we let $M^{s,v} = (M_{ij})_{i \in s, j \in v}$.

For example

$$M^{\{1,2,3\}\{1,2\}} = \begin{bmatrix} M_{11} & M_{12} \\ M_{21} & M_{22} \\ M_{31} & M_{32} \end{bmatrix}.$$

We denote the sequence $x_{t_0}, ..., x_{t_0+t}$ by $x_{t_0:t_0+t}$, and given the history of a random process $r_{0:t}$, we denote the conditional probability of an event $\mathcal{A}$ occurring given this history by $\mathbb{P}_{r_{0:t}}(\mathcal{A})$. If $\mathcal{Y} = \{y^1, \ldots, y^M\}$ is a set of random vectors (possibly of different sizes), we say that $z \in \text{lin}\,(\mathcal{Y})$ if there exist appropriately sized real matrices $C^1, \ldots, C^M$ such that $z = \sum_{i=1}^{M} C^i y^i$.

3.2.1 The two-player problem

This paper focuses on a two plant system with physical propagation delay of D between plants, and varying communication delays $d_t^i \in \{0, \ldots, D\}$ – to ease notation, we let $d_t := (d_t^1, d_t^2)$. We impose some additional assumptions on the stochastic process d_t in Section 3.3 such that the infinite horizon solution is well defined.

The dynamics of the sub-system i are then captured by the following difference

Figure 3.1: The distributed plant considered in (3.6), shown here for $D = 4$. Dummy nodes δ_t^i, $i = 1, \ldots, D-1$, as defined by (3.5), are introduced to make explicit the propagation delay of D between plants.

equation:

$$x_{t+1}^i = A_{ii}x_t^i + A_{ij}x_{t-(D-1)}^j + B_i u_t^i + w_t^i \tag{3.1}$$

with mutually independent Gaussian initial conditions and noise vectors

$$x_0^i \sim \mathcal{N}(\mu_0^i, \Sigma_0^i), \qquad w_t^i \sim \mathcal{N}(0, W_t^i) \tag{3.2}$$

We may describe the information available to controller i at time t, denoted by $\mathcal{I}_t^i$, via the following recursion:

$$\begin{aligned} \mathcal{I}_0^i &= \{x_0^i\} \\ \mathcal{I}_{t+1}^i &= \mathcal{I}_t^i \cup \{x_{t+1}^i\} \cup \{x_k^j \,:\, 1 \le k \le t+1-d_{t+1}^j\} \end{aligned} \tag{3.3}$$

The inputs are then constrained to be of the form

$$u_t^i = \gamma_t^i(\mathcal{I}_t^i) \tag{3.4}$$

for Borel measurable γ_t^i.

In order to build on the results in [15], we model the two plant system as a $D+1$ node graph, with "dummy delay" nodes introduced to explicitly enforce the propagation delay between plants. Specifically, letting

$$\delta_t^i = \begin{bmatrix} x_{t-i}^1 \\ x_{t-(D-i)}^2 \end{bmatrix}, \; i = 1, \ldots, D-1 \tag{3.5}$$

where δ^i is the state of the i^{th} dummy node, we obtain the following state space

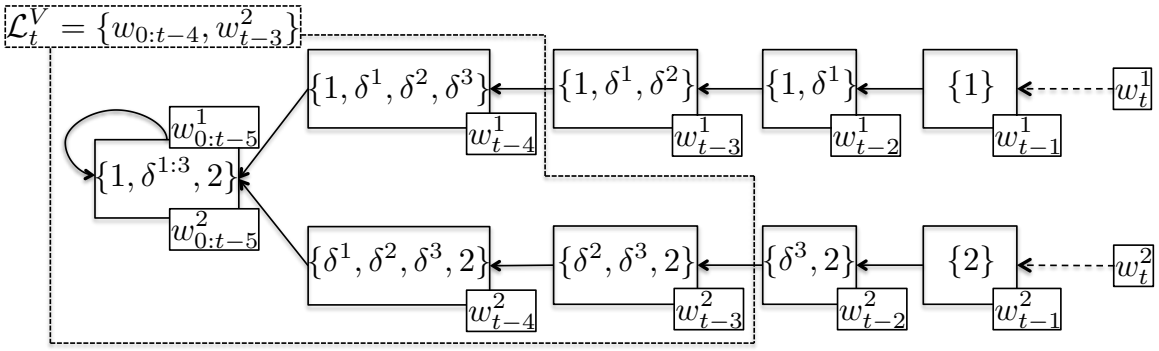

Figure 3.2: The information graph $\mathcal{G} = (\mathcal{V}, \mathcal{E})$, and label sets $\{\mathcal{L}_t^s\}_{s\in\mathcal{V}}$, for system (3.6), shown here for $D = 4$, and $e_t = (3, 2)$. Notice that: (i) for each $(r, s) \in \mathcal{E}$, with $|r| < D+1$, we have that $|s| = |r|+1$, (ii) that $|s|$ corresponds exactly to how delayed the information in the label set is, and (iii) that $\mathcal{L}_t^V$ contains all of the information at nodes s.t. $|s| > e_t^i$, $s \ni i$. We also see that the graph is naturally divided into two branches, with each branch corresponding to information pertaining to a specific plant.

representation for the system

$$x_{t+1} = Ax_t + Bu_t + w_t \tag{3.6}$$

where, to condense notation, we let

$$x = \begin{bmatrix} x^1 \\ \delta^1 \\ \vdots \\ \delta^{D-1} \\ x^2 \end{bmatrix} \quad u = \begin{bmatrix} u^1 \\ 0 \\ \vdots \\ 0 \\ u^2 \end{bmatrix} \quad w = \begin{bmatrix} w^1 \\ 0 \\ \vdots \\ 0 \\ w^2 \end{bmatrix}, \tag{3.7}$$

and A and B are such that (3.6) is consistent with (3.1) and (3.5). The physical topology of the plant is illustrated in Figure 3.1.

Problem 3.1 *Given the linear time invariant (LTI) system described by (3.1), (3.5) and (3.6), with disturbance statistics (3.2), minimize the infinite horizon expected cost*

$$\lim_{N\to\infty} \frac{1}{N} \mathbb{E}\left[\sum_{t=1}^{N} x(t)^T Q x(t) + u(t)^T R u(t)\right] \tag{3.8}$$

subject to the input constraints (3.4).

The weight matrices are assumed to be partitioned into blocks of appropriate dimension, i.e. $Q = (Q_{ij})$ and $R = (R_{ij})$, conforming to the partitions of x and u. We assume Q to be positive semi-definite, and R to be positive definite, and in order to guarantee existence of the stabilizing solution to the corresponding Riccati equation, we assume (A, B) to be stabilizable and $(Q^{\frac{1}{2}}, A)$ to be detectable.

3.3 Main Result

3.3.1 Effective delay

The information constraint sets (3.3) are defined in such a way that controllers do not forget information that they have already received. This leads to the x^j component of the information set $\mathcal{I}_t^i$ being a function of the *effective* delay seen by the controller, as opposed to the current delay value of the communication channel d_t^j.

Definition 3.1 *Let*

$$e_t^j := \min\{d_t^j, d_{t-1}^j + 1, d_{t-2}^j + 2, \ldots, d_{t-(D-2)}^j + (D-2), d_{t-(D-1)}^j + (D-1)\} \quad (3.9)$$

be the effective delay *in transmitting information from controller j to controller i.*

Lemma 3.1 *The information set available to controller i at time t may be written as*

$$\mathcal{I}_t^i = \mathcal{I}_{t-1}^i \cup \{x_t^i\} \cup \mathcal{I}_{t-e_t^j}^j \quad (3.10)$$

Proof: See §3.6. ∎

In order to ensure that the infinite horizon solution is well defined, we assume that

$$\lim_{T\to\infty} \frac{1}{T} \sum_{t=0}^{T-1} \mathbb{P}_{d_{0:t}} \left(e_{t+1}^i \leq d\right) \quad (3.11)$$

exists for any integer d, i.e. we assume that the asymptotic distribution of e^i, conditioned on its history, is stationary and well defined.

3.3.2 Partial Nestedness

Here we show that the information constraints (3.4) and system (3.6) are *partially nested* (c.f. [8]), and hence that the optimal control policies γ_t^i are linear in their information set.

Definition 3.2 *A system (3.6) and information structure (3.4) is partially nested if, for every admissible policy γ, whenever u_τ^i affects $\mathcal{I}_t^j$, then $\mathcal{I}_\tau^i \subset \mathcal{I}_t^j$.*

Lemma 3.2 *(see [8]) Given a partially nested information structure, the optimal control law that minimizes a quadratic cost of the form (3.8) exists, is unique, and is linear.*

Using partial nestedness, the following lemma shows that the optimal state and input lie in the linear span of $\mathcal{I}_t^i$ and $\mathcal{H}_t$, where $\mathcal{H}_t$ is the *noise history* of the system given by

$$\mathcal{H}_t = \{x_0, w_{0:t-1}\} \tag{3.12}$$

Lemma 3.3 *The system (3.6) and information structure (3.4) is partially nested, and for any linear controller, we have that*

$$x_t^i, u_t^i \in \operatorname{lin}\left(\mathcal{I}_t^i\right) \qquad x_t, u_t \in \operatorname{lin}\left(\mathcal{H}_t\right) \tag{3.13}$$

Proof: See §3.6. ∎

3.3.3 Information Graph and Controller Coordinates

Lemma 3.3 indicates that each $\mathcal{I}_t^i$ is a subspace of $\mathcal{H}_t$: in this section, we exploit this observation to define pairwise independent controller coordinates. An explicit characterization of these subspaces is given in Section 3.4.

We begin by defining the *information graph*, as in [15], associated with system (3.6) by $\mathcal{G} = (\mathcal{V}, \mathcal{E})$, with

$$\begin{aligned} \mathcal{V} &:= \left\{\{1\}, \{1, \delta^1\}, \ldots, \left\{1, \delta^1, \ldots, \delta^{D-1}\right\}\right\} \cup \\ &\quad \left\{\{2\}, \left\{\delta^{D-1}, 2\right\}, \ldots, \left\{\delta^1, \ldots, \delta^{D-1}, 2\right\}\right\} \cup V \\ \mathcal{E} &:= \{(r, s) \in \mathcal{V} \times \mathcal{V} : |s| = |r| + 1\} \cup \{(V, V)\} \end{aligned} \tag{3.14}$$

where $V := \left\{1, \delta^1, \ldots, \delta^{D-1}, 2\right\}$. For the case of $D = 4$, the graph $\mathcal{G}$ is illustrated in Figure 3.2.

Before proceeding, we define the following sets, which will help us state the main result. Let

$$\begin{aligned} v_t^{i,+} &:= \{s \in \mathcal{V} \backslash V \,|\, i \in s,\, |s| \geq e_t^i\} \\ v_t^{i,++} &:= \{s \in \mathcal{V} \backslash V \,|\, i \in s,\, |s| > e_t^i\} \end{aligned} \tag{3.15}$$

and similarly define $v_t^{i,-}$ and $v_t^{i,--}$ as in (3.15), but with the (strict) inequality reversed.

Theorem 3.1 *Consider Problem 3.1, and let $\mathcal{G}(\mathcal{V}, \mathcal{E})$ be the associated information graph. Let*

$$\begin{aligned} X^V &= Q + A^\top X^V A + A^\top X^V B K^V \\ K^V &:= -\left(R + B^\top X^V B\right)^{-1} B^\top A, \end{aligned} \tag{3.16}$$

be the stabilizing solution to the discrete algebraic Riccati equation, and the centralized LQR gain, respectively. Now, assume that X^s is given, and let $r \neq s \in \mathcal{V}$ be the unique

node such that $(r,s) \in \mathcal{E}$. *Define the matrices*

$$\begin{aligned}
\Lambda^r &= Q^{rr} + p^r (A^{Vr})^\top X^V A^{Vr} + q^r (A^{sr})^\top X^s A^{sr} \\
\Psi^r &= R^{rr} + p^r (B^{Vr})^\top X^V B^{Vr} + q^r (B^{sr})^\top X^s B^{sr} \\
\Omega^r &= p^r (A^{Vr})^\top X^V B^{Vr} + q^r (A^{sr})^\top X^s B^{sr} \\
X^r &= \Lambda^r + \Omega^r K^r \\
K^r &= -\left(\Psi^r\right)^{-1} \left(\Omega^r\right)^\top
\end{aligned} \tag{3.17}$$

where p^r *is given by*

$$p^r := \lim_{T\to\infty} \frac{1}{T} \sum_{t=0}^{T-1} \mathbb{P}_{d_{0:t}} \left(r \in v_{t+1}^{i,++} \right) \tag{3.18}$$

and $q^r = 1 - p^r$.

The optimal control decisions then satisfy

$$\begin{aligned}
\zeta_{t+1}^V &= A\zeta_t^V + B\varphi_t^V + \\
&\qquad \textstyle\sum_{i=1}^2 \sum_{r \in v_{t+1}^{i,++}} (A^{Vr}\zeta_t^r + B^{Vr}\varphi_t^r) \\
\zeta_{t+1}^s &= \begin{cases} A^{sr}\zeta_t^r + B^{sr}\varphi_t^r \ \textit{if } s \in \cup_i v_{t+1}^{i,-},\ (r,s) \in \mathcal{E} \\ 0 \qquad \textit{otherwise} \end{cases} \\
\zeta_{t+1}^i &= w_t^i \\
\zeta_0^i &= x_0^i \\
u_t^i &= \varphi_t^V + \textstyle\sum_{s \in v_t^{i,-}} I^{V,s} \varphi_t^s \\
\varphi_t^r &= K^r \zeta_t^r
\end{aligned} \tag{3.19}$$

and the corresponding infinite horizon expected cost is

$$\sum_{i=1}^{2} \mathit{Trace}\left(X^{\{i\}} W^i \right) \tag{3.20}$$

Proof: See Section 3.4. ∎

Remark 3.1 *Notice that the global action taken based on* ζ^V *must be taken simultaneously by* both *players. In other words, it is assumed that an acknowledgment*

mechanism is in place such that the e_t is known to both players; relaxing this assumption will be the subject of future work.

Remark 3.2 *The probabilities p^r and q^r can be computed directly if we assume the $\{p_t^{i,d}\}$ to be independently and identically distributed. In this case, e_t^j evolves according to an irreducible and aperiodic Markov chain with transition probability matrix computable directly from the definition of effective delay and the pmf of d_t. As such, p^r and q^r can be computed from the chain's stationary distribution, which is guaranteed to exist. Future work will explore what additional distributions on d_t will lead to closed form expressions for p^r and q^r. Failing the existence of closed form expressions for these asymptotic distributions, computing estimates via simulation should be a feasible option for many interesting pmfs $\{p_t^{i,d}\}$.*

3.4 Controller Derivation

3.4.1 Controller States and Decoupled Dynamics

As mentioned previously, each $\mathcal{I}_t^i$ is a subspace of $\mathcal{H}_t$: in this section, we aim to explicitly characterize these subspaces by assigning label sets $\{\mathcal{L}_{0:t}^s\}_{s\in\mathcal{V}}$ to the graph $\mathcal{G} = (\mathcal{V}, \mathcal{E})$ as defined by (3.14). In particular, they are defined recursively as:

$$\begin{aligned}
\mathcal{L}_0^s &= \emptyset, \text{ for } |s| > 1 \\
\mathcal{L}_0^i &= \{x_0^i\} \\
\mathcal{L}_{t+1}^i &= \{w_t^i\} \\
\mathcal{L}_{t+1}^s &= \mathcal{L}_t^r, \text{ for } (r,s) \in \mathcal{E},\ 1 < |s| < D+1 \\
\mathcal{L}_{t+1}^V &= \mathcal{L}_t^V \cup_i \cup_{s\in v_{t+1}^{i,+}} \mathcal{L}_t^s
\end{aligned} \tag{3.21}$$

where we have let $\cup_i$ denote $\cup_{i=1}^2$ to lighten notational burden. An example of these label sets for the case of $D = 4$ is illustrated in Figure 3.2.

Before delving in to the technical justification for these label sets, we provide some intuition. The information graph $\mathcal{G}$ characterizes how the effect of noise terms spread through the system, and labels are introduced as a means of explicitly tracking this

spreading. As can be seen in Figure 3.2, for each $(r, s) \in \mathcal{E}$, with $|r| < D+1$, we have that $|s| = |r| + 1$, and additionally, that $|s|$ corresponds exactly to how delayed the information in the label set is. We also see that the graph is naturally divided into two *disjoint* branches, with each branch corresponding to information about a specific plant. Finally, the label corresponding to the root node V can be interpreted as the information available to both controllers – this is reflected by its explicit dependence on the effective delay e_t^i.

Remark 3.3 *Note that in contrast to [15], the label sets as defined will in general* not *be disjoint. However, as will be made explicit in Lemma 3.5, an effective delay dependent subset of the label sets will indeed form a partition (i.e. a pairwise disjoint cover) of the noise history.*

We may now characterize the subspaces of $\mathcal{H}_t$ that are associated with each $\mathcal{I}_t^i$. This characterization will be shown to depend on the effective delay e_t^j seen at node i, and will lead to an intuitive partitioning of both the state and the control input.

We begin by pointing out the following useful facts that will be used repeatedly in the derivation to come

Lemma 3.4 *Let $v_t^{i,*}$, $* \in \{-, --\}$, be given as in (3.15). Then, for a fixed i, we have that*

$$\cup_{s \in v_{t+1}^{i,-}} \mathcal{L}_{t+1}^s = \cup_{r \in v_{t+1}^{i,--}} \mathcal{L}_t^r \cup \mathcal{L}_{t+1}^i, \tag{3.22}$$

and for integers $a, b \in \{0, \ldots, D-1\}$

$$\cup_{a<|s|\leq b+1} \mathcal{L}_{t+1}^s = \cup_{a \leq |r| \leq b} \mathcal{L}_t^r \tag{3.23}$$

Proof: Follows immediately by applying the recursion rules (3.21) and the fact that for each $(r, s) \in \mathcal{E}$, with $|r| < D+1$, we have that $|s| = |r| + 1$. ∎

Lemma 3.5 *Consider the information graph $\mathcal{G}$ as defined in equation (3.14), and the label sets defined as in* (3.21)*. We then have that*

1. *For all $t \geq 0$, a subset of the labels form a partition of the noise history. In particular, we have that*

$$\mathcal{H}_t = \mathcal{L}_t^V \cup_i \cup_{s \in v_t^{i,-}} \mathcal{L}_t^s \tag{3.24}$$

where the union is disjoint, i.e. $\mathcal{L}_t^V \cap \mathcal{L}_t^s = \emptyset$ if $s \in v_t^{i,-}$, and $\mathcal{L}_t^s \cap \mathcal{L}_t^{s'} = \emptyset$ for any $s \neq s'$, $s, s' \in \cup_i v_t^{i,-}$.

2. *For $i = 1, 2$*

$$\lin\left(\mathcal{I}_t^i\right) = \lin\left(\mathcal{L}_t^V \cup_{s \in v_t^{i,-}} \mathcal{L}_t^s\right). \tag{3.25}$$

Proof: See §3.6. ∎

Remark 3.4 *Although the proof of this result is notationally cumbersome, it is mainly an exercise in bookkeeping. The idea is illustrated in Figure 3.2: labels for nodes $v \neq V$ track the propagation of a disturbance through the plant, whereas the label for V selects those labels corresponding to globally available information, as dictated by the effective delay.*

With the previous lemmas at our disposal, we may now write

$$\begin{aligned} x_t &= \zeta_t^V + \textstyle\sum_{i=1}^2 \sum_{s \in v_t^{i,-}} I^{V,s} \zeta_t^s \\ u_t &= \varphi_t^V + \textstyle\sum_{i=1}^2 \sum_{s \in v_t^{i,-}} I^{V,s} \varphi_t^s \end{aligned} \tag{3.26}$$

where each ζ_t^s, $\varphi_t^s \in \lin\left(\mathcal{L}_t^s\right)$.

We may accordingly derive update dynamics for these state and control components.

Lemma 3.6 *If the control components are such that $\varphi_s^t \in \lin\left(\mathcal{L}_t^s\right)$, then the state*

components $\{\zeta_t^s\}$ *satisfy the following update dynamics*

$$\begin{aligned}
\zeta_{t+1}^V &= A\zeta_t^V + B\varphi_t^V + \\
&\qquad \textstyle\sum_{i=1}^2 \sum_{r \in v_{t+1}^{i,++}} (A^{Vr}\zeta_t^r + B^{Vr}\varphi_t^r) \\
\zeta_{t+1}^s &= \begin{cases} A^{sr}\zeta_t^r + B^{sr}\varphi_t^r \ \textit{if } s \in \cup_i v_{t+1}^{i,-},\ (r,s) \in \mathcal{E} \\ 0 \quad \textit{otherwise} \end{cases} \\
\zeta_{t+1}^i &= w_t^i \\
\zeta_0^i &= x_0^i
\end{aligned} \tag{3.27}$$

Proof: See §3.6. ∎

In particular, notice that the dynamics (3.27) imply $\zeta_t^s = 0$ for all $s \in \cup_i v_t^{i,++}$, allowing us to rewrite the decomposition for x_t as

$$x_t = \sum_{s \in \mathcal{V}} I^{Vs}\zeta_t^s, \tag{3.28}$$

where have simply added the zero valued state components to the expression in (3.26).

We now have all of the elements required to solve for the optimal control law via dynamic programming.

3.4.2 Finite Horizon Dynamic Programming Solution

Let $\gamma_t = \{\gamma_t^s\}_{s \in \mathcal{V}}$ be the set of policies at time t. By Lemma 3.3, we may assume the γ_t^s to be linear. Define the cost-to-go

$$V_t(\gamma_{0:t-1}) = \min_{\gamma_{t:T-1}} \mathbb{E}^{\gamma \times d} \left(\sum_{k=t}^{T-1} x_k^\top Q x_k + u_k^\top R u_k + x_T^\top Q_T x_T \right) \tag{3.29}$$

where the expectation is taken with respect to the joint probability measure on $(x_{t:T}, u_{t:T-1}) \times (d_{t:T-1})$ induced by the choice of $\gamma = \gamma_{0:T-1}$ (note that the d_t component is assumed to be independent of the policy choice). Via the dynamic programming principle, we may iterate the minimizations and write a recursive formulation for the

cost-to-go:

$$V_t(\gamma_{0:t-1}) = \min_{\gamma_{t:T-1}} \mathbb{E}^{\gamma \times d} \left(x_t^\top Q x_t + u_t^\top R u_t + V_{t+1}(\gamma_{0:t-1}, \gamma_t) \right). \tag{3.30}$$

We begin with the terminal time-step, T, and use the decomposition (3.28) to obtain

$$V_T(\gamma_{0:T-1}) = \mathbb{E}^{\gamma \times d} \left(x_T^\top Q_T x_T \right) = \mathbb{E}^{\gamma} \sum_{s \in \mathcal{V}} (\zeta_T^s)^\top Q_T^{ss}(\zeta_T^s), \tag{3.31}$$

where in the last step we have used the pairwise independence of the coordinates ζ_T^s. By induction, we shall show that the value function, for some $t \geq 0$, always takes the form

$$V_{t+1}(\gamma_{0:t}) = \mathbb{E}^{\gamma} \sum_{s \in \mathcal{V}} ((\zeta_{t+1}^s)^\top X_{t+1}^s (\zeta_{t+1}^s) + c_{t+1} \tag{3.32}$$

where $\{X_{t+1}^s\}_{s \in \mathcal{V}}$ is a set of matrices and c_{t+1} is a scalar. We now solve for $V_t(\gamma_{0:t-1})$ via the recursion (3.30). Given e_t, apply (3.28) and the independence result to write

$$V_t(\gamma_{0:t-1}) = \min_{\gamma_t} \mathbb{E}^{\gamma \times d} \left(\sum_{s \in \mathcal{V}} (\zeta_t^s)^\top Q^{ss}(\zeta_t^s) + (\varphi_t^s)^\top R^{ss}(\varphi_t^s) + \sum_{s \in \mathcal{V}} (\zeta_{t+1}^s)^\top X_{t+1}^s (\zeta_{t+1}^s) + c_{t+1} \right) \tag{3.33}$$

We now substitute the update equations (3.27), average over d_{t+1} and use independence to obtain

$$V_t(\gamma_{0:t-1}) = \min_{\gamma_t} \mathbb{E}^{\gamma} \left(\sum_{r \in \mathcal{V}} \begin{bmatrix} \zeta_t^r \\ \varphi_t^r \end{bmatrix}^\top \Gamma_t^r \begin{bmatrix} \zeta_t^r \\ \varphi_t^r \end{bmatrix} + c_t \right) \tag{3.34}$$

where $\Gamma_{0:T-1}^r$ and $c_{0:T-1}$ are given by:

$$\Gamma_t^r = \begin{bmatrix} Q^{rr} & 0 \\ 0 & R^{rr} \end{bmatrix} + \mathbb{P}_{d_{0:t}}(r \in v_{t+1}^{i,++}) \begin{bmatrix} A^{Vr} & B^{Vr} \end{bmatrix}^\top X_{t+1}^V \begin{bmatrix} A^{Vr} & B^{Vr} \end{bmatrix} + \mathbb{P}_{d_{0:t}}(r \in v_{t+1}^{i,-}) \begin{bmatrix} A^{sr} & B^{sr} \end{bmatrix}^\top X_{t+1}^s \begin{bmatrix} A^{sr} & B^{sr} \end{bmatrix} \tag{3.35}$$

$$c_t = c_{t+1} + \sum_{i=1}^{2} \text{Trace}\left(X_{t+1}^{\{i\}} W^i\right). \tag{3.36}$$

The terminal conditions are $c_T = 0$ and $\Gamma^r = Q_T^{rr}$, and s is the unique node such that $(r,s) \in \mathcal{E}$.

Let $p_t^r := \mathbb{P}_{d_{0:t}}(r \in v_{t+1}^{i,++})$ and $q_t^r := \mathbb{P}_{d_{0:t}}(r \in v_{t+1}^{i,-})$, and introduce the following matrices:

$$\begin{aligned}
\Lambda_{t+1}^r &= Q^{rr} + p_t^r (A^{Vr})^\top X_{t+1}^V A^{Vr} + q_t^r (A^{sr})^\top X_{t+1}^s A^{sr} \\
\Psi_{t+1}^r &= R^{rr} + p_t^r (B^{Vr})^\top X_{t+1}^V B^{Vr} + q_t^r (B^{sr})^\top X_{t+1}^s B^{sr} \\
\Omega_{t+1}^r &= p_t^r (A^{Vr})^\top X_{t+1}^V B^{Vr} + q_t^r (A^{sr})^\top X_{t+1}^s B^{sr}
\end{aligned} \tag{3.37}$$

Then each expression of the sum in (3.34) can be written as

$$(\zeta_t^r)^\top \Lambda_{t+1}^r (\zeta_t^r) + (\varphi_t^r)^\top \Psi_{t+1}^r (\varphi_t^r) + 2(\zeta_t^r)^\top \Omega_{t+1}^r (\varphi_t^r). \tag{3.38}$$

Due to the definitions of ζ and φ, it is clear that the terms (3.38) are pairwise independent and hence can be optimized independently. Removing the information constraints, and optimizing over φ_t^r, we see that the optimal action is given by

$$\varphi_t^r = -\left(\Psi_{t+1}^r\right)^{-1} \left(\Omega_{t+1}^r\right)^\top \zeta_t^r \tag{3.39}$$

which, by construction, satisfies the information constraints $\mathcal{I}_t^i$. Substituting this solution back in to (3.38), we see that the matrices X_t^r must satisfy

$$\begin{aligned}
X_t^r &= \Lambda_{t+1}^r + \Omega_{t+1}^r K_t^r \\
K_t^r &:= -\left(\Psi_{t+1}^r\right)^{-1} \left(\Omega_{t+1}^r\right)^\top
\end{aligned} \tag{3.40}$$

The finite horizon optimal cost is then given by

$$\begin{aligned}
V_0 &= \mathbb{E} \textstyle\sum_{i=1}^2 (x_0^i)^\top X^{\{i\}} (x_0^i) + c_0 \\
&= \mathbb{E} \textstyle\sum_{i=1}^2 (\mu_0^i)^\top X_0^{\{i\}} (\mu_0^i) + \text{Trace}\left(X_0^{\{i\}} \Sigma_0^i\right) + c_0
\end{aligned} \tag{3.41}$$

where c_0 can be computed according to (3.36) beginning with terminal conditions $c_T = 0$.

3.4.3 Infinite Horizon Solution

In order to determine the infinite horizon solution, we first notice that for $r = V$, $p_t^V = 1$, $q_t^V = 0$ and that the recursions (3.40) for $r = V$ are then simply given by

$$\begin{aligned} X_t^V &= Q + A^\top X_{t+1}^V A + A^\top X_{t+1}^V B K_t^V \\ K_t^V &:= \left(R + B^\top X_{t+1}^V B\right)^{-1} B^\top A, \end{aligned} \tag{3.42}$$

that is to say the standard discrete algebraic Riccati recursion/gain. By assumption, we have that $(X_t^V, K_t^V) \to (X^V, K^V)$, where X^V and K_V are, respectively, the stabilizing solution the discrete algebraic riccati equation, and the centralized LQR gain.

Now assume that X_t^s is defined, and let $r \neq s \in \mathcal{V}$ be the unique node such that $(r, s) \in \mathcal{E}$. Much as in the finite horizon case, define the following matrices:

$$\begin{aligned} \Lambda^r &= Q^{rr} + p^r (A^{Vr})^\top X^V A^{Vr} + q^r (A^{sr})^\top X^s A^{sr} \\ \Psi^r &= R^{rr} + p^r (B^{Vr})^\top X^V B^{Vr} + q^r (B^{sr})^\top X^s B^{sr} \\ \Omega^r &= p^r (A^{Vr})^\top X^V B^{Vr} + q^r (A^{sr})^\top X^s B^{sr} \end{aligned} \tag{3.43}$$

where we have let

$$(p^r, q^r) = \lim_{T\to\infty} \tfrac{1}{T} \textstyle\sum_{t=0}^{T-1} (p_t^r, q_t^r). \tag{3.44}$$

Note that these limits are well defined by the assumption (3.11).

We then have that

$$\begin{aligned} X^r &= \Lambda^r + \Omega^r K^r \\ K^r &:= -\left(\Psi^r\right)^{-1} \left(\Omega^r\right)^\top. \end{aligned} \tag{3.45}$$

What remains to be computed is the infinite horizon average cost, which is given by (ignoring without loss the cost incurred by the uncertainty in the initial conditions)

$$\lim_{N\to\infty} \frac{1}{N} \sum_{t=1}^{N} \sum_{i=1}^{2} \text{Trace}\left(X_t^{\{i\}} W^i\right) = \sum_{i=1}^{2} \text{Trace}\left(X^{\{i\}} W^i\right) \tag{3.46}$$

3.5 Conclusion

This chapter presented extensions of a Riccati-based solution to a distributed control problem with communication delays – in particular, we now allow the communication delays to vary, but impose that they preserve partial nestedness. It was seen that the varying delay pattern induces piecewise linear dynamics in the state of the resulting optimal controller, with changes in dynamics dictated by the current *effective* delay regime.

Future work will be to extend the results to systems with several players with more general delay patterns, and to remove the assumption of strong connectedness, much as was done in [15] for the case of constant delays. We will also seek to identify conditions on the delay process d_t such that assumption (3.11) holds. Additionally, we will explore the setting in which the global delay regime is not known. Finally, we are also currently exploring a principled integration of these results with recent deadline based coding techniques developed in [65].

3.6 Proofs of Intermediate Lemmas

Proof of Lemma 3.1: The first two terms of (3.10) follow directly from (3.3). The x^j component of $\mathcal{I}_t^i$ is then given by

$$\cup_{\tau=0}^{t} \{x_k^j \,:\, 0 \le k \le \tau - d_\tau^j\} = \cup_{\tau=0}^{t} \{x_k^j \,:\, 0 \le k \le t - (d_\tau^j + (t-\tau))\} =$$
$$\{x_k^j \,:\, 0 \le k \le t - \min_{\tau=0,\dots,t} (d_\tau^j + (t-\tau))\} = \{x_k^j \,:\, 0 \le k \le t - e_t^j\} \quad (3.47)$$

where the last equality follows from $d_t^j \le D \;\forall t \ge 0$ and the definition of e_t^j. Noting that this is precisely the local information available to plant j at time $t - e_t^j$, and that the x^i component of $\mathcal{I}_{t-e_t^j}^j$ is contained in $\mathcal{I}_{t-1}^i \cup \{x_t^i\}$, the claim follows. ∎

Proof of Lemma 3.3: Note that $\mathcal{I}_t^i \subset \mathcal{I}_{t+1}^i$, and that $\mathcal{I}_t^i \subset \mathcal{I}_{t+D}^j$:

$$\begin{aligned}\mathcal{I}_t^i = \{x_{1:t}^i\} \cup \{x^j \,:\, 1 \leq k \leq t - e_t^j\} \subset \{x_{1:t}^i\} \cup \{x^j \,:\, 1 \leq k \leq t + D\} \subset \\ \{x_k^i \,:\, 1 \leq k \leq t + D - e_{t+D}^i\} \cup \{x_{1:t+D}^j\} = \mathcal{I}_{t+D-1}^j \cup \{x_{t+D}^j\} \cup \mathcal{I}_{t+D-e_{t+D}^i}^i = \mathcal{I}_{t+D}^j\end{aligned} \tag{3.48}$$

where the final inclusion follows from $e_\tau^i \leq D$ for all $\tau \geq 0$, and the final equalities from Lemma 3.1. Partial nestedness then follows from the fact that u_τ^i only affects $\mathcal{I}_t^j$ for $t \geq \tau + D$ due to the propagation delay between plants. By Lemma 3.2, u_t^i is a linear function of $\mathcal{I}_t^i$ and the same is trivially true for $x_t^i \in \mathcal{I}_t^i$. We prove the final claim of the lemma by induction.

We first note that that $x_0, u_0 \in \text{lin}\,(x_0) = \text{lin}\,(\mathcal{H}_0)$. We now proceed by induction, and assume that for some $t \geq 0$ we have that $x_t, u_t \in \text{lin}\,(\mathcal{H}_t)$. We then have that

$$\begin{aligned} x_{t+1} &\in \text{lin}\,(\mathcal{H}_t \cup \{w_t\}) = \text{lin}\,(\mathcal{H}_{t+1}) \\ u_{t+1} &\in \text{lin}\left(\mathcal{I}_{t+1}^1 \cup \mathcal{I}_{t+1}^2\right) = \text{lin}\,(\{x_{t+1}\} \cup \mathcal{H}_t) = \text{lin}\,(\mathcal{H}_{t+1}) \end{aligned} \tag{3.49}$$

■

Proof of Lemma 3.5: (i) We begin by showing that the union in the RHS of (3.24) is disjoint. This easily verified to hold for $t = 0$, as all labels are the empty set except for $\mathcal{L}_0^i = x_0^i$. We now proceed by induction, and suppose that the union in (3.24) is a disjoint one for some $t \geq 0$. We then have that

$$\mathcal{L}_{t+1}^V \cup_i \cup_{s \in v_{t+1}^{i,-}} \mathcal{L}_{t+1}^s = \mathcal{L}_t^V \cup_i \cup_{s \in v_{t+1}^{i,+}} \mathcal{L}_t^s \cup_{s \in v_{t+1}^{i,--}} \mathcal{L}_t^s \cup \mathcal{L}_{t+1}^i \tag{3.50}$$

where the equality follows from simply applying the recursion rules (3.21) and Lemma 3.4. We first note that by the induction hypothesis, $\mathcal{L}_t^V \cap \cup_i \cup_{s \in v_{t+1}^{i,--}} \mathcal{L}_t^s = \emptyset$. Additionally, by construction, we have that $\cup_i \cup_{s \in v_{t+1}^{i,+}} \mathcal{L}_t^s \cap \cup_i \cup_{s \in v_{t+1}^{i,--}} \mathcal{L}_t^s = \emptyset$. We note that $\mathcal{L}_{t+1}^i = w_t^i$ is the new information available at time $t+1$, and thus $\mathcal{L}_{t+1}^i \cap \mathcal{L}_t^s = \emptyset$ for all $s \in \mathcal{V}$. Finally, noting that for all $\mathcal{L}_{t+1}^1 \cap \mathcal{L}_{t+1}^2 = \emptyset$, we have that (3.50) is a disjoint union, proving the claim.

It now suffices to show that (3.24) is also a covering of the noise history. To that end, notice that for $t = 0$, this follows immediately from $\mathcal{L}_0^i = \{x_0^i\}$, and $\mathcal{H}_0 = \{x_0\}$. Now suppose that (3.24) is a covering for some $t \geq 0$. We then have that

$$\begin{aligned}\mathcal{H}_{t+1} = \mathcal{H}_t \cup_i \mathcal{L}_{t+1}^i = \mathcal{L}_t^V \cup_i \cup_{s \in v_t^{i,-}} \mathcal{L}_t^s \cup \mathcal{L}_{t+1}^i = \mathcal{L}_t^V \cup_i \cup_{s \ni i,\, |s| \leq e_t^i + 1} \mathcal{L}_{t+1}^s \\ = \mathcal{L}_t^V \cup_i \cup_{s \in v_{t+1}^{i,-}} \mathcal{L}_{t+1}^s \cup_{s' \ni i,\, e_{t+1}^i < |s'| \leq e_t^i + 1} \mathcal{L}_{t+1}^{s'} = \mathcal{L}_{t+1}^V \cup_i \cup_{s \in v_{t+1}^{i,-}} \mathcal{L}_{t+1}^s. \quad (3.51)\end{aligned}$$

The third equality follows from applying the induction hypothesis, the fourth by applying the recursion rules for the label sets, and the before last equality noticing that $e_{t+1}^i \leq e_t^i + 1$. To prove the final equality, it suffices to show that $\mathcal{L}_t^V \cup_i \cup_{s' \ni i,\, e_{t+1}^i < |s'| \leq e_t^i + 1} \mathcal{L}_{t+1}^{s'} = \mathcal{L}_{t+1}^V$. This follows by applying the recursion rules and Lemma 3.4 as follows:

$$\begin{aligned}\mathcal{L}_t^V \cup_i \cup_{s' \ni i,\, e_{t+1}^i < |s'| \leq e_t^i + 1} \mathcal{L}_{t+1}^{s'} = \mathcal{L}_t^V \cup_i \cup_{s' \ni i} \cup_{e_{t+1}^i \leq |s'| \leq e_t^i} \mathcal{L}_t^{s'} \cup_{|s'| \geq e_t^i} \mathcal{L}_{t-1}^{s'} \\ = \mathcal{L}_t^V \cup_i \cup_{s' \ni i} \cup_{e_{t+1}^i \leq |s'| \leq e_t^i} \mathcal{L}_t^{s'} \cup_{|s'| \geq e_t^i + 1} \mathcal{L}_t^{s'} = \mathcal{L}_t^V \cup_i \cup_{s \in v_{t+1}^{i,+}} \mathcal{L}_t^s = \mathcal{L}_{t+1}^V \quad (3.52)\end{aligned}$$

(ii) We proceed by induction once again. This holds trivially for $t = 0$. Now suppose it to be true for some $t \geq 0$. We have that $\mathcal{I}_{t+1}^i = \mathcal{I}_t^i \cup \mathcal{I}_{t-(e_{t+1}^j - 1)}^j \cup \{x_{t+1}^i\}$. Taking the linear span of both sides, we then obtain

$$\begin{aligned}\operatorname{lin}\left(\mathcal{I}_{t+1}^i\right) = \operatorname{lin}\left(\mathcal{I}_t^i\right) + \operatorname{lin}\left(\mathcal{I}_{t-(e_{t+1}^j - 1)}^j\right) + \operatorname{lin}\left(w_t^i\right) \\ = \operatorname{lin}\left(\mathcal{L}_t^V\right) + \sum_{s \in v_t^{i,-}} \operatorname{lin}\left(\mathcal{L}_t^s\right) + \sum_{r \in v_{t+1}^{j,--}} \operatorname{lin}\left(\mathcal{L}_{t-(e_{t+1}^j - 1)}^r\right) + \operatorname{lin}\left(\mathcal{L}_{t+1}^i\right) \quad (3.53)\end{aligned}$$

By the same arguments used in the second part of the proof of part (i), we have that $\operatorname{lin}\left(\sum_{s \in v_t^{i,++}} \mathcal{L}_t^s\right) \subset \operatorname{lin}\left(\mathcal{L}_t^V\right)$. Also notice that applying the recursion for $\mathcal{L}_{t+1}^s$ to the $\mathcal{L}_{t-(e_{t+1}^j - 1)}^r$ term $e_{t+1}^j - 1$ times, and that for $r \to \cdots \to s'$, we have that

$|s'| = |r| + e^j_{t+1} - 1 \geq e^j_{t+1}$. We may then write (3.53) as

$$\begin{aligned}
&\lin\left(\mathcal{L}^V_t\right) + \sum_{s\ni i} \lin\left(\mathcal{L}^s_t\right) + \sum_{s'\in v^{j,+}_{t+1}} \lin\left(\mathcal{L}^{s'}_t\right) \\
&\qquad = \lin\left(\mathcal{L}^V_t\right) + \sum_{k=1}^{2} \sum_{s\in v^{k,+}_{t+1}} \lin\left(\mathcal{L}^s_t\right) + \sum_{s\in v^{i,--}_{t+1}} \lin\left(\mathcal{L}^s_t\right) + \lin\left(\mathcal{L}^i_{t+1}\right). \quad (3.54)
\end{aligned}$$

The first two terms of the final equality are precisely the expression for $\lin\left(\mathcal{L}^V_{t+1}\right)$, whereas the final two terms may be combined by applying the recursion rules to the summation, yielding $\sum_{s\in v^{i,-}_{t+1}} \lin\left(\mathcal{L}^s_{t+1}\right)$. We therefore have that (3.54) is equal to

$$\lin\left(\mathcal{L}^V_{t+1}\right) + \sum_{s\in v^{i,-}_{t+1}} \lin\left(\mathcal{L}^s_{t+1}\right) = \lin\left(\mathcal{L}^V_{t+1} \cup_{s\in v^{i,-}_{t+1}} \mathcal{L}^s_{t+1}\right) \quad (3.55)$$

proving the claim. ∎

Proof of Lemma 3.6: The recursive nature of the label sets ensure that $\zeta^s \in \lin\left(\mathcal{L}^s_t\right)$ for all $t \geq 0$. Thus it suffices to show that these dynamics preserve the state decomposition (3.26).

$$\begin{aligned}
&\zeta^V_{t+1} + \sum_{i=1}^{2} \sum_{s\in v^{i,-}_{t+1}} I^{V,s}\zeta^s_{t+1} \\
&= A\zeta^V_t + B\varphi^V_t + \sum_{i=1}^{2} \sum_{r\in v^{i,++}_{t+1}} \left(A^{Vr}\zeta^r_t + B^{Vr}\varphi^r_t\right) + \sum_{i=1}^{2} \sum_{s\in v^{i,-}_{t+1}} I^{V,s}\left(A^{sr}\zeta^r_t + B^{sr}\varphi^r_t\right) + w_t \\
&\qquad = A\left(\zeta^V_t + \sum_{s\in\mathcal{V}} I^{V,s}\zeta^s_t\right) + B\left(\varphi^V_t + \sum_{s\in\mathcal{V}} I^{V,s}\varphi^s_t\right) + w_t \\
&\qquad = A\left(\zeta^V_t + \sum_{i=1}^{2} \sum_{s\in v^{i,-}_t} I^{V,s}\zeta^s_t\right) + B\left(\varphi^V_t + \sum_{i=1}^{2} \sum_{s\in v^{i,-}_t} I^{V,s}\varphi^s_t\right) + w_t \\
&\qquad\qquad = Ax_t + Bu_t + w_t = x_{t+1} \quad (3.56)
\end{aligned}$$

where the first equality followed from applying the update dynamics (3.27), and the third from noting that certain components of the state and control decomposition are

zero due to the effective delays seen by the controllers. The fourth equality follows from equation (3.26), and the final one from (3.6). ∎

Chapter 4

Regularization for Design

4.1 Introduction

As argued in the previous chapters of this thesis, the move to large-scale systems such as the smart-grid, software defined networking and automated highways, makes the design of control systems much more challenging. Thus far we have focused on settings for which the *controller architecture*, that is to say the sensors, actuators and communication links between them, is taken as a given. However, as we now argue, in large-scale distributed settings, *designing* the controller architecture is now as important as the traditional design of the control laws themselves.

A conceptually useful viewpoint in the design of controller architectures is to consider complicated systems as being composed of multiple simpler *atomic* subsystems. For example, if the task is to design the actuation architecture of a controller, a natural atomic element is a controller with a single actuator – it is then clear that a general architecture can be built out of such atoms. In general, controllers with a dense actuation, sensing and communication architecture (i.e., systems that consist of many atomic subsystems) achieve better closed loop performance in comparison with those with sparse architectures (i.e., systems composed of a small number of atomic subsystems). However, as these architectural resources translate into actual hardware requirements, it is desirable from both a maintenance and a cost perspective that we minimize the total number of atomic elements used. Hence, the problem of controller architecture/control law co-design is one of jointly optimizing an appropriately de-

fined structural measure of the controller and its closed loop performance by trading off between these two competing metrics in a principled manner. In other words, we seek an approximation of a given optimal controller by one that utilizes fewer atomic elements without a significant loss in performance. This goal has parallels with the approximation theory literature in which one seeks approximations of complicated functions as combinations of elements from a simpler class of functions such as the Fourier basis or a wavelet basis [66].

In an appropriate parameterization, pure controller synthesis methods in a model matching framework can be interpreted as techniques for solving a particular linear inverse problem in which one is given an open loop response of a system Y and a linear map $\mathfrak{L}$ from the controller to the closed loop response, and one seeks a controller U such that $Y - \mathfrak{L}(U) \approx 0$ (as measured in a suitable performance metric). From this perspective, our objective in joint controller architecture/control law co-design is to obtain *structured* solutions to the linear inverse problem underlying controller synthesis. Such *structured linear inverse problems* (SLIP) are of interest in diverse applications across applied mathematics – for instance, computing sparse solutions to linear inverse problems or computing low-rank solutions to systems of linear matrix equations arise prominently in many contexts in signal processing and in statistics [67–70].

In these problem domains, minimizing the ℓ_1 norm subject to constraints described by the specified equations is useful for obtaining sparse solutions [67,68], and similarly, nuclear norm minimization is useful for obtaining low-rank solutions to linear matrix equations [69, 70]. These ideas were extended in [20], where the authors describe a generic convex programming approach – based on minimizing an appropriate *atomic norm* [66]– for inducing a desired type of structure in solutions to linear inverse problems. Motivated by these developments, our approach to the problem of joint architecture/control law co-design is to augment variational formulations of controller synthesis methods with suitable convex regularization functions. The role of these regularizers is to penalize controllers with more complex architectures in favor of those with less complex ones, thus inducing controllers with a simpler architecture. We call

this framework *Regularization for Design* (RFD).

Related work: Regularization techniques based on ℓ_1 norms and, more generally, atomic norms have already been employed extensively in system identification, e.g., to identify systems of small Hankel order (cf. [24, 71, 72]), and in linear regression based methods [73]. Although the resulting solutions yield structured systems, they typically do not have a direct interpretation in terms of the architecture of a control system (i.e., actuators, sensors and the communication links between them). The use of regularization explicitly for the purpose of designing the architecture of a controller can also be found in the literature. Examples include the use of ℓ_1 regularization to design sparse structures in $\mathcal{H}_2$ static state feedback gains [27], treatment therapies [74], and synchronization topologies [75]; the use of group norm penalties to design actuation/sensing schemes [21,76]; and the use of an atomic norm to design communication delay constraints that are well-suited to $\mathcal{H}_2$ distributed optimal control [23, 56]. Although these methods provide an algorithmic approach for designing controller architectures in certain specialized settings, they do not enjoy the same theoretical support that regularization techniques for structured inverse problems enjoy in other settings [66–70].

Chapter contributions: This chapter is based on [21, 22] and presents novel computational and theoretical contributions to the area of optimal controller architecture/control law co-design. From a computational perspective, we propose a general RFD framework that is applicable in a much broader range of settings than the previous approaches mentioned above. We restrict ourselves to problems for which the linear optimal structured controller is specified as the solution to a convex optimization problem [9, 10, 77]. As a result, RFD optimization problems with convex regularization functions for inducing a desired architecture are convex programs. Specifically, (i) we provide a catalog of atomic norms useful for control architecture design. In particular, in addition to known penalties for actuator, sensor and communication design, we provide novel penalties for *simultaneous* actuator, sensor and/or communication design; (ii) we describe a unifying framework for RFD that encompasses state and output feedback problems in centralized and distributed settings,

and in which any subset of actuation, sensing, and/or communication architectures are co-designed; and (iii) we present a two-step algorithm that first identifies the controller architecture via a finite-dimensional convex RFD optimization problem, and then solves for the potentially infinite dimensional linear optimal controller restricted to the designed architecture using methods from classical and distributed optimal control [2, 12–17].

To provide theoretical support for our computational framework, we make explicit links between RFD optimization problems and the use of convex optimization based approaches for structured inference problems. We build on these links to analyze the properties of the structured controllers generated by RFD synthesis methods, which leads to conditions under which RFD methods successfully identify optimally-structured controllers. Our analysis and results are natural control-theoretic analogs of similar results in the structured inference literature. Specifically, (i) we show that finite-horizon finite-order convex approximations of an RFD optimization problem can recover the structure of an underlying infinite dimensional optimal controller; (ii) we define control-theoretic analogs of identifiability conditions and signal-to-noise ratios (SNRs), and we provide sufficient conditions based on these for a controller architecture to be identified by RFD. In particular, we show that controllers that maximize this SNR-like quantity are more easily recovered via RFD than those that do not, and (iii) we provide a concrete example of a system satisfying the above identifiability and SNR conditions. As far as we are aware, this is the first example in the literature of a system for which convex optimization provably recovers the actuation architecture of an underlying optimally structured controller.

Chapter organization: In §4.2, we define notation and discuss the relevant concepts from operator theory. This chapter is then organized in a modular fashion: §4.3-4.5 focus on the computational aspects of controller architecture design, whereas §4.6 and §4.8 focus on conditions for optimal architecture recovery. Specifically, in §4.3, we introduce the RFD framework as a natural blend of controller synthesis methods and regularization techniques. In §4.4, we focus on RFD problems with an $\mathcal{H}_2$ performance metric and an atomic norm penalty; we present a catalog of atomic

norms that are useful for controller architecture design, and make connections to the structured inference literature. The computational component of the chapter concludes in §4.5, in which we formally describe the two-step RFD procedure, and we apply the RFD framework to a simultaneous actuator, sensor and communication design problem. In §4.6, we shift our focus to analyzing the theoretical properties of the RFD procedure: we make connections between structured controller design and structured inference problems by framing both tasks as finding structured solutions to linear inverse problems, and we leverage these connections to describe sufficient conditions for the success of a finite-dimensional RFD optimization problem. In §4.8, we provide a case study to further illustrate the applicability of these results.

4.2 Preliminaries & Notation

We use standard definitions of the Hardy spaces $\mathcal{H}_2$ and $\mathcal{H}_\infty$. We denote the restrictions of $\mathcal{H}_2$ and $\mathcal{H}_\infty$ to the space of real rational proper transfer matrices $\mathcal{R}_p$ by $\mathcal{RH}_2$ and $\mathcal{RH}_\infty$. As we work in discrete time, the two spaces are equal, and as a matter of convention we refer to this space as $\mathcal{RH}_\infty$. We refer the reader to [2] for a review of this material. Let $\mathcal{RH}_\infty^{\leq t}$ denote the subspace of $\mathcal{RH}_\infty$ composed of finite impulse response (FIR) transfer matrices of length t, i.e., $\mathcal{RH}_\infty^{\leq t} := \{G \in \mathcal{RH}_\infty \,|\, G = \sum_{i=0}^{t} \frac{1}{z^i} G^{(i)}\}$. We denote the projection of an element $G \in \mathcal{R}_p$ onto the subspace $\mathcal{RH}_\infty^{\leq t}$ by $G^{\leq t}$. Unless required, we do not explicitly denote dimensions and we assume that all vectors, operators and spaces are of compatible dimension throughout. We denote elements of $\mathcal{R}_p$ with upper case Latin letters, and temporal indices and horizons by lower case Latin letters. Linear maps from $\mathcal{R}_p$ to $\mathcal{R}_p$ are denoted by upper case Fraktur letters such as $\mathfrak{L}$. For such a linear map, we denote the i^{th} impulse response element of $\mathfrak{L}$ by $\mathfrak{L}^{(i)}$. We further use $\mathfrak{L}^{\leq t}$ to denote the restriction of the range of $\mathfrak{L}$ to $\mathcal{RH}_\infty^{\leq t}$, and $\mathfrak{L}^{\leq t,v}$ to denote the restriction of $\mathfrak{L}^{\leq t}$ to the domain $\mathcal{RH}_\infty^{\leq v}$. Thus $\mathfrak{L}^{\leq t,v}$ is a map from $\mathcal{RH}_\infty^{\leq v}$ to $\mathcal{RH}_\infty^{\leq t}$. In particular, if $\mathfrak{L}$ is represented as a semi-infinite lower block triangular matrix, then $\mathfrak{L}^{\leq t,v}$ corresponds to the t by v block row by block column sub matrix $(\mathfrak{L})_{ij}$, $i = 1, \ldots, t$, $j = 1, \ldots, v$. Sets are denoted by upper case script

letters, such as $\mathscr{S}$, whereas subspaces of an inner product space are denoted by upper case calligraphic letters, such as $\mathcal{S}$. The restriction of a linear map $\mathfrak{L}$ to a subspace $\mathcal{S} \in \mathcal{RH}_\infty$ is denoted by $\mathfrak{L}_{\mathcal{S}}$; similarly, the projection of an operator $G \in \mathcal{R}_p$ onto a subspace $\mathcal{A} \subset \mathcal{R}_p$ is denoted by $G_{\mathcal{A}}$. We denote the adjoint of a linear map $\mathfrak{L}$ by $\mathfrak{L}^\dagger$. The most complicated expression that we use is of the form $\left[\mathfrak{L}_{\mathcal{S}}^{\leq t,v}\right]^\dagger$: this denotes the adjoint of the map $\mathfrak{L}^{\leq t}$ restricted to $\mathcal{RH}_\infty^{\leq v} \cap \mathcal{S}$. We denote the n-dimensional identity matrix and down-shift matrices by I_n and Z_n, respectively. In particular, Z_n is a matrix with all ones along its first sub-diagonal and zero elsewhere. We use e_i to denote a standard basis element in $\mathbb{R}^n$, and E_{ij} to denote the matrix with $(i,j)^{\text{th}}$ element set to 1 and all others set to 0.

4.3 RFD as Structured Approximation

Under standard assumptions [2], traditional controller synthesis methods within the framework of *model matching* can be framed as linear inverse problems of the form

$$\underset{U \in \mathcal{RH}_\infty}{\text{minimize}} \quad \Psi\left(U; Y, \mathfrak{L}\right) \tag{4.1}$$

where Y is the open loop response of the system, U is the Youla parameter, $\mathfrak{L}$ is a suitably defined linear map from the Youla parameter U to the closed loop response, and $\Psi\left(\cdot; Y, \mathfrak{L}\right)$ is a performance metric that measures the size of the closed loop response (i.e., the size of the deviation between Y and $\mathfrak{L}(U)$), such as the $\mathcal{H}_2$ or $\mathcal{H}_\infty$ norm. We make this connection clear in the following subsection and we also recall how to incorporate *quadratically invariant* [9] distributed constraints on the controller into this framework.

Remark 4.1 *We use this non-standard notation to facilitate comparisons with the structured inference literature. This notation emphasizes that the optimal linear controller synthesis task can be viewed as one of solving a linear inverse problem with "data" specified by the open loop response Y and the map $\mathfrak{L}$ from the Youla parameter to the closed loop response.*

4.3.1 Convex Model Matching

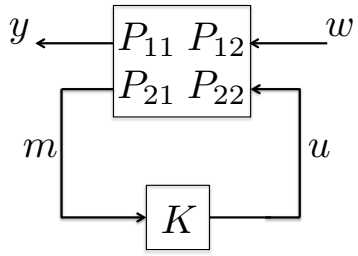

Figure 4.1: A diagram of the generalized plant defined in (4.2).

In order to discuss a broad range of model matching problems, we introduce the *generalized plant*, a standard tool in robust and optimal control [2]. In particular, consider the system described by

$$P = \begin{bmatrix} P_{11} & P_{12} \\ P_{21} & P_{22} \end{bmatrix} = \left[\begin{array}{c|cc} A & B_1 & B_2 \\ \hline C_1 & 0 & D_{12} \\ C_2 & D_{21} & 0 \end{array}\right] \tag{4.2}$$

where $P_{ij} = C_i(zI - A)^{-1}B_j + D_{ij}$. As illustrated in Figure 4.1, this system describes the four transfer matrices from the disturbance and control inputs w and u, respectively, to the controlled and measured outputs y and m, respectively. We make the standard orthogonality assumptions that

$$D_{12}\begin{bmatrix} C_1^\top & D_{12}^\top \end{bmatrix} = \begin{bmatrix} 0 & \rho_u I \end{bmatrix}, \; D_{21}^\top \begin{bmatrix} B_1 & D_{21} \end{bmatrix} = \begin{bmatrix} 0 & \rho_w I \end{bmatrix} \tag{4.3}$$

for some $\rho_u, \rho_w \geq 0$. At times we separate the state component of the open and closed loop responses from the components of these transfer matrices that measure control effort. To that end, we define the *state component* of an element X to be the projection of X onto the range of C_1.

Letting $u(z) = K(z)m(z)$ for a causal linear controller $K \in \mathcal{R}_p$, the closed loop map from the disturbance w to the controlled output y is given by the linear fractional transform $P_{11} - P_{12}K(I - P_{22}K)^{-1}P_{21}$. When the open-loop plant is stable (we remark on the unstable case at the end of the subsection), a typical optimal control problem

in this framework is then formulated as

$$\begin{aligned} \underset{K \in \mathcal{R}_p}{\text{minimize}} \quad & \|P_{11} - P_{12}K(I - P_{22}K)^{-1}P_{21}\| \\ \text{s.t.} \quad & K(I - P_{22}K)^{-1} \in \mathcal{RH}_\infty \end{aligned} \tag{4.4}$$

where $\|\cdot\|$ is a suitable norm, and the constraint ensures internal stability of the closed loop system [2]. Notice however that the optimal control problem (4.4) is non-convex as stated.

A standard and general approach to solving the optimal control problem (4.4) is to convert it into a *model matching problem* through the *Youla* change of variables $U := K(I - P_{22}K)^{-1}$; the optimal controller K can then be recovered via $K = (I + UP_{22})^{-1}U$. The resulting convex optimization problem is then given by

$$\underset{U \in \mathcal{RH}_\infty}{\text{minimize}} \quad \|P_{11} - P_{12}UP_{21}\|, \tag{4.5}$$

which is of the form of the linear inverse problem (4.1) if we take $Y := P_{11}$, $\mathfrak{L} = P_{12} \otimes P_{21}$ (where $(P_{12} \otimes P_{21})(U) := P_{12}UP_{21}$) and $\Psi(U; Y, \mathfrak{L}) := \|Y - \mathfrak{L}(U)\|$.

We also often want to impose a *distributed constraint* on the controller K by requiring K to lie in some subspace $\mathcal{S}$, which specifies information exchange constraints between the sensors and actuators of the controller. It is known that a necessary and sufficient condition for such a distributed constraint to be invariant under the Youla change of variables is that it be *quadratically invariant* with respect to P_{22} [9, 10, 77].

Definition 4.1 *A subspace $\mathcal{S}$ is* quadratically invariant *(QI) with respect to P_{22} if $KP_{22}K \in \mathcal{S}$ $\forall K \in \mathcal{S}$.*

In particular, when a subspace $\mathcal{S}$ is QI with respect to P_{22}, we have that $K \in \mathcal{S}$ if and only if $K(I - P_{22}K)^{-1} \in \mathcal{S}$, allowing us to convert the general optimal control problem (4.1) with the additional constraint that $K \in \mathcal{S}$ to the following convex optimization problem

$$\underset{U \in \mathcal{RH}_\infty}{\text{minimize}} \quad \Psi(U; Y, \mathfrak{L}) \text{ s.t. } U \in \mathcal{S}. \tag{4.6}$$

This optimization problem is again precisely of the form of the linear inverse problem (4.1) save for the addition of the subspace constraint $U \in \mathcal{S}$. This framework is fairly general in that it allows for a unified treatment of all structured optimal control problems in which the linear optimal structured controller can be computed via convex optimization [9, 77]. These include state and output feedback problems in either centralized or QI distributed settings. Further, if the optimal control problem is centralized with respect to the $\mathcal{H}_2$, $\mathcal{H}_\infty$ or $\mathcal{L}_1$ metrics, or is QI distributed with a finite horizon $\mathcal{H}_2$ cost, the linear optimal control is globally optimal [2, 8, 77, 78].

Remark 4.2 (Unstable Plants) *The above discussion extends to unstable plants through the use of an appropriate* structure preserving *Youla-Kucera parameterization built around* arbitrary coprime factorizations*, which are always available. See [4, 16, 79] for examples of such parameterizations, and [23] for an example of using such a parameterization with a structure inducing penalty. Note that although the structured synthesis task for unstable plants is addressed by these previous results, finding a structured realization for the resulting optimal controller may still be challenging [80].*

4.3.2 Architecture Design through Structured Solutions

We seek a modification of the optimal controller synthesis procedure to design the controller's architecture. We reiterate that by the architecture of a controller, we mean the actuators, sensors, and communication links between them. In particular, we view the controller K as a map from all potential sensors to all potential actuators, using all potential communication links between these actuators and sensors. The architectural design task is that of selecting which actuators, sensors and communication links need to be used to achieve a certain performance level. This task is naturally viewed as one of finding a structured approximation of the optimal controller (4.4) that utilizes all of the available architectural choices.

The components of the controller architecture being designed determine the type of structured approximation that we attempt to identify. In particular, each nonzero

row of $K(z)$ corresponds to an actuator used by the controller, and likewise, each nonzero column corresponds to a sensor employed by the controller. Further sparsity patterns present within rows/columns of the power series elements $K^{(t)}$ of $K(z)$ can be interpreted as information exchange constraints imposed by an underlying communication network between the sensors and actuators. It is thus clear that specific sparsity patterns in K have direct interpretations in terms of the architectural components of the controller: nonzero rows correspond to actuators, nonzero columns correspond to sensors, and additional sparsity structure corresponds to communication constraints.

Although we seek seek to identify a suitably structured controller K, for the computational reasons described in §4.3.1 it is preferable to solve a problem in terms of the Youla parameter U as this parameterization leads to the convex optimization problem (4.6). Therefore, in the following definition RFD problems are defined as a regularized version of the model matching problem (4.6) with a penalty function added to the objective to induce suitable structure, rather than as a modification of the controller synthesis problem (4.4). In the sequel, we justify that for architectural design problems of interest, the structure underlying the controller K is equivalent to the structure underlying the Youla parameter U; to that end, we show that in the case of actuator, sensor, and/or QI communication topology design, the structure of the Youla parameter U corresponds to the structure of the controller K.

Definition 4.2 *Let $U, Y \in \mathcal{RH}_\infty$, and $\mathfrak{L} : \mathcal{RH}_\infty \to \mathcal{RH}_\infty$ be of compatible dimension. The optimization*

$$\underset{U \in \mathcal{RH}_\infty}{\text{minimize}} \quad \Psi\left(U; Y, \mathfrak{L}\right) + 2\lambda\Omega\left(U\right) \;\; s.t. \; U \in \mathcal{S} \tag{4.7}$$

is called a RFD optimization problem *with cost function $\Psi\left(\cdot; Y, \mathfrak{L}\right)$ and penalty $\Omega\left(\cdot\right)$.*

Remark 4.3 *With the exception of the centralized state-feedback setting, it is known that the optimal linear controller is dynamic [2], and therefore restricting our analysis to dynamic controllers is natural. In the centralized setting (given the equivalence*

between static and dynamic state-feedback), once an actuation architecture is identified, traditional methods can then be used to solve for a static state-feedback controller restricted to that architecture. Further as we show in §4.6, the dynamic controller synthesis approach is amenable to analysis that guarantees optimal structure recovery.

We discuss natural costs $\Psi(\cdot; Y, \mathfrak{L})$ and penalties $\Omega(\cdot)$ in §4.4, and we focus now on justifying why we can perform the structural design on the Youla parameter U rather than the controller K.

Actuator/Sensor Design Recall that the actuators (sensors) that a controller K uses are identified by the nonzero rows (columns) of K: the actuator (sensor) design problem therefore corresponds to finding a controller K that achieves a good closed loop response and that is sparse row-wise (column-wise). This corresponds exactly to finding a row (column) sparse solution U to the RFD optimization problem (4.7). This is true because any subspace $\mathcal{D}$ that is defined solely in terms of row (column) sparsity is QI with respect to any P_{22}. In particular, it is easily verified that if $K \in \mathcal{D}$, then right (left) multiplication leaves $\mathcal{D}$ invariant, i.e., $KX \in \mathcal{D}$ ($XK \in \mathcal{D}$) for all compatible X. It then follows from Definition 4.1 that $\mathcal{D}$ is QI with respect to any plant P_{22}. We can extend this analysis to incorporate additional QI distributed constraints $\mathcal{S}$ by leveraging the results in [10]: in particular, if $\mathcal{S}$ is QI with respect to P_{22}, then so is $\mathcal{D} \cap \mathcal{S}$.[1]

Joint Actuator and Sensor Design By virtue of the previous discussion joint actuator and sensor design corresponds to finding a controller K that is simultaneously sparse row-wise and column-wise. It follows immediately from the previous discussion that this corresponds exactly to finding a simultaneously row and column sparse solution U to the RFD optimization problem (4.7). In particular, any subspace $\mathcal{D}$ defined solely in terms of row and column sparsity is QI with respect to any plant P_{22},

[1] In particular, since removing actuators does not change the communication delays between the remaining actuators and sensors, if the delay based conditions in [10] hold when all actuators (sensors) are present they also hold with any subset of them being present.

we can incorporate additional QI distributed constraints $\mathcal{S}$ by leveraging the results in [10].

Communication Design In an analogous manner to the above, one can also associate subspaces to structures corresponding to suitable information exchange constraints that a distributed controller must satisfy.[2] Recall in particular that the information exchange constraints between the sensors and actuators of a controller K are identified by the sparsity structure found within the nonzero rows and columns of K. In [23], the first author showed that a specific type of sparsity structure in K corresponds exactly to sensors and actuators exchanging information according to an underlying communication graph. In particular, given a communication graph between sensors and actuators with adjacency matrix Γ, a distributed controller K can be implemented using the graph defined by Γ if the power series elements $K^{(t)}$ of the controller satisfy $\operatorname{supp}\left(K^{(t)}\right) \subseteq \operatorname{supp}\left(\Gamma^{t-1}\right)$.[3] The interpretation of the support nesting condition is that the delay from sensor j to actuator i is given by the length of the shortest path from node j to node i in the graph defined by Γ. This support nesting condition thus defines the distributed subspace constraint $\mathcal{S}$ in which K must lie – based on the discussion in §4.3.1, one can pose the distributed controller synthesis problem as a distributed model matching problem (4.6) if and only if $\mathcal{S}$ is QI with respect to P_{22}. In light of this, we consider the communication design task proposed in [23]: given an initial graph with adjacency matrix Γ_{QI} that induces a QI distributed subspace constraint $\mathcal{S}$, what minimal set of additional edges should be added to the graph to achieve a desired performance level.[4] It is additionally shown in [23] that any communication graph constructed in this manner results in a subspace constraint $\mathcal{S}$ that is QI with respect to P_{22}. Therefore the structure imposed on the controller K by an underlying QI communication graph corresponds exactly to the structure

[2] We restrict ourselves to communications delays that satisfy the triangle inequality defined in [10]. This assumption implies that information exchanged between sensors and actuators is transmitted along shortest delay paths in the underlying communication graph.

[3] We assume that K is square for simplicity; cf. [23] for the general case.

[4] It is shown in [23] that under mild assumptions on the plant P_{22}, the propagation delays of P_{22} can be used to define an adjacency matrix Γ_{QI} that induces a distributed subspace constraint that is QI with respect to P_{22}.

imposed on the Youla parameter U.

Joint Communication, Actuator and/or Sensor Design By virtue of the previous discussion and the results of [10], combining QI communication design with actuator and/or sensor design still leads to the underlying structure of the controller K corresponding to the underlying structure of the Youla parameter U.

Thus for architecture design problems the RFD task can be performed via a model matching problem.

Example 4.1 *Suppose that different RFD optimization problems are solved for a system with three possible actuators and three possible sensors, resulting in the various sparsity patterns in $U(z)$ shown on the far right of Figure 4.2. It is easily seen by inspection that the resulting sparsity patterns are QI. In particular Figures 4.2a) through 4.2c) correspond to centralized RFD optimization problems (this can be seen from the full matrices in the center of the left hand side), and 2d) to a RFD optimization problem subject to lower triangular constraints, a special case of a nested information constraint.*[5]

$$
\begin{array}{ll}
\text{a)} & \begin{bmatrix} 0 & 0 & 0 \\ * & * & * \\ * & * & * \end{bmatrix} \begin{bmatrix} * & * & * \\ * & * & * \\ * & * & * \end{bmatrix} \begin{bmatrix} 0 & 0 & 0 \\ * & * & * \\ * & * & * \end{bmatrix} \subseteq \begin{bmatrix} 0 & 0 & 0 \\ * & * & * \\ * & * & * \end{bmatrix} \\
\text{b)} & \begin{bmatrix} 0 & * & * \\ 0 & * & * \\ 0 & * & * \end{bmatrix} \begin{bmatrix} * & * & * \\ * & * & * \\ * & * & * \end{bmatrix} \begin{bmatrix} 0 & * & * \\ 0 & * & * \\ 0 & * & * \end{bmatrix} \subseteq \begin{bmatrix} 0 & * & * \\ 0 & * & * \\ 0 & * & * \end{bmatrix} \\
\text{c)} & \begin{bmatrix} 0 & 0 & 0 \\ 0 & * & * \\ 0 & * & * \end{bmatrix} \begin{bmatrix} * & * & * \\ * & * & * \\ * & * & * \end{bmatrix} \begin{bmatrix} 0 & 0 & 0 \\ 0 & * & * \\ 0 & * & * \end{bmatrix} \subseteq \begin{bmatrix} 0 & 0 & 0 \\ 0 & * & * \\ 0 & * & * \end{bmatrix} \\
\text{d)} & \begin{bmatrix} * & 0 & 0 \\ 0 & 0 & 0 \\ * & * & * \end{bmatrix} \begin{bmatrix} * & 0 & 0 \\ * & * & 0 \\ * & * & * \end{bmatrix} \begin{bmatrix} * & 0 & 0 \\ 0 & 0 & 0 \\ * & * & * \end{bmatrix} \subseteq \begin{bmatrix} * & 0 & 0 \\ 0 & 0 & 0 \\ * & * & * \end{bmatrix}
\end{array}
$$

Figure 4.2: Examples of QI sparsity patterns generated via a) actuator, b) sensor, and c) actuator/sensor RFD procedures without any distributed constraints, and d) actuator RFD subject to nested information constraints.

[5]Nested information constraints are a well studied class of QI distributed constraints, cf. [12–14] for examples.

4.4 RFD Cost Functions and Regularizers

In this section we examine convex formulations of the RFD optimization problem (4.7) by restricting our attention to convex cost functions $\Psi(\cdot; Y, \mathfrak{L})$ and convex penalty functions $\Omega(\cdot)$.

4.4.1 Convex Cost Functions

Any suitable convex cost function $\Psi(\cdot; Y, \mathfrak{L})$ can be used in (4.7): traditional examples from robust and optimal control include the $\mathcal{H}_2$, $\mathcal{H}_\infty$ [2] and $\mathcal{L}_1$ norms [78]. We focus on the $\mathcal{H}_2$ norm as a performance metric because it allows us to make direct connections between the RFD optimization problem (4.7) and well-established methods employed in structured inference such as ordinary least squares, Ridge Regression [81], Group Lasso [82] and Group Elastic Net [83].

We begin by introducing a specialized form of the model matching problem (4.6), and show how state-feedback problems with $\mathcal{H}_2$ performance metrics can be put into this form.

Definition 4.3 *Let $U, Y \in \mathcal{RH}_\infty$, and $\mathfrak{L} : \mathcal{RH}_\infty \to \mathcal{RH}_\infty$ be of compatible dimension. The optimization problem*

$$\underset{U \in \mathcal{RH}_\infty}{\text{minimize}} \quad \|Y - \mathfrak{L}(U)\|_{\mathcal{H}_2}^2 + \rho_u \|U\|_{\mathcal{H}_2}^2 \ s.t.\ U \in \mathcal{S} \tag{4.8}$$

is the $\mathcal{H}_2$ optimal control problem *for a suitable control penalty weight ρ_u and a distributed constraint $\mathcal{S}$.*

In this definition, Y is the state component of the open loop response, and $\mathfrak{L}$ is the map from the Youla parameter to state component of the closed loop response. Explicitly separating the cost of the state component $\|Y - \mathfrak{L}(U)\|_{\mathcal{H}_2}^2$ of the closed loop response from the control cost $\rho_u \|U\|_{\mathcal{H}_2}^2$ allows us to connect the $\mathcal{H}_2$ RFD optimization to several well-established methods in the inference literature. Before elaborating on some of these connections, we provide two examples of standard control problems that can be put into this form.

Example 4.2 (Basic LQR) *Consider the basic LQR problem given by*

$$\begin{aligned} \underset{u\in\ell_2}{\text{minimize}} \quad & \textstyle\sum_{t=0}^{\infty} \|Cx_t\|_{\ell_2}^2 + \|Du_t\|_{\ell_2}^2 \\ s.t. \quad & x_{t+1} = Ax_t + Bu_t,\ x_0 = \xi, \end{aligned} \tag{4.9}$$

and assume that $D^\top D = \rho_u I$*, for some* $\rho_u \geq 0$*. Define* $\rho = \rho_u$*,* $X^{(t)} = CA^t\xi$ *for* $t \geq 0$*,* $U^{(t)} = u_t$*, and* $\mathfrak{L}(U) = -H * U$*, where* $H \in \mathcal{R}_p$ *with* $H^{(0)} = 0$*, and* $H^{(t)} = CA^{t-1}B$ *for* $t \geq 1$*. We can then rewrite the basic LQR problem in the form of optimization problem* (4.8) *(with no distributed constraint* $\mathcal{S}$*).*

Example 4.3 ($\mathcal{H}_2$ State Feedback) *Assume either that the generalized plant* (4.2) *is open-loop stable or that the control problem is over a finite horizon. Let* $C_2 = I$ *and* $D_{21} = 0$ *in the generalized plant* (4.2) *such that the problem is one of synthesizing an optimal state-feedback controller, and for clarity of exposition, assume that* B_1 *is invertible.*[6] *Define the Youla parameterization for the controller synthesis problem* (4.4) *as follows [2]:*

$$\tilde{P}_{12} = \tfrac{1}{z}P_{12},\ \tilde{P}_{21} = AP_{21} + B_1,\ \tilde{U} = K(I - P_{22}K)^{-1}\tilde{P}_{21},$$

with all other parameters remaining the same. Under this parameterization, the optimal control problem (4.4) *(with additional QI distributed constraint* $\mathcal{S}$*) with performance metric* $\|\cdot\|_{\mathcal{H}_2}^2$ *can be written as*

$$\underset{\tilde{U}\in\mathcal{RH}_\infty}{\text{minimize}} \|P_{11} - \tilde{P}_{12}\tilde{U}\|_{\mathcal{H}_2}^2 + \rho_u\|\tilde{U}\|_{\mathcal{H}_2}^2 \ s.t.\ \tilde{U}\tilde{P}_{21}^{-1} \in \mathcal{S}, \tag{4.10}$$

The optimal controller K *is then recovered from the solution to* (4.10) *as* $K = (I + \tilde{U}\tilde{P}_{21}^{-1}P_{22})^{-1}\tilde{U}\tilde{P}_{21}^{-1}$*. The state-feedback assumption and the choice of Youla parameterization ensure that* $\tilde{P}_{21}$ *is invertible in* $\mathcal{RH}_\infty$ *and that* $K \in \mathcal{S}$*.*

Remark 4.4 *A dual argument applies to* $\mathcal{H}_2$ *filter design by considering the "full-*

[6]The assumption that B_1 is invertible simply implies that no component of the state is deterministic, and can be relaxed at the expense of more complicated formulas.

control" setting, cf. [2] for more details.

As illustrated by Example 4.3, the $\mathcal{H}_2$ optimal control problem (4.8) is simply a more general way of writing the $\mathcal{H}_2$ state feedback model matching problem – in Remark 4.7 we show how $\mathcal{H}_2$ output feedback model matching problems can also be put in a similar form. Writing the $\mathcal{H}_2$ problem as a linear inverse problem with a least squares like state cost and an explicitly separated control cost already allows us to make connections to classical techniques from structured inference. These connections (along with others we make later in this section) are summarized in Table 4.1. In order to keep the discussion as streamlined as possible, we make these connections in the context of the Basic LQR problem presented in Example 4.2.

4.4.1.1 $\rho_u = 0$

In an inferential context, this is simply ordinary least squares, and is commonly used when U_* is not known *a priori* to have any structure. Further, the resulting estimate of U_* is unbiased, but often suffers from high error variance. Moving now to a control context, It is easy to see that this setting corresponds to "cheap control" LQR, in which there is no cost on u_t – under suitable controllability and observability assumptions, the resulting state trajectory is deadbeat, but the optimal control law is not necessarily unique.

4.4.1.2 $\rho_u > 0$

This corresponds to Ridge Regression or Tikhonov Regularization [81]. In an inferential context, this regularizer has the effect of *shrinking* estimates towards 0 – this introduces bias into the estimator, but reduces its variance, and is often a favorable tradeoff from a statistical perspective. From a linear algebraic perspective, this is a commonly used technique to improve the numerical conditioning of an inverse problem. Once again, the interpretation in RFD is clear: this corresponds to standard LQR control with $R = \rho I$; the parameter ρ allows for a tradeoff between control effort

and state deviation. The optimal control action is then unique and the resulting state trajectory is generally not deadbeat.

4.4.2 The $\mathcal{H}_2$ RFD Problem with an Atomic Norm Penalty

Recall that our strategy for designing controller architectures is to augment the traditional model matching problem (4.6) with a structure inducing penalty, resulting in the RFD optimization problem (4.7). In light of the previous subsection, we further specialize the RFD optimization problem to have an $\mathcal{H}_2$ performance metric and an atomic norm penalty $\|\cdot\|_{\mathscr{A}}$.

Definition 4.4 *Let $U, Y \in \mathcal{RH}_\infty$ and $\mathfrak{L} : \mathcal{RH}_\infty \to \mathcal{RH}_\infty$ be of compatible dimension. The optimization problem*

$$\underset{U \in \mathcal{RH}_\infty}{\text{minimize}} \|Y - \mathfrak{L}(U)\|_{\mathcal{H}_2}^2 + \rho \|U\|_{\mathcal{H}_2}^2 + 2\lambda \|U\|_{\mathscr{A}} \;\; s.t.\; U \in \mathcal{S} \tag{4.11}$$

is called the $\mathcal{H}_2$ RFD optimization problem *with parameters (ρ, λ), distributed constraint $\mathcal{S}$, and atomic norm penalty $\|\cdot\|_{\mathscr{A}}$.*

There are two components of note in this definition. The first is that ρ need not be equal to ρ_u, the control cost parameter of the original non-penalized control problem (4.8); the reasons why a different choice of ρ may be desirable are explained in §4.6. The second is the use of an atomic norm penalty function to induce structure. Indeed, if one seeks a solution U_* that can be composed as a linear combination of a small number of "atoms" $\mathscr{A}$, then a useful approach, as described in [20, 67–70], to induce such structure in the solution of an inverse problem is to employ a convex penalty function that is given by the atomic norm induced by the atoms $\mathscr{A}$ [66]. Examples of the types of structured solutions one may desire in linear inverse problems include sparse, group sparse and signed vectors, and low-rank, permutation and orthogonal matrices (cf. [20]).

Specifically, if one assumes that

$$U = \sum_{i=1}^{r} c_i A_i, \;\; A_i \in \mathscr{A}, \;\; c_i \geq 0 \tag{4.12}$$

for a set of appropriately scaled and centered atoms $\mathscr{A}$, and a small number r relative to the ambient dimension, then solving

$$\underset{U}{\text{minimize}} \quad \Psi\left(U; Y, \mathfrak{L}\right) + 2\lambda \|U\|_{\mathscr{A}} \tag{4.13}$$

with the atomic norm $\|\cdot\|_{\mathscr{A}}$ given by the gauge function[7]

$$\begin{array}{rcl} ||U||_{\mathscr{A}} : & = & \inf\{t \geq 0 \,\big|\, U \in t\text{conv}(\mathscr{A})\} \\ & = & \inf\{\sum_{A\in\mathscr{A}} c_A \,\big|\, U = \sum_{A\in\mathscr{A}} c_A A, \; c_A \geq 0\} \end{array} \tag{4.14}$$

results in solutions that are both consistent with the data as measured in terms of the cost function $\Psi\left(\cdot; Y, \mathfrak{L}\right)$, and that are sparse in terms of their atomic descriptions, i.e., are a combination of a small number of elements from $\mathscr{A}$.

Our discussion in §4.3.2 on designing controller architecture by finding structured solutions to the model matching problem (4.6) suggests natural atomic sets for constructing suitable penalty functions for RFD. We make this point precise by showing that actuator, sensor, and/or communication delay design can all be performed through the use of a purposefully constructed atomic norm. We introduce several novel penalty functions for controller architecture design, most notably for the simultaneous design of actuator, sensor and communication delays. Further, all regularizers that have been considered for control architecture design in the literature (cf. [21, 23, 27, 56, 74–76], among others) may be viewed as special instances of the atomic norms described below.

In what follows, the atomic sets that we define are of the form

$$\mathscr{A} = \bigcup_{\mathcal{A}\in\mathscr{M}} \mathcal{A} \cap k_{\mathcal{A}} \mathcal{B}_{\mathcal{H}_2}, \tag{4.15}$$

[7] If no such t exists, then $\|X\|_{\mathscr{A}} = \infty$.

for $\mathscr{M}$ an appropriate set of subspaces, $\{k_{\mathcal{A}}\}$ a set of normalization constants indexed by the subspaces $\mathcal{A} \in \mathscr{M}$, and $\mathcal{B}_{\mathcal{H}_2}$ the $\mathcal{H}_2$ unit norm ball; see the concrete examples below. Note that we normalize our atoms relative to the $\mathcal{H}_2$ norm as this norm is isotropic; hence this normalization ensures that no atom is preferred over another within a given family of atoms $\mathscr{A}$. We use n_s and n_a to denote the total number of sensors and actuators, respectively, available for the RFD task.

4.4.2.1 Actuator/Sensor Norm

For the *Actuator Norm*, we choose the atomic set to be transfer functions in $\mathcal{RH}_\infty^{n_a \times n_s}$ that have exactly one nonzero row with unit $\mathcal{H}_2$ norm, i.e., suitably normalized Youla parameters that use only one actuator. Specifically, the set of subspaces (4.15) in this context is

$$\mathscr{M}_{\text{act}} := \left\{ \mathcal{A} \subset \mathcal{RH}_\infty^{n_a \times n_s} \,\middle|\, \mathcal{A} \text{ has one nonzero row} \right\}, \tag{4.16}$$

leading to the atomic set

$$\mathscr{A}_{\text{act}} := \left\{ e_i V \,\middle|\, V \in \mathcal{RH}_\infty^{1 \times n_s},\, \|V\|_{\mathcal{H}_2} = 1 \right\}. \tag{4.17}$$

The resulting atomic norm is then given by

$$\|U\|_{\text{act}} = \sum_{i=1}^{n_a} \|e_i^\top U\|_{\mathcal{H}_2}. \tag{4.18}$$

In particular, each "group" corresponds to a row of the Youla parameter. For the *Sensor Norm*, we similarly choose transfer functions with exactly one nonzero column with unit $\mathcal{H}_2$ norm, leading to the atomic norm

$$\|U\|_{\text{sns}} = \sum_{i=1}^{n_s} \|U e_i\|_{\mathcal{H}_2}. \tag{4.19}$$

Both of these norms are akin to a Group Lasso penalty [82].

4.4.2.2 Joint Actuator and Sensor Norm

Conceptually, each atom corresponds to a controller that uses only a small subset of actuators and sensors. As each row of the Youla parameter U corresponds to an actuator and each column to a sensor, the atomic transfer matrices have support defined by a submatrix of $U(z)$. Specifically, we choose atoms with at most k_a actuators and k_s sensors:

$$\begin{aligned}\mathscr{M}_{\text{act+sns}} := \big\{\mathcal{A} \subset \mathcal{RH}_\infty^{n_s \times n_a} \,\big|\, &\operatorname{supp}(\mathcal{A}) \text{ is a submatrix} \\ &\text{with at most } k_a \text{ nonzero rows and } k_s \text{ nonzero columns}\big\}\end{aligned} \tag{4.20}$$

The scaling terms $k_{\mathcal{A}}$ in the definition of the atomic set (4.15) are given by $k_{\mathcal{A}} = (\operatorname{card}(\mathcal{A}) + .1)^{-\frac{1}{2}}$, and are necessary as some of the atoms are nested within others – the additional .1 can be any positive constant, and controls how much an atom of larger cardinality is preferred over several atoms of lower cardinality. The resulting *Actuator+Sensor Norm* is then constructed according to (4.15) and is akin to the latent Group Lasso [84].

4.4.2.3 Communication Link Norm

As described in §4.3.2, the communication design task is to select which additional links to introduce into an existing base communication graph. An atom in $\mathscr{A}_{\text{comm}}$ corresponds to such an additional link. We provide an example of such an atomic set for a simple system, and refer the reader to Chapter 5 and [23] for a more general construction. In particular, consider a three player chain system, with physical

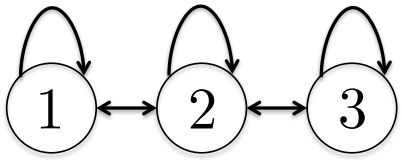

Figure 4.3: Three player chain system

topology illustrated in Figure 4.3, such that P_{22} lies in the subspace

$$\mathcal{S} := \frac{1}{z}\begin{bmatrix} * & 0 & 0 \\ 0 & * & 0 \\ 0 & 0 & * \end{bmatrix} \oplus \frac{1}{z^2}\begin{bmatrix} * & * & 0 \\ * & * & * \\ 0 & * & * \end{bmatrix} \oplus \frac{1}{z^3}\mathcal{R}_p,$$

where $*$ is used to denote $\mathbb{R}$ to reduce notational clutter. We consider an existing communication graph matching the physical topology illustrated in Figure 4.3 so that the induced distributed subspace constraint, as described in §4.3.2, is given precisely by $\mathcal{S}$. It can be checked that $\mathcal{S}$ is then QI with respect to P_{22}. We consider choosing from two additional links to augment the communication graph: a directed link from node 1 to node 3, and a directed link from node 3 to node 1. Then $\mathscr{M}_{\text{comm}} = \{\mathcal{A}_{13}, \mathcal{A}_{31}\}$, where its component subspaces are given by

$$\mathcal{A}_{13} = \tfrac{1}{z^2}\begin{bmatrix} 0 & 0 & 0 \\ 0 & 0 & 0 \\ * & 0 & 0 \end{bmatrix}, \mathcal{A}_{31} = \tfrac{1}{z^2}\begin{bmatrix} 0 & 0 & * \\ 0 & 0 & 0 \\ 0 & 0 & 0 \end{bmatrix}.$$

In particular, each subspace $\mathcal{A}_{ij}$ corresponds to the additional information available to the controller *uniquely* due to the added link from sensor j to actuator i. The resulting *Communication Link Norm* $\|\cdot\|_{\text{comm}}$ is then constructed according to (4.15) with all normalization constants $k_{\mathcal{A}} = 1$. We note that this penalty is also akin to the latent Group Lasso [84].

4.4.2.4 Joint Actuator (and/or Sensor) and Communication Link Norm

This penalty can be viewed as simultaneously inducing sparsity at the communication link level, while further inducing row sparsity as well. The general strategy is to combine the actuator and communication link penalties in a convex manner. We suggest two such approaches, one based on taking their weighted sums and the other based on taking their "weighted maximum." In particular, we define the joint actuator

plus communication link penalty to be:

$$\|U\|_{\text{act+comm}} = (1-\theta)\,\|U\|_{\text{comm}} + \theta\,\|U\|_{\text{act}}\,, \tag{4.21}$$

for some $\theta \in [0,1]$, and the *max* actuator/communication link penalty to be

$$\|U\|_{\max\{\text{act,comm}\}} = \max\left\{(1-\theta)\,\|U\|_{\text{comm}}\,, \theta\,\|U\|_{\text{act}}\right\}, \tag{4.22}$$

for some $\theta \in [0,1]$. The analogous Sensor and Communication Link penalties, as well as Sensor+Actuator and Communication link penalties can be derived by replacing $\mathscr{A}_{\text{act}}$ with either $\mathscr{A}_{\text{sns}}$ or $\mathscr{A}_{\text{act+sns}}$.

4.4.3 Further Connections with Structured Inference

As already noted in §4.4.1, by choosing different values of ρ for $\lambda = 0$ we are able to recover control-theoretic analogs to Ordinary Least Squares and Ridge Regression [81]. Noting that the actuator norm penalty (4.18) is akin to the Group Lasso [82], we now discuss how control theoretic analogs of the Group Lasso and Group Elastic Net [83] can be obtained by setting $\lambda > 0$ in (4.11) and using the Actuator Norm (4.18) penalty – these connections are summarized in Table 4.1. To simplify the discussion, we once again consider these connections in the context of the basic LQR problem introduced in Example 4.2, now augmented with the actuator norm penalty (4.18).

In structured inference problems, the setting $\lambda > 0$, $\rho > 0$ corresponds to Group Elastic-Net regression. If the groups are single elements, this becomes the traditional Elastic Net and Lasso. The singleton group setting with $\lambda > 0$, $\rho = 0$ corresponds to Lasso regression, and this inference method is employed when the underlying model is known to be sparse – in particular, the Lasso penalty is used to select which elements U_i^* of the model are non-zero [67, 68]. Continuing with the singleton group setting, if both $\lambda > 0$ and $\rho > 0$, then the corresponding inferential approach is called the Elastic Net. In addition to the sparsity-inducing properties of the Lasso, the Elastic Net also encourages automatic clustering of the elements [83] – in particular, $\rho > 0$

Parameters	Inference Method	Inference Structure	Inference Tradeoff	RFD Method	RFD Structure	RFD Tradeoff
$\lambda = 0$, $\rho = 0$	Ordinary Least Squares	None	N/A	Cheap Control LQR	Deadbeat response	N/A
$\lambda = 0$, $\rho > 0$	Ridge Regression	Small Euclidean norm	Bias, Variance	LQR	Small control action	State deviation, Control effort
$\lambda > 0$, $\rho = 0$	Group LASSO	Group sparsity	Bias, Variance, Model complexity	RFD LQR	Sparse actuation	State deviation, Control effort, Actuation complexity
$\lambda > 0$, $\rho > 0$	Group Elastic Net	Correlated group sparsity	Bias, Variance, Model complexity	RFD LQR	Correlated sparse actuation	State deviation, Control effort, Actuation complexity

Table 4.1: A dictionary relating various SLIP methods in structured inference and Actuator RFD problems.

encourages the simultaneous selection of highly correlated elements (two elements U_i^* and U_j^* are said to be highly correlated if $\mathfrak{L}(U_i^*) \approx \mathfrak{L}(U_j^*)$). Thus ρ can be seen as a parameter that can be adjusted to leverage a prior of *correlation* in the underlying measurement operator $\mathfrak{L}$. These interpretations carry over to more general groups in a natural way.

In RFD, this setting corresponds to our motivating Example 4.2 augmented with the actuator norm penalty, in which we design the controller's actuation architecture. As each atom corresponds to an actuator, this RFD procedure then selects a small number of actuators. Porting the clustering effect interpretation from the structured inference setting, we see that ρ promotes the selection of actuators that have similar effects on the closed loop response. In particular, this suggests that for systems in which no such similarities are expected, ρ should be chosen to be small (or 0) during the RFD process, even if the original LQR problem had non-zero control cost.

4.5 The RFD Procedure

4.5.1 The Two-Step Algorithm

We now introduce the convex optimization based RFD procedure for the co-design of an optimal controller and the architecture on which it is implemented. The remaining computational challenge is the possibly infinite dimensional nature of the RFD optimization problem (4.7). To address this issue, we propose a two step procedure: first, a finite dimensional approximation of optimization problem (4.7) is solved to identify a potential controller architecture and its defining subspace constraint $\mathcal{D}$. Once this architecture has been identified, a traditional (and possibly infinite dimensional) optimal control problem (4.1) with Youla prameter restricted to lie in $\mathcal{D} \cap \mathcal{S}$ is then solved – in particular, in many interesting settings the resulting optimal controller restricted to the designed architecture can then be computed exactly leveraging results from the optimal controller synthesis literature [2, 12–17].

Formally, we begin by fixing an optimization horizon t and a controller order v. We suggest initially choosing t and v to be small (i.e., 2 or 3), and then gradually increasing these parameters until a suitable controller architecture/control law pair is found. Our motivations for this approach are twofold: (i) first, selecting a small horizon t and small controller order v leads to a smaller optimization problem that is computationally easier to solve; and (ii) as we show in the next section, a smaller horizon t and smaller controller order v can actually aid in the identification of optimal controller architectures. For a given performance metric $\Psi(\cdot; Y, \mathfrak{L})$ and atomic norm penalty $\|\cdot\|_{\mathcal{A}}$, the two step RFD procedure consists of an architecture design step and an optimal control law design step:

1) Architecture design: Select the regularization weight λ and solve the *finite dimensional* RFD optimization problem

$$\underset{U \in \mathcal{RH}_\infty^{\leq v} \cap \mathcal{S}}{\text{minimize}} \quad \Psi\left(U; Y^{\leq t}, \mathfrak{L}^{\leq t, v}\right) + 2\lambda \|U\|_{\mathcal{A}} \tag{4.23}$$

The actuators, sensors and communication links defining the designed architecture are

specified by the non-zero atoms that constitute the solution $\hat{U}$ to optimization problem (4.23). The architectural components employed in $\hat{U}$ in turn define a subspace $\mathcal{D}(\hat{U})$ which corresponds to all controllers (within the Youla parameterization) that have the same architecture as $\hat{U}$.[8]

2) Optimal control law design: Solve the infinite dimensional optimal control problem with Youla parameter additionally constrained to lie in the designed subspace $\mathcal{D}(\hat{U}) \cap \mathcal{S}$:

$$\underset{U \in \mathcal{RH}_\infty}{\text{minimize}} \quad \Psi\left(U; Y, \mathfrak{L}\right) \text{ s.t. } U \in \mathcal{D}(\hat{U}) \cap \mathcal{S}. \tag{4.24}$$

If the resulting controller architecture and controller performance are acceptable, the RFD procedure terminates. Otherwise, adjust λ accordingly to vary the tradeoff between architectural complexity and closed loop performance. If no suitable controller architecture/controller can be found, increase t and v and repeat the procedure.

Remark 4.5 (Removing Bias) *The method of solving a regularized optimization problem to identify the architectural structure of a controller and then solving a standard model matching problem restricted to the identified architecture is analogous to a procedure that is commonly employed in structured inference. In structured inference problems, a regularized problem is solved first to identify a subspace corresponding to the structure of an underlying model U_*. Subsequently, a non-regularized optimization problem with solution restricted to that identified subspace is solved to obtain an unbiased estimator of the underlying model U_*.*

4.5.2 Simultaneous Actuator, Sensor and Communication RFD

In this subsection we demonstrate the full power and flexibility of the RFD framework in designing a distributed controller architecture, jointly incorporating actuator, sensor and communication link design. In particular we consider a plant with eleven subsystems with topology as illustrated in Figure 4.4. The solid lines correspond to the physical interconnection between subsystems. Choosing $C_2 = B_2 = I$, the adja-

[8] As described in §4.3, the subspace $\mathcal{D}(\hat{U}) \cap \mathcal{S}$ is QI by construction, and hence this subspace also corresponds to all controllers with the same architecture as $\hat{K} = (I + \hat{U}P_{22})^{-1}\hat{U}$.

cency matrix of this graph then defines the support of the A matrix in the state space realization of the generalized plant (4.2), as well as the required communication links between nodes such that the distributed constraint is QI under P_{22} [10, 23].

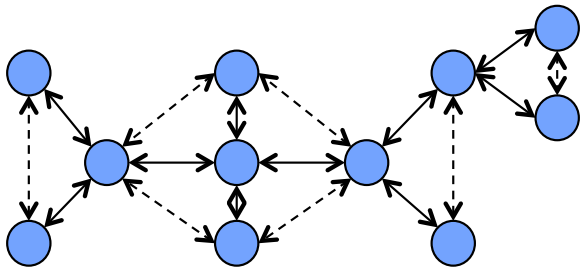

Figure 4.4: Topology of system considered for RFD example. Solid lines indicate both physical interconnections and existing communication links between controllers. Dashed lines correspond to possible additional edges to be added.

The non-zero entries of A were generated randomly and normalized such that $|\lambda_{\max}(A)| = .999$. The remaining state space parameters of the generalized plant (4.2) satisfy $D_{12}\begin{bmatrix} C_1^\top & D_{12}^\top \end{bmatrix} = \begin{bmatrix} 0 & 25I \end{bmatrix}$, and $D_{21}^\top \begin{bmatrix} B_1 & D_{21} \end{bmatrix} = \begin{bmatrix} 0 & .01I \end{bmatrix}$, with $C_1 C_1^\top = 100I$ and $B_1^\top B_1 = I$.

For the RFD task, we choose an $\mathcal{H}_2$ norm performance metric; we allow each node to be equipped with an actuator and/or a sensor (for a total of 11 possible actuators and sensors), and we allow the communication graph to be augmented with any subset of the interconnections denoted by the dashed lines in Figure 4.4, in addition to the already present links given by the solid lines. This leads to 536,870,911 different possible controller architectures.

We solved the RFD optimization (4.43) with atomic norm $\|\cdot\|_{\text{act+sns+comm}}$ as defined in §4.4.2, with weighting parameter $\theta = .75$ and with $k_s = k_a = 1$. We performed the RFD procedure for two different horizon/order pairs: $t = 4$ and $v = 2$, as well as $t = 6$ and $v = 3$; for these latter horizon/order values acceptable tradeoffs between architecture complexity and closed loop performance were identified, and hence the RFD procedure terminated. For each horizon/order pair (t, v), we vary λ, and for each resulting optimal solution $\hat{U}$, we identified the designed architecture and corresponding subspace $\mathcal{D}(\hat{U})$. We then used the method from [16] to exactly solve the resulting non-regularized distributed $\mathcal{H}_2$ model matching problem with subspace con-

straint $\mathcal{D}(\hat{U})$. Note that the Youla parameter solving this non-regularized problem is not restricted to have a finite impulse response. In particular, we can compute the optimal Youla parameter and the corresponding optimal controller restricted to the architecture underlying $\hat{U}$ in a computationally tractable fashion because we guarantee that the subspace corresponding to the designed architecture is QI, as per the discussion in Section 4.4.

For horizon $t = 6$ and order $v = 3$, the resulting architectural complexity is plotted against the closed loop norm of the system in Figure 4.5. As λ is increased, the architectural complexity (i.e. the number of actuators, sensors and communication links) decreases, but at the expense of deviations from the performance achieved by the controller that uses all of the available architectural resources. We also show the resulting architecture for $\lambda = 500$ in Figure 4.6: as can be seen, a non-obvious combination of eight actuators, eight sensors and five additional communication links are chosen, resulting in only a 0.71% degradation in performance over the distributed controller using all eleven actuators, eleven sensors and seven additional communication links.

As this example shows, the RFD procedure is effective at identifying simple controller architectures that approximate the performance of a controller that maximally utilizes the available architectural resources. In the next section, we offer some theoretical justification for the success of our procedure by suitably interpreting the RFD optimization problem (4.7) in the context of approximation theory and by making connections to analogous problems in structured inference.

4.6 Recovery of Optimal Actuation Structure

This section is dedicated to the analysis of the $\mathcal{H}_2$ RFD optimization problem (4.11) with no distributed constraint, actuator norm penalty (4.18), and Y and $\mathfrak{L}$ as given in Example 4.3 – a nearly identical argument applies to a sensor norm regularized problem. We discuss how to extend the analysis to output feedback and distributed problems at the end of the section.

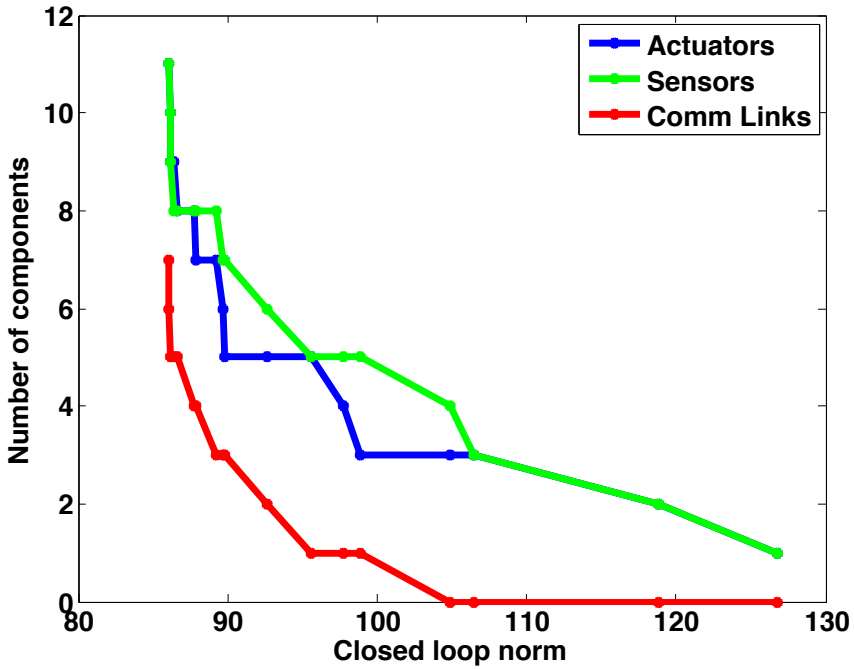

Figure 4.5: A small degradation in closed loop performance allows for a significant decrease in architectural complexity.

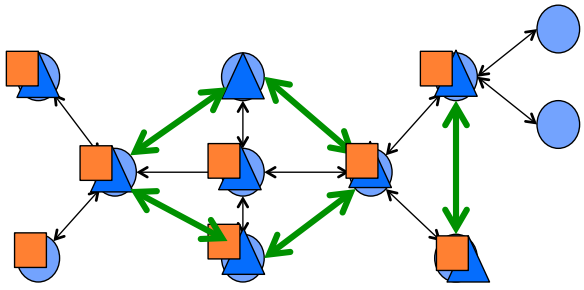

Figure 4.6: Resulting architecture for $\lambda = 500$: despite only using eight actuators (orange squares), eight sensors (blue triangles) and five additional communication links (green arrows), the performance only degraded by 0.71% relative to the distributed controller using all eleven actuators, eleven sensors and seven communication links.

Viewing the model matching problem (4.6) as a linear inverse problem makes it clear that designing a structured controller is akin to obtaining a structured solution to a linear inverse problem. The problem of obtaining structured solutions to linear inverse problems arises prominently in many contexts, most notably in statistical

estimation and inference. In that setting, one posits a linear measurement model[9]

$$Y = \mathfrak{L}(U_*) + W, \tag{4.25}$$

where Y is the vector of observations, $\mathfrak{L}$ is the measurement map, U_* parametrizes an underlying model and W is the measurement error. The linear model (4.25) also has an appealing interpretation from a control-theoretic perspective. In particular, letting $Y \in \mathcal{RH}_\infty$ be the state component of the open loop response of a LTI system, $U_* \in \mathcal{RH}_\infty$ be a suitably defined Youla parameter, and $\mathfrak{L} : \mathcal{RH}_\infty \to \mathcal{RH}_\infty$ be the map from Youla parameter to the state component of the closed loop response, it is then immediate that

$$W := Y - \mathfrak{L}(U_*) \tag{4.26}$$

represents the state component of the closed loop response achieved by the controller U_*. Table 4.2 summarizes the correspondence between these two perspectives.

Parameter	Structured Controller Design	Structured Inference
Y	Open loop system	Observations
$\mathfrak{L}$	Map to closed loop	Measurement map
U_*	Desired controller	Underlying model
W	Closed loop response	Measurement noise

Table 4.2: Interpretation of parameters in Structured Controller Design and Structured Inference.

This conceptual connection suggests a novel interpretation of the role of the closed loop response W achieved by a controller U_*. In an inferential context, since W corresponds to measurement noise, a smaller W makes the task of identifying the structure of the underlying model U_* much easier, as the measurements are more accurate. In a similar spirit, we demonstrate that structured controller design is easier (via the solution to an RFD optimization problem (4.7)) if the corresponding state component of the closed loop response is small. Thus the state component of the closed loop response of the system plays the role of noise when trying to identify the

[9]We purposefully use non-standard notation to facilitate comparisons between RFD and SLIP.

structure of a suitably defined controller U_*. In the sequel, we describe an appropriate notion of smallness for the state component of the closed loop response in the context of designing structured controllers.

The remainder of the discussion in this section builds on prominent results from the structured inference literature [67–70]. The flavor of these results is somewhat non-standard in the controls literature, and we therefore pause briefly to frame the setup in this section appropriately and to discuss how the results of this section should be interpreted. The main result of this section proceeds by assuming that there exists an architecturally simple controller U_* (i.e., one with a small number of actuators) that achieves a good closed loop response, (i.e., that achieves a small W as defined in (4.26)). Under suitable conditions, Theorems 4.1 and 4.2 state that the architectural structure of U_* can be recovered via tractable convex optimization using the RFD procedure. These conditions are phrased in terms of quantities associated to U_* which are typically unknown in advance – however, these conditions are not meant to be checked prior to solving a RFD optimization problem. Although the results are stated in terms of a nominal controller U_*, they should be interpreted as describing the properties satisfied by controller architectures identified via the RFD procedure of §4.5. In particular, the RFD procedure requires solving RFD optimization problems across a range of controller orders v, optimization horizons t and regularization weights λ: this process leads to a set of controller architectures being identified. Our results allow a practitioner to be confident that all controller architectures satisfying the conditions of our theorems – i.e., those that have a small number of actuators and that achieve a small closed loop state response – are included in this set of identified controller architectures. In this way, the RFD procedure provably identifies good controller architectures, should they exist.

We study finite dimensional variants of the $\mathcal{H}_2$ RFD optimization problem (4.11) with the actuator norm penalty (4.18), and show that such finite dimensional approximations are sufficient to identify the structure of a desired controller U_*. In particular, we truncate the optimization problem (4.11) to a finite horizon t by restricting $Y - \mathfrak{L}(U) \in \mathcal{RH}_\infty$ to the first t elements of its impulse response, and to

a finite controller order v by restricting U to lie in $\mathcal{RH}_\infty^{\leq v}$. The resulting optimization problem is thus finite dimensional, and corresponds to the first step of the RFD procedure defined in the previous section. At this point, it is convenient to introduce the temporally truncated version of (4.26) for a fixed optimization horizon t and controller order v:

$$\begin{aligned} W^{\leq t} &= Y^{\leq t} - \mathfrak{L}^{\leq t,t}(U_*^{\leq t}) \\ &= Y^{\leq t} - \mathfrak{L}^{\leq t,v}(U_*^{\leq v}) - T^{\leq t,v} \end{aligned} \tag{4.27}$$

with

$$T^{\leq t,v} := \mathfrak{L}^{\leq t,t}\left(U_*^{\leq t} - U_*^{\leq v}\right) \tag{4.28}$$

corresponding to the effect of the "tail" of U_* on the state component $W^{\leq t}$ of the truncated closed loop response.

The flexibility in the choice of the optimization horizon t and controller order v will be the focus of much of our discussion. In particular, it is of interest to find the smallest t and v for which we can guarantee that the RFD procedure recovers the structure underlying U_* – the smaller the horizon and controller order, the smaller the size of the optimization problem that needs to be solved. Perhaps counter-intuitively, we show that larger t and v do not necessarily help in recovering the structure of an underlying parameter U_*. We make this statement precise in what follows, but again drawing on intuition from the structured inference literature, we note that increasing v in RFD is analogous to increasing the allowed model complexity when solving an inference problem: if the model class is too rich, we risk over-fitting and thus obfuscating the structure of the underlying model U_*.

Our goal is to prove that the solution $\tilde{U}$ to the finite dimensional $\mathcal{H}_2$ RFD optimization problem

$$\tilde{U} = \underset{U \in \mathcal{RH}_\infty^{\leq v}}{\operatorname{argmin}} \|Y^{\leq t} + \mathfrak{L}^{\leq t,v}(U)\|_{\mathcal{H}_2}^2 + \rho\|U\|_{\mathcal{H}_2}^2 + 2\lambda \left\|U\right\|_{\text{act}} \tag{4.29}$$

has the same architectural structure as U_* for appropriately chosen t and v. To show

this, we study the solution $\hat{U}$ to the following *architect* optimization problem:

$$\begin{aligned} \hat{U} = \underset{U \in \mathcal{RH}_\infty^{\leq v}}{\operatorname{argmin}} & \|Y^{\leq t} + \mathfrak{L}^{\leq t,v}(U)\|_{\mathcal{H}_2}^2 + \rho\|U\|_{\mathcal{H}_2}^2 + 2\lambda \|U\|_{\text{act}} \\ & \text{s.t. } U \in \mathcal{A}_* \end{aligned} \tag{4.30}$$

where $\mathcal{A}_*$ is a subspace of Youla parameters U with the property that a row of U_* being zero implies that the corresponding row of U is zero. In words, $\mathcal{A}_*$ may be viewed as the set of Youla parameters corresponding to actuation schemes matching the actuation scheme of U_*. We also define $\mathscr{M}_* \subset \mathscr{M}_{\text{act}}$, with $\mathscr{M}_{\text{act}}$ defined as in (4.16), to be

$$\mathscr{M}_* := \{\mathcal{A} \in \mathscr{M}_{\text{act}} \,|\, (U_*)_{\mathcal{A}} \neq 0\}\,. \tag{4.31}$$

In words, the elements of $\mathscr{M}_*$ correspond to actuation schemes that use a single actuator, where these actuators are defined by the nonzero rows of the desired controller U_*.

We show under suitable conditions on t, v, U_* and $\mathfrak{L}^{\leq t,v}$ that $\hat{U} = \tilde{U}$; that is to say that the architect solution $\hat{U}$ is also the unique optimal solution to the RFD optimization problem (4.29) without the additional constraint $U \in \mathcal{A}_*$. As a result, since $\hat{U}$ is constrained to lie in $\mathcal{A}_*$, the solution to the RFD optimization problem $\tilde{U}$ also lies in $\mathcal{A}_*$ and hence has the same architectural structure as U_*. We emphasize that at no stage during the RFD procedure described in §4.5 do we require knowledge of $\mathcal{A}_*$ and $\mathscr{M}_*$ – the investigation of the architect problem (4.30) is only a theoretical tool used to prove structural recovery results.

4.6.1 Identifiability Conditions in Control

We begin by introducing two *restricted gains* in terms of the subspace $\mathcal{A}_*$ and its orthogonal complement $\mathcal{A}_*^\perp$. In order to do so, we introduce the dual norm to $\|\cdot\|_{\text{act}}$, which is given by

$$\|U\|_{\text{act}}^\star = \max_{\mathcal{A} \in \mathscr{M}_{\text{act}}} \|U_{\mathcal{A}}\|_{\mathcal{H}_2}. \tag{4.32}$$

These restricted gains are then

$$\begin{aligned} \alpha^{\leq t,v} := \min_{\Delta} \quad & \left\| \left(\left[\mathfrak{L}_{\mathcal{A}_*}^{\leq t,v} \right]^{\dagger} \mathfrak{L}_{\mathcal{A}_*}^{\leq t,v} + \rho I \right) (\Delta) \right\|_{\text{act}}^{\star} \\ \text{s.t.} \quad & \|\Delta\|_{\text{act}}^{\star} = 1,\ \Delta \in \mathcal{A}_* \cap \mathcal{RH}_{\infty}^{\leq v} \end{aligned} \tag{4.33}$$

$$\begin{aligned} \beta^{\leq t,v} := \max \quad & \left\| \left[\mathfrak{L}_{\mathcal{A}_*^{\perp}}^{\leq t,v} \right]^{\dagger} \mathfrak{L}_{\mathcal{A}_*}^{\leq t,v}(\Delta) \right\|_{\text{act}}^{\star} \\ \text{s.t.} \quad & \|\Delta\|_{\text{act}}^{\star} \leq 1,\ \Delta \in \mathcal{A}_* \cap \mathcal{RH}_{\infty}^{\leq v}. \end{aligned} \tag{4.34}$$

The minimum gain $\alpha^{\leq t,v}$ is a quantitative measure of the injectivity of the operator $\mathfrak{L}^{\leq t,v} \times \sqrt{\rho} I$ restricted to the subspace $\mathcal{A}_*$. Intuitively, it characterizes the distinctions among the effects of the different actuators within $\mathcal{A}_*$. The maximum gain $\beta^{\leq t,v}$, on the other hand, is a measure of how different the effects of actuators in $\mathcal{A}_*$ are from those of actuators in $\mathcal{A}_*^{\perp}$.

We can already see some immediate implications of different choices of the horizon t and and controller order v on these quantities. In particular, $\alpha^{\leq t,v}$ is non-increasing in the controller order v. This minimum gain's dependence on the horizon t is more subtle. Define the *mixing time of* $\mathscr{M}_*$ to be

$$\tau_{\mathscr{M}_*} := \max \left\{ t \in \mathbb{Z}_+ \;\middle|\; \left[\mathfrak{L}_{\mathcal{A}}^{\leq t} \right]^{\dagger} \mathfrak{L}_{\mathcal{B}}^{\leq t} = 0,\ \forall \mathcal{A} \neq \mathcal{B} \in \mathscr{M}_* \right\}. \tag{4.35}$$

If no t exists such that the condition within the $\max\{\cdot\}$ is satisfied, we set $\tau_{\mathscr{M}_*} = 0$. The mixing time $\tau_{\mathscr{M}_*}$ measures how long it takes for the effects of the distinct actuators used by U_* to overlap, or mix, in the closed loop response. Consequently the minimum gain $\alpha^{\leq t,v}$ is non-decreasing in t so long as $t \leq \tau_{\mathscr{M}_*}$, i.e., so long as t is sufficiently small that the effects of the different actuators used by U_* do not overlap. We then have the following lemma:

Lemma 4.1 *Let $\tau_{\mathscr{M}_*}$ be as defined in* (4.35)*. Then*

$$\alpha^{\leq t,v} = \rho + \min_{\mathcal{A} \in \mathscr{M}_*} \sigma_{\min} \left(\left[\mathfrak{L}_{\mathcal{A}}^{\leq t,v} \right]^{\dagger} \mathfrak{L}_{\mathcal{A}}^{\leq t,v} \right) \tag{4.36}$$

for all $1 \leq t \leq \tau_{\mathscr{M}_*}$. In particular, $\alpha^{\leq t,v}$ is non-decreasing in t for all $1 \leq t \leq \tau_{\mathscr{M}_*}$.

Proof: It is easily verified that for $\mathcal{A} \neq \mathcal{B} \in \mathscr{M}_*$ and $t \leq \tau_{\mathscr{M}_*}$, we have $\left[\mathfrak{L}_{\mathcal{A}}^{\leq t,v} \right]^{\dagger} \mathfrak{L}_{\mathcal{B}}^{\leq t,v} =$

0, from which (4.36) follows. To see that $\alpha^{\leq t,v}$ as given in (4.36) is non-decreasing in t, it suffices to note that

$$\left[\mathfrak{L}_{\mathcal{A}}^{\leq t+1,v}\right]^{\dagger}\mathfrak{L}_{\mathcal{A}}^{\leq t,v} = \left[\mathfrak{L}_{\mathcal{A}}^{\leq t,v}\right]^{\dagger}\mathfrak{L}_{\mathcal{A}}^{\leq t,v}, \tag{4.37}$$

leading to the conclusion that

$$\left[\mathfrak{L}_{\mathcal{A}}^{\leq t+1,v}\right]^{\dagger}\mathfrak{L}_{\mathcal{A}}^{\leq t+1,v} = \left[\mathfrak{L}_{\mathcal{A}}^{\leq t,v}\right]^{\dagger}\mathfrak{L}_{\mathcal{A}}^{\leq t,v} + \left[\mathfrak{L}_{\mathcal{A}}^{\leq t+1,v} - \mathfrak{L}_{\mathcal{A}}^{\leq t,v}\right]^{\dagger}\left(\mathfrak{L}_{\mathcal{A}}^{\leq t+1,v} - \mathfrak{L}_{\mathcal{A}}^{\leq t,v}\right). \tag{4.38}$$

The result follows by noting that the final term in this expression is positive semidefinite. ∎

In particular, this result suggests that actuation schemes with more evenly distributed actuators (i.e., those with larger mixing times $\tau_{\mathscr{M}_*}$ (4.35)) are easier to identify.

The maximum gain $\beta^{\leq t,v}$, however, is clearly seen to be non-decreasing both in the controller order v and the horizon t. This is consistent with our interpretation of $\beta^{\leq t,v}$ as a measure of similarity between actuators: as either v or t increase, there is more time for the mixing of the actuators' control actions via the propagation of dynamics in the system, increasing their worst-case "similarity." We now assume that the following *identifiability condition* is satisfied.

Assumption 4.1 (Identifiability) *There exist* $1 \leq v \leq t < \infty$ *such that*

$$\frac{\beta^{\leq t,v}}{\alpha^{\leq t,v}} =: \delta \in [0,1). \tag{4.39}$$

In light of the previous discussion, it is immediate that a larger controller order v decreases the likelihood of the identifiability condition being satisfied, and should therefore be taken as small as possible. The effect of increasing the horizon t is less clear, but we see that it may help if the minimum gain $\alpha^{\leq t,v}$ increases sufficiently fast with t relative to the increase in the gain $\beta^{\leq t,v}$ with respect to t – further there is no

need to increase t beyond the mixing time $\tau_{\mathscr{M}_*}$.

In the inference literature, the analog of these identifiability assumptions are given by conditions known as the *restricted eigenvalue condition* [85] and the *restricted isometry property* [86]. In the sequel, we give an example of deterministic and structured state space matrices that satisfy these identifiability conditions. Specifically, we focus on systems (4.2) that have block diagonal B_2 and C_1 matrices (i.e., decoupled actuators and state costs), and block banded state matrices A (i.e., locally coupled dynamics).

Remark 4.6 *Notice that if $\mathfrak{L}^{\leq t,v} = I$, then $\alpha^{\leq t,v} \geq 1$, $\beta^{\leq t,v} = 0$ and $\delta = 0$. These conditions are satisfied if $B = C = I$ and $v = t = 1$ in Example 4.2 (Basic LQR), or if $C_1 = B_2 = I$ and $v = 1$, $t = 2$ in Example 4.3 ($\mathcal{H}_2$ State Feedback). Thus sufficiently small values of v and t ensure that condition* (4.39) *holds. However, the resulting optimization problem only incorporates low order effects of the dynamics (as encoded in $\mathfrak{L}^{\leq t,v}$) in the RFD optimization problem, suggesting that t and v should be also be chosen large enough to sufficiently capture the dynamics of the system. This observation and Lemma 4.1 motivate our suggestion in Section 4.5 to begin with small horizon t and controller order v and to then gradually increase these values until a suitable controller architecture/control law pair is found.*

4.6.2 Sufficient Conditions for Recovery

The following theorem provides sufficient conditions for (i) the architect solution $\hat{U}$ to be the unique optimal solution to the finite dimensional RFD optimization (4.29), and (ii) an actuator of the desired controller, identified by a subspace $\mathcal{A} \in \mathscr{M}_*$, to be identified by the RFD procedure.

Theorem 4.1 (Structural Recovery) *Fix a horizon $1 \leq t < \infty$, and a controller*

order $1 \leq v \leq t$ *such that Assumption 4.1 holds. If*

$$\lambda > \tfrac{\delta}{1-\delta}\left(\left\|\left[\mathfrak{L}_{\mathcal{A}_*}^{\leq t,v}\right]^{\dagger}\left(W^{\leq t}+T^{\leq t,v}\right)\right\|_{\text{act}}^{\star}+\rho\left\|U_*^{\leq v}\right\|_{\text{act}}^{\star}\right)+\frac{\left\|\left[\mathfrak{L}_{\mathcal{A}_*^{\perp}}^{\leq t,v}\right]^{\dagger}\left(W^{\leq t}+T^{\leq t,v}\right)\right\|_{\text{act}}^{\star}}{1-\delta} \tag{4.40}$$

we have that $\hat{U}$ *as defined in* (4.30) *is the unique optimal solution to* (4.29)*, and that the row support of* $\hat{U}$ *is contained within the row support of* U_**. Further if* $\mathcal{A} \in \mathscr{M}_*$ *and*

$$\|(U_*^{\leq v})_{\mathcal{A}}\|_{\mathcal{H}_2} > \tfrac{1}{\alpha}\left(\lambda+\left\|\left[\mathfrak{L}_{\mathcal{A}_*}^{\leq t,v}\right]^{\dagger}\left(W^{\leq t}+T^{\leq t,v}\right)\right\|_{\text{act}}^{\star}+\rho\left\|U_*^{\leq v}\right\|_{\text{act}}^{\star}\right), \tag{4.41}$$

then $\hat{U}_{\mathcal{A}} \neq 0$*.*

The condition (4.40) states that, under suitable identifiability assumptions, the regularization weight λ needs to be sufficiently large to guarantee that the architect solution $\hat{U}$ is also the solution to (4.30). However, this can always be made to hold by choosing λ sufficiently large so that $\hat{U} = \tilde{U} = 0$. The second condition (4.41) provides an upper bound on the values of λ for which a specific actuator (i.e., a specific component $(U_*^{\leq v})_{\mathcal{A}}$, $\mathcal{A} \in \mathscr{M}_*$) is identified by the architect solution $\hat{U}$. The following corollary then guarantees the recovery of $\mathscr{M}_*$.

Corollary 4.1 *Let* $\mu := \min_{\mathcal{A}\in\mathscr{M}_*} \|(U_*^{\leq v})_{\mathcal{A}}\|_{\mathcal{H}_2}$*, and suppose that the open interval*

$$\Lambda := \left(\begin{array}{c}\tfrac{\delta}{1-\delta}\left[\left\|\left[\mathfrak{L}_{\mathcal{A}_*}^{\leq t,v}\right]^{\dagger}\left(W^{\leq t}+T^{\leq t,v}\right)\right\|_{\text{act}}^{\star}+\rho\left\|U_*^{\leq v}\right\|_{\text{act}}^{\star}\right]+\frac{\left\|\left[\mathfrak{L}_{\mathcal{A}_*^{\perp}}^{\leq t,v}\right]^{\dagger}\left(W^{\leq t}+T^{\leq t,v}\right)\right\|_{\text{act}}^{\star}}{1-\delta}, \\ \alpha^{\leq t,v}\mu-\left\|\left[\mathfrak{L}_{\mathcal{A}_*}^{\leq t,v}\right]^{\dagger}\left(W^{\leq t}+T^{\leq t,v}\right)\right\|_{\text{act}}^{\star}-\rho\left\|U_*^{\leq v}\right\|_{\text{act}}^{\star}\end{array}\right) \tag{4.42}$$

is non-empty. Then the solution $\tilde{U}$ *to the RFD optimization* (4.29)*, with any regularization weight* λ *chosen within* Λ*, has row support* equal *to that of* U_**.*

Note that it is useful to have a given architecture be identifiable for a range of regularization weights λ, as prior information about the values needed to specify (4.42)

are typically not available. We exploited this fact when we defined the RFD procedure in Section 4.5 by suggesting that λ be varied until a suitable architecture/control law pair is identified. This corollary also makes explicit that larger values of ρ shrinks the range of λ for which the RFD procedure is successful. It also shows that larger $T^{\leq t,v}$ tail terms (4.28) are deleterious to the performance of the RFD procedure as well – therefore although we previously stated that the controller order v should be chosen as small as possible, it should not be so small that the tail term $T^{\leq t,v}$ is too large.

Remark 4.7 (Extension to Output Feedback) *A similar argument applies to the output feedback problem, but at the expense of more complicated formulas. In particular the $\mathcal{H}_2$ RFD optimization takes the form*

$$\underset{U \in \mathcal{RH}_\infty}{\text{minimize}} \quad \|Y - \mathfrak{L}(U)\|_{\mathcal{H}_2}^2 + \|\mathfrak{F}(U)\|_{\mathcal{H}_2}^2 + 2\lambda \|U\|_{act}, \tag{4.43}$$

for $Y = P_{11}$, $\mathfrak{L}(U) = P_{12}UP_{21}$, and $\mathfrak{F}(U) = \begin{bmatrix} P_{12}UD_{21} & D_{12}UP_{21} & D_{12}UD_{21} \end{bmatrix}$. Notice that if D_{12} and D_{21} are set to 0 in the RFD optimization problem (4.43), we recover an optimization problem of exactly the same form as (4.11) with $\rho = 0$, in which case the analyses of this section and the next section are applicable.

Remark 4.8 (Extension to Distributed Constraints) *For the purposes of analysis, the additional constraint that $U \in \mathcal{S}$ can be incorporated by considering the restriction of $\mathfrak{L}$ to $\mathcal{S}$, resulting in a centralized problem (cf. [9] for an example of how this can be done).*

4.7 A RFD Signal to Noise Ratio

Theorem 4.1 as stated does not yet provide an immediate interpretation of the effect of the choices of the horizon t and the controller order v on the performance of the RFD procedure. In order to better understand the effects of the horizon t and controller order v on the success of the RFD procedure, we describe more interpretable bounds on $\alpha^{\leq t,v}$ and $\beta^{\leq t,v}$.

Lemma 4.2 *Fix $1 \leq t < \infty$ and $1 \leq v \leq t$. The parameters $\alpha^{\leq t,v}$ and $\beta^{\leq t,v}$, as defined in equations* (4.33) *and* (4.34)*, can be bounded from below and above, respectively, as follows:*

$$\alpha^{\leq t,v} \geq \rho + \gamma^{\leq t,v}, \tag{4.44}$$

where

$$\gamma^{\leq t,v} := \min_{\mathscr{B} \subseteq \mathscr{M}_*, |\mathscr{B}| \geq 1} \max_{\mathcal{A} \in \mathscr{B}} \left[\sigma_{\min} \left(\left[\mathfrak{L}_{\mathcal{A}}^{\leq t,v} \right]^{\dagger} \mathfrak{L}_{\mathcal{A}}^{\leq t,v} \right) - \sum_{\mathcal{B} \neq \mathcal{A} \in \mathscr{B}} \sigma_{\max} \left(\left[\mathfrak{L}_{\mathcal{A}}^{\leq t,v} \right]^{\dagger} \mathfrak{L}_{\mathcal{B}}^{\leq t,v} \right) \right] \tag{4.45}$$

and

$$\beta^{\leq t,v} \leq \max_{\mathcal{A} \in (\mathscr{M}_{act} \setminus \mathscr{M}_*)} \sum_{\mathcal{B} \in \mathscr{M}_*} \sigma_{\max} \left(\left[\mathfrak{L}_{\mathcal{A}}^{\leq t,v} \right]^{\dagger} \mathfrak{L}_{\mathcal{B}}^{\leq t,v} \right). \tag{4.46}$$

Consequently, we can upper bound the ratio (4.39) *as*

$$\delta \leq \frac{\beta^{\leq t,v}}{\rho + \gamma^{\leq t,v}}. \tag{4.47}$$

In particular, it is a straightforward consequence of Lemma 4.1 that for all $t \leq \tau_{\mathscr{M}_*}$ (where the mixing time $\tau_{\mathscr{M}_*}$ is as in (4.35)), the intermediate quantity $\gamma^{\leq t,v}$, as introduced in Lemma 4.2, is given by

$$\gamma^{\leq t,v} = \min_{\mathcal{A} \in \mathscr{M}_*} \sigma_{\min} \left(\left[\mathfrak{L}_{\mathcal{A}}^{\leq t,v} \right]^{\dagger} \mathfrak{L}_{\mathcal{A}}^{\leq t,v} \right),$$

and is non-decreasing in t. Further it is easily verified that the bounds (4.44), (4.46) and (4.47) can be taken with equality if $v = 1$, as each $\mathfrak{L}_{\mathcal{A}}^{\leq t,1}$ is isomorphic to a column vector.

The bounds computed in Lemma 4.2 can be combined with the sufficient conditions of Theorem 4.1 to describe sufficient conditions for the successful recovery of the architecture of U_* in terms of a signal to noise like quantity – to that end, we introduce the following definitions.

Definition 4.5 (RFD Noise) *We define the* RFD Noise *level $\eta_{\mathscr{M}_*}^{\leq t,v}$ for an $\mathcal{H}_2$ RFD*

optimization problem (4.29) *to be*

$$\eta_{\mathscr{M}_*}^{\leq t,v} := \left\| \left[\mathfrak{L}_{\mathcal{A}_*}^{\leq t,v} \right]^\dagger \left(W^{\leq t} + T^{\leq t,v} \right) \right\|_{\text{act}}^\star + \left\| \left[\mathfrak{L}_{\mathcal{A}_*^\perp}^{\leq t,v} \right]^\dagger \left(W^{\leq t} + T^{\leq t,v} \right) \right\|_{\text{act}}^\star . \tag{4.48}$$

The control theoretic interpretation (4.26) of the linear model (4.25) used in inference problems motivates our terminology – recall in particular that in (4.26) the state component of the closed loop response W is interpreted as measurement noise in the context of identifying a structured controller. Likewise, $T^{\leq t,v}$ can be viewed as additional noise introduced into the architecture identification procedure by the temporal truncation procedure described in (4.27). We proceed to define a control theoretic analog to the signal in the context of RFD optimization problems.

Definition 4.6 (RFD SNR) *In the context of architecture recovery via RFD, the magnitude of each atom,* $\|(U_*^{\leq v})_{\mathcal{A}}\|_{\mathcal{H}_2}$ *plays the role of a signal, and the RFD Noise level* $\eta_{\mathscr{M}_*}^{\leq t,v}$ *that of noise, leading to the definition of the SNR of a component* $(U_*^{\leq v})_{\mathcal{A}}$, $\mathcal{A} \in \mathscr{M}_*$ *as*

$$\text{SNR}\left((U_*^{\leq v})_{\mathcal{A}} \right) := \frac{\|(U_*^{\leq v})_{\mathcal{A}}\|_{\mathcal{H}_2}}{\eta_{\mathscr{M}_*}^{\leq t,v}}. \tag{4.49}$$

These definitions allow us to state simple conditions in terms of the SNR (4.49) for the successful recovery of an actuation architecture via the solution to the $\mathcal{H}_2$ RFD optimization problem (4.29).

Theorem 4.2 *Let* $\rho = 0$, $\lambda = \lambda' + \kappa$, *where* λ' *is given by the right hand side of* (4.40), *and* $\kappa > 0$ *is an arbitrarily small constant, and assume that* $\beta^{\leq t,v}/\gamma^{\leq t,v} < 1$. *If*

$$\text{SNR}\left((U_*^{\leq v})_{\mathcal{A}} \right) > \frac{1}{\gamma^{\leq t,v} - \beta^{\leq t,v}} \tag{4.50}$$

for all $\mathcal{A} \in \mathscr{M}_*$, *then for sufficiently small* κ, *the solution* $\tilde{U}$ *to the* $\mathcal{H}_2$ *RFD optimization problem* (4.29) *has the same row support as* $U_*^{\leq v}$.

Proof: Follows from rearranging terms in (4.41), Definition 4.6 and letting κ tend to 0 from above. ∎

Setting $\rho = 0$ increases the range Λ, as defined in (4.42), for which the RFD optimization problem is successful in recovering the structure of U_*, and the assumption that $\beta^{\leq t,v}/\gamma^{\leq t,v} < 1$ ensures that Assumption 4.1 holds. Thus Theorem 4.2 can be viewed as a slightly stronger, but more interpretable, set of sufficient conditions for the success of the RFD procedure.

Notice in particular that the left hand side of condition (4.50), i.e., the SNR, is mainly a function of the desired controller $U_*^{\leq v}$ and the closed loop performance $W^{\leq t}$ that it achieves, whereas the right hand side of (4.50) is mainly a function of the structure of the optimal controller and $\mathfrak{L}^{\leq t,v}$. Thus we expect controllers with sparse and evenly distributed actuation, i.e., controllers that minimize the SNR threshold $(\gamma^{\leq t,v} - \beta^{\leq t,v})^{-1}$, that act quickly and aggressively to achieve a good closed loop norm, i.e., controllers that maximize the SNR (4.49), to be recovered by the RFD procedure.

4.8 Case Study

The following case study illustrates the concepts introduced in the previous section on a concrete system that satisfies our sufficient conditions.

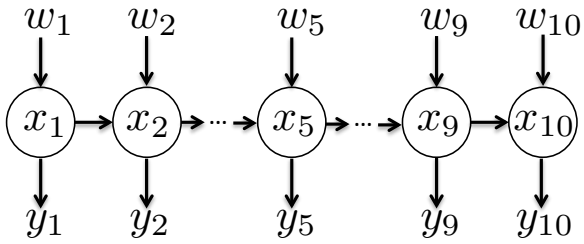

Figure 4.7: A diagram of the Stable Unidirectional Chain System case study.

We consider a $\mathcal{H}_2$ RFD optimization with control cost $\rho_u = .1$, and the remaining generalized plant (4.2) state space parameters set as $B_2 = C_1 = I_{10}$, $A = \frac{1}{2}I_{10} + \frac{1}{2}Z_{10}$, and $B_1 = 1.1(E_{11} + E_{55}) + .7E_{99} + .1I_{10}$. This system is illustrated in Figure 4.7. This simple example is chosen in order to allow a direct computation of various bounds and parameters, and to easily interpret the propagation of inputs and disturbances.

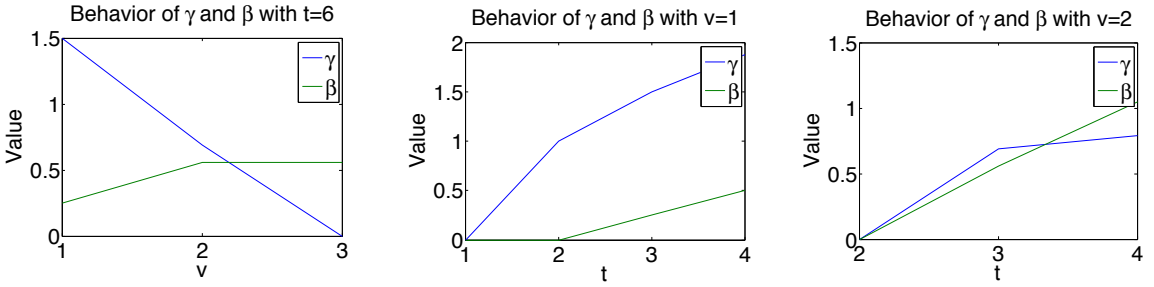

(a) Fixed horizon $t = 6$. (b) Fixed controller order $v = 1$. (c) Fixed controller order $v = 2$.

Figure 4.8: Behavior of identifiability parameters $\gamma^{\leq t,v}$ and $\beta^{\leq t,v}$.

We consider the task of recovering the optimal actuation schemes that use either 2 actuators or 3 actuators. In particular, we take the desired controller U_s, for $s = 2$ and $s = 3$, to be

$$\begin{aligned} U_s := \underset{U \in \mathcal{RH}_\infty}{\operatorname{argmin}} \quad & \|Y - \mathfrak{L}(U)\|_{\mathcal{H}_2}^2 + .1\|U\|_{\mathcal{H}_2}^2 \\ \text{s.t.} \quad & U \text{ has at most } s \text{ nonzero rows,} \end{aligned} \tag{4.51}$$

with open loop state response Y and map $\mathfrak{L}$ as defined in Example 4.3. We solve this optimization problem by enumerating all possible actuation schemes, and we find that the optimal actuation scheme for $s = 2$ is given by actuators at nodes 1 and 5, and for $s = 3$ by actuators at nodes 1, 5 and 9.

We emphasize that the goal of this case study is to illustrate the concepts introduced in the previous section, and to help the reader understand how the various parameters affect the recovery conditions – in practice, $\mathscr{M}_*$ and $\mathcal{A}_*$ are not available. Further, we note that the case study presented is, as far as we are aware, the first example in the literature of a system for which convex optimization provably identifies an optimal actuation architecture.

With these optimal actuation schemes at our disposal, we vary the parameters t and v to investigate how our recovery conditions are affected. As per the discussion in §4.7, we set $\rho = 0$. We also show that for appropriate fixed controller order v and horizon t, increasing λ shifts the identified architecture from actuators at nodes 1, 5 and 9 to actuators at nodes 1 and 5. This is a very desirable property from

an architecture design perspective, as it suggests that increasing the regularization weight λ causes the identified architecture to move to a simpler, but still optimal, actuator configuration. As predicted by Corollary 4.1, each optimal architecture is identified for a range of regularization weights λ. Further, as predicted by Theorem 4.2, the identified architectures are those for which the optimal control law achieves a small closed loop norm.

We begin by examining how the lower bound parameter $\gamma^{\leq t,v}$ and the maximum gain $\beta^{\leq t,v}$ are affected as we vary the horizon t and the controller order v. In particular, for actuation sparsity $s = 2$, we compute $\gamma^{\leq t,v}$ and $\beta^{\leq t,v}$ for (i) $t = 6$ and $v \in \{1, 2, 3\}$ (shown in Figure 4.8a), (ii) for $v = 1$ and $t \in \{1, 2, 3, 4\}$ (shown in Figure 4.8b), and (iii) for $v = 2$ and $t \in \{2, 3, 4\}$ (shown in Figure 4.8c). As expected, there is a decrease in the lower bound parameter $\gamma^{\leq t,v}$ and an increase in the maximum gain $\beta^{\leq t,v}$ as v increases, while both $\gamma^{\leq t,v}$ and $\beta^{\leq t,v}$ are non-decreasing for a fixed controller order v and increasing horizon t as long as $t \leq \tau_{\mathscr{M}_*}$. For this problem, the mixing time $\tau_{\mathscr{M}_*} = 5$. Further we see that $\gamma^{\leq t,v}$ begins to decrease for horizons $t > 6$ when $v = 2$.

t	$\frac{1}{\gamma^{\leq t,v} - \beta^{\leq t,v}}$	SNR_1	SNR_5	λ	$\|\Delta\|^{\star}_{\text{act}}$	Bound
2	1	1.27	1.27	.8	.73	.89
3	.8	.87	.88	1.46	.91	1.03
4	.727	.732	.735	2.01	1.00	1.12
5	.7	.67	.68	2.45	1.05	1.16

Table 4.3: Summary of relevant values for the controller U_2 with actuators at nodes 1 and 5.

The conditions of Theorem 4.2 are satisfied for $v = 1$ and several values of t. For example, if we select $t = 4$, $v = 1$, $\rho = 0$ and U_* as defined in (4.51), we can compute $(\gamma^{\leq 4,1} - \beta^{\leq 4,1})^{-1} = .7273$, $\text{SNR}\left((U_*^{\leq 1})_1\right) = .7324$, and $\text{SNR}\left((U_*^{\leq 1})_5\right) = .7353$, thus satisfying condition (4.50) for each of the two actuators. Further, selecting $\lambda = 2.0119 \in \Lambda$, and using this value for λ in the truncated RFD optimization (4.29) recovers a solution with non-zero first and fifth rows.

Perhaps surprisingly, similar positive recovery results can be verified for all $2 \leq t \leq \tau_{\mathscr{M}_*}$ – the relevant values are summarized in Table 4.3. In this table, SNR_i

corresponds to the SNR achieved by the controller component corresponding to the actuator at node i. Further, $\Delta := \hat{U} - U_*^{\leq v}$ is the approximation error between the architect parameter $\hat{U}$ and underlying parameter $U_*^{\leq v}$, and the values in the "Bound" column are given by equation (4.52) in the appendix giving upper bounds on $\|\Delta\|_{\text{act}}^{\star}$. It is worth noting that for $t = 5$, we do not satisfy the sufficient conditions of Theorem 4.2, but nonetheless recover the correct actuation architecture.

We now consider the case of actuation sparsity $s = 3$. Much as in the $s = 2$ case, we can verify that the conditions of Theorem 4.2 hold for $v = 1$, and $2 \leq t \leq \tau_{\mathscr{M}_*}$, where the mixing time $\tau_{\mathscr{M}_*}$ is still 5. However, since the controller with 3 actuators is able to achieve a much better closed loop norm, the SNRs are significantly larger, while the SNR threshold $(\gamma^{\leq t,v} - \beta^{\leq t,v})^{-1}$ does not change significantly. In particular, for the case of $t = 5$, we have a threshold of $(\gamma^{\leq 5,1} - \beta^{\leq 5,1})^{-1} = .82$, and SNRs of 4.04, 4.04 and 2.67 for the three actuator components.

This is consistent with our original interpretation of the closed loop state response $W^{\leq t}$ playing the role of measurement noise – the better the performance of the controller, the easier it is to identify via RFD. These experiments demonstrate that controllers with sparse and diffuse actuation schemes that achieve a small state response $W^{\leq t}$ are easy to identify as the solutions to RFD optimization problems. In summary, our analysis and case studies demonstrate that: (i) the parameter ρ can be set to 0 in the RFD optimization problem (4.7), even if the original model matching problem (4.6) had non-zero control cost ρ_u; (ii) choosing small controller order v and horizon t can actually lead to a favorable threshold $(\gamma^{\leq t,v} - \beta^{\leq t,v})^{-1}$ (4.50); (iii) actuation schemes that are more evenly distributed (so that they lead to large mixing times $\tau_{\mathscr{M}_*}$ in (4.35)) are easier to identify; and (iv) controller components that maximize the RFD analog of a SNR (4.49) are more likely to satisfy our recovery conditions. These consist of controllers that have a concentration of energy in their early impulse response elements, and that achieve a closed loop with small state response component.

4.9 Future Work

A priori bounds on incoherence: It is of great interest to derive *a priori* bounds on the gain parameters $\alpha^{\leq t,v}$ (4.33) and $\beta^{\leq t,v}$ (4.34) in terms of the state-space parameters of the system and a lower bound on the mixing time $\tau_{\mathscr{M}_*}$ (4.35). We are currently pursuing semidefinite relaxation based methods to obtain bounds on these parameters [87].

Scalability: The scalability of the RFD framework is limited by the underlying quadratic invariance based controller synthesis algorithms upon which it is built. In order to allow the RFD framework, and distributed optimal control theory in general, to scale to large heterogeneous systems, the first author and co-authors have developed the localized optimal control framework (cf. [88] and references therein). The algorithmic component of the RFD framework has already been ported [89]; it is of interest to see if analogous recovery conditions can also be developed.

4.10 Proofs

Proof: [Proof of Theorem 4.1] The proof of Theorem 4.1 centers around showing that under Assumption 4.1, the unique solution to the architect optimization (4.30) is also the unique solution of the original unconstrained optimization (4.29). We emphasize that at no point during the RFD process do we assume knowledge of $\mathcal{A}_*$ or of the architect optimization problem (4.30).

The proof consists of two parts: we first show that if $\alpha^{\leq t,v} > 0$, the architect optimization problem (4.30) has a unique optimal solution $\hat{U}$, and control its deviation from the underlying desired controller $U_*^{\leq v}$. We then use $\hat{U}$ and its error bound to construct a strictly dual-feasible primal/dual pair for the original RFD optimization problem (4.29), showing that $\hat{U}$ is indeed its unique optimal solution as well.

Proposition 4.1 (Bounded Errors) *Fix a horizon $1 \leq t < \infty$, and a controller order $1 \leq v \leq t$. Assume that $\alpha^{\leq t,v}$ as defined in* (4.33) *is strictly positive, and let $\Delta := \hat{U} - U_*^{\leq v}$. Then*

$$\|\Delta\|_{\text{act}}^{\star} \leq \tfrac{1}{\alpha}\left(\lambda + \left\|\left[\mathfrak{L}_{\mathcal{A}_*}^{\leq t,v}\right]^{\dagger}(W^{\leq t}+T^{\leq t,v})\right\|_{\text{act}}^{\star} + \rho\left\|U_*^{\leq v}\right\|_{\text{act}}^{\star}\right). \tag{4.52}$$

Proof: It is clear that under the assumption that $\alpha^{\leq t,v} > 0$, the architect optimization problem (4.30) is strongly convex, and hence has a unique optimal solution $\hat{U}$. Letting $\Delta := \hat{U} - U_*^{\leq v}$, and using the relation (4.27), the optimality conditions of the architect optimization problem (4.30) are then given by

$$\left(\left[\mathfrak{L}_{\mathcal{A}_*}^{\leq t,v}\right]^{\dagger}\mathfrak{L}_{\mathcal{A}_*}^{\leq t,v} + \rho I\right)(\Delta) - \left[\mathfrak{L}_{\mathcal{A}_*}^{\leq t,v}\right]^{\dagger}(W^{\leq t}+T^{\leq t,v}) + \rho U_*^{\leq v} + \lambda Z + \Lambda_{\mathcal{A}_*^{\perp}} \ni 0,$$

where $Z \in \partial\left\|\hat{U}\right\|_{\text{act}}$ satisfies $\|Z_{\mathcal{A}_*}\|_{\text{act}}^{\star} = 1$, $\left\|Z_{\mathcal{A}_*^{\perp}}\right\|_{\text{act}}^{\star} \leq 1$, and $\Lambda_{\mathcal{A}_*^{\perp}} \in \mathcal{A}_*^{\perp}$ is the Lagrange multiplier corresponding to the architect constraint $U \in \mathcal{A}_*$. Projecting (4.10) onto $\mathcal{A}_*$, and leveraging that $\Delta \in \mathcal{A}_*$, we then obtain

$$\left(\left[\mathfrak{L}_{\mathcal{A}_*}^{\leq t,v}\right]^{\dagger}\mathfrak{L}_{\mathcal{A}_*}^{\leq t,v} + \rho I\right)(\Delta) = \left(\left[\mathfrak{L}_{\mathcal{A}_*}^{\leq t,v}\right]^{\dagger}(W^{\leq t}+T^{\leq t,v}) - \rho U_*^{\leq v} - \lambda Z_{\mathcal{A}_*}\right). \tag{4.53}$$

We then have the following chain of inequalities

$$\begin{aligned}\alpha^{\leq t,v}\|\Delta\|_{\text{act}}^{\star} &\leq \left\|\left(\left[\mathfrak{L}_{\mathcal{A}_*}^{\leq t,v}\right]^{\dagger}\mathfrak{L}_{\mathcal{A}_*}^{\leq t,v} + \rho I\right)(\Delta)\right\|_{\text{act}}^{\star} \\ &\leq \lambda + \left\|\left[\mathfrak{L}_{\mathcal{A}_*}^{\leq t,v}\right]^{\dagger}(W^{\leq t}+T^{\leq t,v})\right\|_{\text{act}}^{\star} + \rho\left\|U_*^{\leq v}\right\|_{\text{act}}^{\star}\end{aligned}$$

where the first inequality follows from (4.33), and the second from (4.53) and the triangle inequality. Rearranging terms yields the error bound (4.52). ∎

Strict dual feasibility

In order to construct a primal/dual feasible pair for optimization (4.29) from $\hat{U}$, we first set $Z_{\mathcal{A}_*}$ to be a member of the sub differential $\partial\|\cdot\|_{\text{act}}$ evaluated at $\hat{U}$. We now choose $Z_{\mathcal{A}_*^{\perp}}$ to be

$$Z_{\mathcal{A}_*^{\perp}} := \frac{\left(\left[\mathfrak{L}_{\mathcal{A}_*^{\perp}}^{\leq t,v}\right]^{\dagger}(W^{\leq t}+T^{\leq t,v}) - \left[\mathfrak{L}_{\mathcal{A}_*^{\perp}}^{\leq t,v}\right]^{\dagger}\mathfrak{L}_{\mathcal{A}_*}^{\leq t,v}(\Delta)\right)}{\lambda} \tag{4.54}$$

In doing so, we guarantee that $(\hat{U}, Z)$ satisfy the optimality conditions of optimization (4.29). What remains to be shown is the $Z_{\mathcal{A}_*^\perp}$ is an element of the sub-differential. In order to do so, we show that under the assumptions of the theorem, $\left\|Z_{\mathcal{A}_*^\perp}\right\|_{\text{act}}^\star < 1$. This guarantees that Z is indeed in $\partial \left\|\hat{U}\right\|_{\text{act}}$, and that $\hat{U}_{\mathcal{A}} = 0$ for all $\mathcal{A} \notin \mathscr{M}_*$.

To that end, notice that $\left\|Z_{\mathcal{A}_*^\perp}\right\|_{\text{act}}^\star$ can be upper bounded by

$$\begin{aligned}
&\frac{\left(\left\|\left[\mathfrak{L}_{\mathcal{A}_*^\perp}^{\leq t,v}\right]^\dagger \mathfrak{L}_{\mathcal{A}_*}^{\leq t,v}(\Delta)\right\|_{\text{act}}^\star + \left\|\left[\mathfrak{L}_{\mathcal{A}_*^\perp}^{\leq t,v}\right]^\dagger (W^{\leq t} + T^{\leq t,v})\right\|_{\text{act}}^\star\right)}{\lambda} \\
&\qquad \leq \frac{1}{\lambda}\left(\beta^{\leq t,v}\left\|\Delta\right\|_{\text{act}}^\star + \left\|\left[\mathfrak{L}_{\mathcal{A}_*^\perp}^{\leq t,v}\right]^\dagger (W^{\leq t} + T^{\leq t,v})\right\|_{\text{act}}^\star\right) \\
&\qquad \leq \frac{1}{\lambda}\delta\left(\rho\left\|U_*^{\leq v}\right\|_{\text{act}}^\star + \left\|\left[\mathfrak{L}_{\mathcal{A}_*}^{\leq t,v}\right]^\dagger (W^{\leq t} + T^{\leq t,v})\right\|_{\text{act}}^\star\right) \\
&\qquad\qquad + \delta + \frac{1}{\lambda}\left\|\left[\mathfrak{L}_{\mathcal{A}_*^\perp}^{\leq t,v}\right]^\dagger (W^{\leq t} + T^{\leq t,v})\right\|_{\text{act}}^\star < 1,
\end{aligned}$$

where the first inequality follows from applying the triangle inequality to (4.54), the second from applying definition (4.34), the third from applying the error bound (4.52), and the fourth from (4.40). Thus we have shown that under the assumptions of the Theorem, $\hat{U}$ is also the optimal solution of the original problem (4.29) – its uniqueness follows from the *local* strong convexity of the cost function around $\hat{U}$. Finally, if for $\mathcal{A} \in \mathscr{M}_*$, we have that (4.41) holds, then $\hat{U}_{\mathcal{A}} \neq 0$. ∎

Proof: [Proof of Lemma 4.2] The gain $\alpha^{\leq t,v}$ is bounded below by

$$\begin{aligned}
&\min_{\substack{\|\Delta\|_{\text{act}}^\star = 1 \\ \Delta \in \mathcal{A}_*}} \max_{\mathcal{A} \in \mathscr{M}_*} \left\|\left(\left[\mathfrak{L}_{\mathcal{A}}^{\leq t,v}\right]^\dagger \mathfrak{L}_{\mathcal{A}}^{\leq t,v} + \rho I\right)\Delta_{\mathcal{A}}\right\|_{\mathcal{H}_2} - \sum_{\mathcal{B} \neq \mathcal{A} \in \mathscr{M}_*} \left\|\left[\mathfrak{L}_{\mathcal{A}}^{\leq t,v}\right]^\dagger \mathfrak{L}_{\mathcal{B}}^{\leq t,v}\Delta_{\mathcal{B}}\right\|_{\mathcal{H}_2} \\
&\quad \geq \rho + \min_{\mathscr{B} \subseteq \mathscr{M}_*, |\mathscr{B}| \geq 1} \max_{\mathcal{A} \in \mathscr{B}} \sigma_{\min}\left(\left[\mathfrak{L}_{\mathcal{A}}^{\leq t,v}\right]^\dagger \mathfrak{L}_{\mathcal{A}}^{\leq t,v}\right) - \sum_{\mathcal{B} \neq \mathcal{A} \in \mathscr{B}} \sigma_{\max}\left(\left[\mathfrak{L}_{\mathcal{A}}^{\leq t,v}\right]^\dagger \mathfrak{L}_{\mathcal{B}}^{\leq t,v}\right),
\end{aligned}$$

where the inequalities follow from the fact that $\|\Delta\|_{\text{act}}^\star = 1$ implies that there exists $\mathcal{A} \in \mathscr{M}_*$ such that $\|\Delta_{\mathcal{A}}\|_{\mathcal{H}_2} = 1$, and the definition of the respective norms. The derivation of the bound on $\beta^{\leq t,v}$ is similar, and hence omitted. ∎

Chapter 5

Communication Delay Co-design in $\mathcal{H}_2$ Distributed Control Using Atomic Norm Minimization

5.1 Introduction

In the previous chapter, we address the problem of jointly optimizing the architectural complexity of a distributed optimal controller and the closed loop performance that it achieves by introducing the Regularization for Design (RFD) framework. In RFD, controllers with complicated architectures are viewed as being composed of atomic controllers with simpler architectures – this family of simple controllers is then used to construct various *atomic norms* [20, 66, 90] that penalize the use of specific architectural resources, such as actuators, sensors or additional communication links. These atomic norms are then added as a penalty function to the variational solution to an optimal control problem (formulated in the model matching framework), allowing the controller designer to explore the tradeoff between architectural complexity and closed loop performance by varying the weight on the atomic norm penalty in the resulting convex optimization problem.

In [22] we give explicit constructions of atomic norms useful for the design of actuation, sensing and joint actuation/sensing architectures, but do not address how to construct an atomic norm for communication architecture design. Indeed constructing a suitable atomic norm for communication architecture design has substantial

technical challenges that do not arise in actuation and sensing architecture design: we address these challenges in this chapter. We model a distributed controller as a collection of sub-controllers, each equipped with a set of actuators and sensors, that exchange their respective measurements with each other subject to *communication delays* imposed by an underlying communication graph. Keeping with the philosophy adopted in RFD [22], we view dense communication architectures, i.e., ones with a large number of communication links between sub-controllers, as being composed of multiple simple *atomic* communication architectures, i.e., ones with a small number of communication links between sub-controllers. Thus the problem of controller communication architecture/control law co-design can be framed as the joint optimization of a suitably defined measure of the communication complexity of the distributed controller and its closed loop performance, in which these two competing metrics are traded off against each other in a principled manner.

In general one can select communication architectures that range in complexity from completely decentralized, i.e., distributed controllers with no communication allowed between sub-controllers, to essentially centralized and without delay, i.e., distributed controllers with instantaneous communication allowed between all sub-controllers. However, if we ask that the distributed optimal controller restricted to the designed communication architecture be specified by the solution to a convex optimization problem then this limits the simplicity of the designed communication scheme [5, 9, 10, 77]. In particular a sufficient, and under mild assumptions necessary, condition for a distributed optimal controller to be specified by the solution to a convex optimization problem[1] is that the communication architecture allow sub-controllers to communicate with each other as quickly as their control actions propagate through the plant [10]. Although this condition may seem restrictive, it can often be met in practice by constructing a communication topology that mimics or is a superset of the physical topology of the plant. For example, these delay based conditions may be satisfied in a smart-grid setting if fiber-optic cables are laid down

[1]For a more detailed overview of the relationship between information exchange constraints and the convexity of distributed optimal control problems, we refer the reader to [4, 9, 10, 25] and the references therein.

in parallel to transmission lines; in a SDN setting if control packets are given priority in routing protocols; and in an automated highway system setting if vehicles are allowed to communicate wirelessly with nearby vehicles.

When the aforementioned delay based condition is satisfied by a distributed constraint, it is said to be *quadratically invariant* (QI) [9, 10]. While the resulting distributed optimal control problem is convex when quadratic invariance holds, it may still be infinite dimensional. Recently it has been shown that in the case of $\mathcal{H}_2$ distributed optimal control subject to QI constraints imposed by a strongly connected communication architecture, i.e. one in which every sub-controller can exchange information with every other sub-controller subject to delay, the resulting distributed optimal controller synthesis problem can be reduced to a finite dimensional convex program, and hence admits an efficient solution [16, 91].[2] In light of these observations, we look to design *strongly connected communication architectures* that induce *QI* constraint sets – once such a communication architecture is obtained, the methods from [16,91] can then be used to compute the optimal distributed controller restricted to that communication architecture exactly.

Related work: We refer the reader to the related work paragraph of §4.1 for an overview of literature relevant to the use of regularization in the control literature.

Chapter contributions: We show that the communication complexity of a distributed controller can be inferred from the structure of its impulse response elements. We use this observation to provide an explicit construction of an atomic norm [20,66,90], which we call the communication link norm, that can be incorporated into the RFD framework [22] to design strongly connected communication graphs that generate QI subspaces. As argued above, these two structural properties allow for the distributed optimal controller implemented using the designed communication architecture to be specified by the solution to a finite dimensional convex optimization problem [16, 91]. We also show that by augmenting the variational solution to the $\mathcal{H}_2$ distributed optimal control problem presented in [16, 91] with the communication link

[2] Other solutions exist to the $\mathcal{H}_2$ distributed control problem subject to delay constraints – we refer the reader to the discussion and references in [16] for a more extensive overview of this literature.

norm as a regularizer, the communication architecture/control law co-design problem can be formulated as a second order cone program. By varying the weight on the communication link norm penalty function, the controller designer can use our co-design algorithm to explore the tradeoff between communication architecture complexity and closed loop performance in a principled way via convex optimization. We use these results to formulate a communication architecture/control law co-design algorithm that yields a distributed optimal controller and the communication architecture on which it is to be implemented.

Chapter organization: In §5.2 we introduce necessary operator theoretic concepts and establish notation. In §5.3 we formulate the communication architecture/control law co-design problem as the joint optimization of a suitably defined measure of the communication complexity of a distributed controller and the closed loop performance that it achieves. In §5.4, we show how communication graphs can be used to generate distributed constraints, and show that if a communication graph that generates a QI subspace is augmented with additional communication links, the subspace generated by the resulting communication graph is also QI. We use this observation and techniques from structured linear inverse problems [20] in §5.5 to construct a convex regularizer that penalizes the use of additional communication links by a distributed controller, and formulate the co-design procedure. In §5.6 we discuss the computational complexity of the co-design procedure and illustrate the usefulness of our approach with two numerical examples. We end with a discussion in §5.7.

5.2 Preliminaries

5.2.1 Operator Theoretic Preliminaries

We use standard definitions of the Hardy spaces $\mathcal{H}_2$ and $\mathcal{H}_\infty$. We denote the restrictions of $\mathcal{H}_\infty$ and $\mathcal{H}_2$ to the space of real rational proper transfer matrices $\mathcal{R}_p$ by $\mathcal{RH}_\infty$ and $\mathcal{RH}_2$, respectively. As we work in discrete time, the two spaces are equal, and as

a matter of convention we refer to this space as $\mathcal{RH}_\infty$. We refer the reader to [2] for a review of this standard material. For a signal $\mathbf{f} = (f^{(t)})_{t=0}^{\infty}$, we use $\mathbf{f}^{\leq d}$ to denote the truncation of $\mathbf{f}$ to its elements $f^{(t)}$ satisfying $t \leq d$, i.e., $\mathbf{f}^{\leq d} := (f^{(t)})_{t=0}^{d}$. We extend the Banach space ℓ_2^n to the space

$$\ell_{2,e}^n := \{\mathbf{f} : \mathbb{Z}_+ \to \mathbb{R}^n \,|\, \mathbf{f}^{\leq d} \in \ell_2^n \text{ for all } d \in \mathbb{Z}_+\}, \tag{5.1}$$

where $\mathbb{Z}_+$ ($\mathbb{Z}_{++}$) denotes the set of non-negative (positive) integers. A plant $G \in \mathcal{R}_p^{m\times n}$ can then be viewed as a linear map from $\ell_{2,e}^n$ to $\ell_{2,e}^m$. Unless required, we do not explicitly denote dimensions and we assume that all vectors, operators and spaces are of compatible dimension throughout.

5.2.2 Notation

We denote elements of $\ell_{2,e}$ with boldface lower case Latin letters, elements of $\mathcal{R}_p$ (which include matrices) with upper case Latin letters, and affine maps from $\mathcal{RH}_\infty$ to $\mathcal{RH}_\infty$ with upper case Fraktur letters such as $\mathfrak{M}$. We denote temporal indices, horizons and delays by lower case Latin letters.

We denote the elements of the power series expansion of a map $G \in \mathcal{RH}_\infty$ by $G^{(t)}$, i.e., $G = \sum_{t=0}^{\infty} \frac{1}{z^t} G^{(t)}$. We use $\mathcal{RH}_\infty^{\leq d}$ to denote the subspace of $\mathcal{RH}_\infty$ composed of finite impulse response (FIR) transfer matrices of horizon d, i.e., $\mathcal{RH}_\infty^{\leq d} := \{G \in \mathcal{RH}_\infty \,|\, G = \sum_{t=0}^{d} \frac{1}{z^t} G^{(t)}\}$. Similarly, we use $\mathcal{RH}_\infty^{\geq d+1}$ to denote the subspace of $\mathcal{RH}_\infty$ composed of transfer matrices with power series expansion elements satisfying $G^{(t)} = 0$ for all $t \leq d$, i.e., $\mathcal{RH}_\infty^{\geq d+1} := \{G \in \mathcal{RH}_\infty \,|\, G = \sum_{t=d+1}^{\infty} \frac{1}{z^t} G^{(t)}\}$. For an element $G \in \mathcal{RH}_\infty$, we use $G^{\leq d}$ to denote the projection of G onto $\mathcal{RH}_\infty^{\leq d}$, and $G^{\geq d+1}$ to denote the projection of G onto $\mathcal{RH}_\infty^{\geq d+1}$, i.e., $G^{\leq d} = \sum_{t=0}^{d} \frac{1}{z^t} G^{(t)}$ and $G^{\geq d+1} = \sum_{t=d+1}^{\infty} \frac{1}{z^t} G^{(t)}$.

Sets are denoted by upper case script letters, such as $\mathscr{S}$, whereas subspaces of an inner product space are denoted by upper case calligraphic letters, such as $\mathcal{S}$. We denote the orthogonal complement of $\mathcal{S}$ with respect to the standard inner product on $\mathcal{RH}_2$ by $\mathcal{S}^\perp$. We use the greek letter Γ to denote the adjacency matrix of a graph,

and use labels in the subscript to distinguish among different graphs, i.e., Γ_{base} and Γ_1 correspond to different graphs labeled "base" and "1." We use E_{ij} to denote the matrix with (i,j)th element set to 1 and all others set to 0. We use I_n and 0_n to denote the $n \times n$ dimensional identity matrix and all zeros matrix, respectively. For a p by q block row by block column transfer matrix M partitioned as $M = (M_{ij})$, we define the block support $\text{bsupp}(M)$ of the transfer matrix M to be the p by q integer matrix with (i,j)th element set to 1 if M_{ij} is nonzero, and 0 otherwise. Finally, we use the $\star$ superscript to denote that a parameter is the solution to an optimization problem.

5.3 Communication Architecture Co-Design

In this section we formulate the communication architecture/control law co-design problem as the joint optimization of a suitably defined measure of the communication complexity of the distributed controller and its closed loop performance. In particular, we introduce the convex optimization based solution to the $\mathcal{H}_2$ distributed optimal control problem subject to delays presented in [16, 91], and modify this method to perform the communication architecture/control law co-design task.

5.3.1 Distributed $\mathcal{H}_2$ Optimal Control subject to Delays

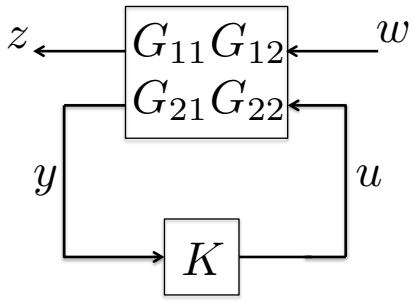

Figure 5.1: A diagram of the generalized plant defined in (5.2).

To review the relevant results of [16,91], we introduce the discrete-time generalized

plant G given by

$$G = \left[\begin{array}{c|cc} A & B_1 & B_2 \\ \hline C_1 & 0 & D_{12} \\ C_2 & D_{21} & 0 \end{array}\right] = \begin{bmatrix} G_{11} & G_{12} \\ G_{21} & G_{22} \end{bmatrix} \tag{5.2}$$

with inputs of dimension p_1, p_2 and outputs of dimension q_1, q_2. As illustrated in Figure 5.1, this system describes the four transfer matrices from the disturbance and control inputs $\mathbf{w}$ and $\mathbf{u}$, respectively, to the controlled and measured outputs $\mathbf{z}$ and $\mathbf{y}$, respectively. In order to ensure the existence of solutions to the necessary Riccati equations and to obtain simpler formulas, we assume that (A, B_1, C_1) and (A, B_2, C_2) are both stabilizable and detectable, and that

$$D_{12}^\top D_{12} = I,\ D_{21} D_{21}^\top = I,\ C_1^\top D_{12} = 0,\ B_1 D_{21}^\top = 0. \tag{5.3}$$

Let $\mathcal{S}$ be a subspace that encodes the distributed constraints imposed on the controller K. For example, when some sub-controllers cannot access the measurements of other sub-controllers, the subspace $\mathcal{S}$ enforces corresponding sparsity constraints on the controller K. Alternatively, when sub-controllers can only gain access to other sub-controllers' measurements after a given delay, the subspace $\mathcal{S}$ enforces corresponding delay constraints on the controller K.

The distributed $\mathcal{H}_2$ optimal control problem with subspace constraint $\mathcal{S}$ is then given by

$$\begin{aligned} \underset{K \in \mathcal{R}_p}{\text{minimize}} \quad & \|G_{11} - G_{12} K (I - G_{22} K)^{-1} G_{21}\|_{\mathcal{H}_2}^2 \\ \text{s.t.} \quad & K \in \mathcal{S} \\ & K \text{ internally stabilizes } G \end{aligned} \tag{5.4}$$

where the objective function measures the $\mathcal{H}_2$ norm of the closed loop transfer function from the exogenous disturbance $\mathbf{w}$ to the controlled output $\mathbf{z}$, and the first constraint ensures that the controller K respects the distributed constraints imposed by the subspace $\mathcal{S}$.

Optimization problem (5.4) is in general both infinite dimensional and non-convex. In [16, 91], the authors provide an exact and computationally tractable solution to

optimization problem (5.4) when the distributed constraint $\mathcal{S}$ is *QI* [9] with respect to G_{22}[3] and is generated by a *strongly connected* communication graph. We say that a distributed constraint $\mathcal{S}$ is generated by a strongly connected communication graph[4] if it admits a decomposition of the form

$$\mathcal{S} = \mathcal{Y} \oplus \frac{1}{z^{d+1}}\mathcal{R}_p,\ \mathcal{Y} = \oplus_{t=1}^{d} \frac{1}{z^t}\mathcal{Y}^{(t)} \tag{5.5}$$

for some positive integer d, and some subspaces $\mathcal{Y}^{(t)} \subset \mathbb{R}^{p_2 \times q_2}$. In §5.4 we show how a strongly connected communication graph between sub-controllers can be used to define a subspace $\mathcal{S}$ that admits a decomposition (5.5).

Restricting ourselves to distributed constraints $\mathcal{S}$ that are QI with respect to G_{22} and that admit a decomposition of the form (5.5) allows us to pose the optimal control problem (5.4) as the following convex model matching problem

$$\begin{aligned} \underset{Q \in \mathcal{RH}_\infty}{\text{minimize}} \quad & \|P_{11} - P_{12} Q P_{21}\|_{\mathcal{H}_2}^2 \\ \text{s.t.} \quad & \mathfrak{C}\left(Q^{\leq d}\right) \in \mathcal{Y} \end{aligned} \tag{5.6}$$

through the use of a suitable Youla parameterization, where the $P_{ij} \in \mathcal{RH}_\infty$ are appropriately defined stable transfer matrices and $\mathfrak{C} : \mathcal{RH}_\infty^{\leq d} \to \mathcal{RH}_\infty^{\leq d}$ is an appropriately defined affine map (cf. §III-B of [16]). It is further shown in [16] that the solution $Q^\star$ to the distributed model matching problem (5.6) with QI constraint $\mathcal{S}$ admitting decomposition (5.5) is specified in terms of the solution to a finite dimensional convex quadratic program.

Theorem 5.1 (Theorem 3 in [16]) *Let $\mathcal{S}$ be QI under G_{22} and admit a decomposition as in* (5.5)*. Let $Q^\star \in \mathcal{S} \cap \mathcal{RH}_\infty$ be the optimal solution to the convex model*

[3] A subspace $\mathcal{S}$ is said to be QI with respect to G_{22} if $KG_{22}K \in \mathcal{S}$ for all $K \in \mathcal{S}$. When quadratic invariance holds, we have that $K \in \mathcal{S}$ if and only if $K(I - G_{22}K)^{-1} \in \mathcal{S}$; this key property allows for the convex parameterization (5.6) of the distributed optimal control problem (5.4).

[4] We consider subspaces $\mathcal{S}$ that are strictly proper so that the reader can use the exact results presented in [16]. The authors of [16] do however note that their method extends to non-strictly proper controllers at the expense of more complicated formulas.

matching problem (5.6). *Then* $(Q^\star)^{\geq d+1} = 0$ *and*

$$(Q^\star)^{\leq d} = \underset{V \in \mathcal{RH}_\infty^{\leq d}}{\arg\min} \quad \| \mathfrak{L}(V) \|_{\mathcal{H}_2}^2 \ \textit{s.t.} \ \mathfrak{C}(V) \in \mathcal{Y}, \tag{5.7}$$

where $\mathfrak{L}$ *is a linear map from* $\mathcal{RH}_\infty^{\leq d}$ *to* $\mathcal{RH}_\infty^{\leq d}$, *and* $\mathfrak{C}$ *is the affine map from* $\mathcal{RH}_\infty^{\leq d}$ *to* $\mathcal{RH}_\infty^{\leq d}$ *used to specify the model matching problem* (5.6). *Furthermore, the optimal cost achieved by* $Q^\star$ *in the optimization problem* (5.6) *is given by*

$$\|P_{11}\|_{\mathcal{H}_2}^2 + \| \mathfrak{L}\left((Q^\star)^{\leq d}\right) \|_{\mathcal{H}_2}^2. \tag{5.8}$$

Remark 5.1 *The term* $\| \mathfrak{L}\left((Q^\star)^{\leq d}\right) \|_{\mathcal{H}_2}^2$ *in the optimal cost* (5.8) *quantifies the deviation of the performance achieved by the distributed optimal controller from that achieved by the centralized optimal controller.*

The optimization problem (5.7) is finite dimensional because the maps $\mathfrak{L}$ and $\mathfrak{C}$ are both finite dimensional (they map the finite dimensional space $\mathcal{RH}_\infty^{\leq d}$ into itself) and act on the finite dimensional transfer matrix $V \in \mathcal{RH}_\infty^{\leq d}$. These maps can be computed in terms of the state-space parameters of the generalized plant (5.2) and the solution to appropriate Riccati equations (cf. §III-B and §IV-A of [16]). Under the assumptions (5.3) the map $\mathfrak{L}$ is injective, and hence the convex quadratic program (5.7) has a unique optimal solution $(Q^\star)^{\leq d}$.

As the distributed constraint $\mathcal{S}$ is assumed to be QI, the optimal distributed controller $K^\star \in \mathcal{S}$ specified by the solution to the non-convex optimization problem (5.4) can be recovered from the optimal Youla parameter $Q^\star \in \mathcal{S}$ through a suitable linear fractional transformation (cf. Theorem 3 of [16]).

Remark 5.2 *If the state-space matrix* A *specified in the generalized plant* (5.2) *is of dimension* $s \times s$, *then the resulting optimal controller* $K^\star$ *admits a state-space realization of order* $s + q_2 d$. *As argued in [16], this is at worst within a constant factor of the minimal realization order.*

5.3.2 Communication Delay Co-Design via Convex Optimization

Although our objective is to design the communication graph on which the distributed controller K is implemented, for the computational reasons described in §5.3.1 it is preferable to solve a problem in terms of the Youla parameter Q as this leads to the convex optimization problems (5.6) and (5.7). In order to perform the communication architecture/control law co-design task in the Youla domain, we restrict ourselves to designing strongly connected communication architectures that generate QI subspaces, i.e., subspaces that are QI and that admit a decomposition of the form (5.5). As argued in §5.1, this is a practically relevant class of communication architectures to consider, and further, based on the previous discussion it is then possible to solve for the resulting distributed optimal controller restricted to the designed communication architecture using the results of Theorem 5.1.

Our approach to accomplish the co-design task is to remove the subspace constraint $\mathfrak{C}(V) \in \mathcal{Y}$, which encodes the distributed structure of the controller, from the optimization problem (5.7) and to augment the objective of the optimization problem with a convex penalty function that instead induces suitable structure in $\mathfrak{C}(V)$. In particular, we seek a convex penalty function $\|\cdot\|_{\text{comm}}$ and horizon d such that the structure of $\mathfrak{C}(V^\star)$, where $V^\star$ is the solution to

$$\underset{V \in \mathcal{RH}_\infty^{\leq d}}{\text{minimize}} \quad \|\mathfrak{L}(V)\|_{\mathcal{H}_2}^2 + \lambda \|\mathfrak{C}(V)\|_{\text{comm}}, \tag{5.9}$$

can be used to define an appropriate QI subspace $\mathcal{S}$ that admits a decomposition of the form (5.5). Imposing that the designed subspace $\mathcal{S}$ be QI ensures that the structure induced in $\mathfrak{C}(V^\star)$ corresponds to the structure of the resulting distributed controller $K^\star$. Further imposing that the designed subspace $\mathcal{S}$ admit a decomposition of the form (5.5) ensures that the distributed optimal controller restricted to lie in the subspace $\mathcal{S}$ can be computed using Theorem 5.1.

Remark 5.3 *The regularization weight $\lambda \geq 0$ allows the controller designer to trade-*

off between closed loop performance (as measured by $\|\mathfrak{L}(V)\|_{\mathcal{H}_2}^2$*) and communication complexity (as measured by* $\|\mathfrak{C}(V)\|_{\text{comm}}$*).*

In order to define an appropriate convex penalty $\|\cdot\|_{\text{comm}}$, we need to understand how a communication graph between sub-controllers defines the subspace $\mathcal{Y}$ in which $\mathfrak{C}(V)$ is constrained to lie in optimization problem (5.7) – this in turn informs what structure to induce in $\mathfrak{C}(V^\star)$ in the regularized optimization problem (5.9). To that end, in §5.4 we define a simple communication protocol between sub-controllers that allows communication graphs to be associated with distributed subspace constraints in a natural way. Within this framework, we show that if a communication graph generates a distributed subspace $\mathcal{S}$ that is QI with respect to G_{22}, then adding additional communication links to this graph preserves the QI property of the distributed subspace that it generates. We use this observation to pose the communication architecture design problem as one of augmenting a suitably defined base communication graph, namely a simple graph that generates a QI subspace, with additional communication links.

5.4 Communication Graphs and Quadratically Invariant Subspaces

This section first shows how a communication graph connecting sub-controllers can be used to define the subspace $\mathcal{S}$ in which the controller K is constrained to lie in the distributed optimal control problem (5.4). In particular, if two sub-controllers exchange information using the shortest path between them on an underlying communication graph, then there is a natural way of generating a subspace constraint from the adjacency matrix of that graph. Under this information exchange protocol, we then define a set of strongly connected communication graphs that generate subspace constraints that are QI with respect to a plant G_{22} in terms of a *base* and a *maximal* communication graph. This approach allows the controller designer to specify which communication links between sub-controllers are *physically realizable*,

i.e., which communication links can be built subject to the physical constraints of the system.

5.4.1 Generating Subspaces from Communication Graphs

Consider a generalized plant (5.2) comprised of n sub-plants, each equipped with its own sub-controller. Let $\mathcal{N} := \{1, \ldots, n\}$ and label each sub-controller by a number $i \in \mathcal{N}$. To each such sub-controller i associate a space of possible control actions $\mathcal{U}_i = \ell_{2,e}^{p_{2,i}}$ and a space of possible output measurements $\mathcal{Y}_i = \ell_{2,e}^{q_{2,i}}$, and define the overall control and measurement spaces as $\mathcal{U} := \mathcal{U}_1 \times \cdots \times \mathcal{U}_n$ and $\mathcal{Y} := \mathcal{Y}_1 \times \cdots \times \mathcal{Y}_n$, respectively.

Then, for any pair of sub-controllers i and j, the $(i,j)^{\text{th}}$ block of G_{22} is the mapping from the control action $\mathbf{u}_j$ taken by sub-controller j to the measurement $\mathbf{y}_i$ of sub-controller i, i.e., $(G_{22})_{ij} : \mathcal{U}_j \to \mathcal{Y}_i$. Similarly, the mapping from the measurement $\mathbf{y}_j$, transmitted by sub-controller j, to the control action $\mathbf{u}_i$ taken by sub-controller i is given by $K_{ij} : \mathcal{Y}_j \to \mathcal{U}_i$.

We then form the overall measurement and control vectors

$$\mathbf{y} = \begin{bmatrix} (\mathbf{y}_1)^\top & \cdots & (\mathbf{y}_n)^\top \end{bmatrix}^\top, \qquad \mathbf{u} = \begin{bmatrix} (\mathbf{u}_1)^\top & \cdots & (\mathbf{u}_n)^\top \end{bmatrix}^\top \tag{5.10}$$

leading to the natural block-wise partitions of the plant G_{22}

$$G_{22} = \begin{bmatrix} (G_{22})_{11} & \cdots & (G_{22})_{1n} \\ \vdots & \ddots & \vdots \\ (G_{22})_{n1} & \cdots & (G_{22})_{nn} \end{bmatrix} \tag{5.11}$$

and of the controller K

$$K = \begin{bmatrix} K_{11} & \cdots & K_{1n} \\ \vdots & \ddots & \vdots \\ K_{n1} & \cdots & K_{nn} \end{bmatrix}. \tag{5.12}$$

We assume that sub-controllers exchange measurements with each other subject to

delays imposed by an underlying communication graph – specifically, we assume that sub-controller i has access to sub-controller j's measurement $\mathbf{y}_j$ with delay specified by the length of the shortest path from sub-controller j to sub-controller i in the communication graph. Formally, let Γ be the adjacency matrix of the communication graph between sub-controllers, i.e., Γ is the integer matrix with rows and columns indexed by $\mathcal{N}$, such that Γ_{kl} is equal to 1 if there is an edge from l to k, and 0 otherwise. The *communication delay* from sub-controller j to sub-controller i is then given by the length of the shortest path from j to i as specified by the adjacency matrix gamma Γ. In particular, we define[5] the communication delay from sub-controller j to sub-controller i to be given by

$$c_{ij} := \min \left\{ d \in \mathbb{Z}_+ \,\middle|\, \Gamma_{ij}^d \neq 0 \right\} \tag{5.13}$$

if an integer satisfying the condition in (5.13) exists, and set $c_{ij} = \infty$ otherwise.

We say that a strictly proper distributed controller K can be *implemented* on a communication graph with adjacency matrix Γ if for all $i, j \in \mathcal{N}$, we have that the the (i,j)th block of the controller K satisfies $K_{ij}^{(t)} = 0$ for all positive integers $t \leq c_{ij}$, or equivalently, that $K_{ij} \in \frac{1}{z^{c_{ij}+1}} \mathcal{R}_p$. In words, this says that sub-controller j only has access to the measurement $\mathbf{y}_i$ from sub-controller i after c_{ij} time steps, the length of the shortest path from j to i in the communication graph, and can only take actions based on this measurement after a computational delay of one time step.[6] More succinctly, this condition holds if $\operatorname{bsupp}\left(K^{(t)}\right) \subseteq \operatorname{supp}\left(\Gamma^{t-1}\right)$ for all $t \geq 1$.

If Γ is the adjacency matrix of a strongly connected graph, then there exists a path between all ordered pairs of sub-controllers $(i,j) \in \mathcal{N} \times \mathcal{N}$ – this implies that there exists a positive delay $d(\Gamma)$ after which a given measurement $\mathbf{y}_j$ is available to all sub-controllers. In particular, we define the delay $d(\Gamma)$ associated with the adjacency matrix Γ to be

$$d\left(\Gamma\right) := \sup \left\{ \tau \in \mathbb{Z}_{++} \,\middle|\, \exists (k,l) \in \mathcal{N} \times \mathcal{N} \text{ s.t. } \Gamma_{kl}^{\tau-1} = 0 \right\}. \tag{5.14}$$

[5] See Lemma 8.1.2 of [92] for a graph theoretic justification of this definition.

[6] This computational delay is included to ensure that the resulting controller is strictly proper.

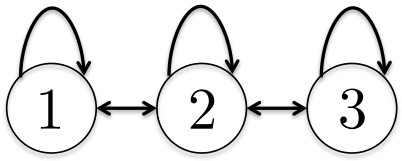

Figure 5.2: Three subsystem chain example

Using this convention all measurements $y_j^{(t)}$ are available to all sub-controllers by time $t + d(\Gamma) + 1$. When the delay $d(\Gamma)$ is finite, we say that Γ is a *strongly connected adjacency matrix*, as it defines a strongly connected communication graph.

We define the subspace $\mathcal{S}(\Gamma)$ generated by a strongly connected adjacency matrix Γ to be

$$\mathcal{S}(\Gamma) := \mathcal{Y}(\Gamma) \oplus \frac{1}{z^{d(\Gamma)+1}}\mathcal{R}_p, \tag{5.15}$$

where $d(\Gamma)$ is as defined in (5.14), and $\mathcal{Y}(\Gamma) := \oplus_{t=1}^{d} \frac{1}{z^t}\mathcal{Y}^{(t)}(\Gamma)$ is specified by the subspaces

$$\mathcal{Y}^{(t)}(\Gamma) := \left\{ M \in \mathbb{R}^{p_2 \times q_2} \,\middle|\, \text{bsupp}\,(M) \subseteq \text{supp}\left(\Gamma^{t-1}\right) \right\}. \tag{5.16}$$

It is then immediate that a controller K can be implemented on the communication graph Γ if and only if $K \in \mathcal{S}(\Gamma)$.

Example 5.1 *Consider the communication graph illustrated in Figure 5.2 with strongly connected adjacency matrix $\Gamma_{3\text{-}chain}$ given by*

$$\Gamma_{3\text{-}chain} = \begin{bmatrix} 1 & 1 & 0 \\ 1 & 1 & 1 \\ 0 & 1 & 1 \end{bmatrix}. \tag{5.17}$$

This communication graph generates the subspace

$$\mathcal{S}(\Gamma_{3\text{-}chain}) := \frac{1}{z}\begin{bmatrix} * & 0 & 0 \\ 0 & * & 0 \\ 0 & 0 & * \end{bmatrix} \oplus \frac{1}{z^2}\begin{bmatrix} * & * & 0 \\ * & * & * \\ 0 & * & * \end{bmatrix} \oplus \frac{1}{z^3}\mathcal{R}_p, \tag{5.18}$$

where $*$ is used to denote a space of appropriately sized real matrices. The communi-

cation delays associated with this graph are then given by $c_{ij} = |i-j|$ *(e.g.,* $c_{11} = 0$*,* $c_{12} = 1$ *and* $c_{13} = 2$*). We also have that* $d(\Gamma_{\textit{3-chain}}) = 2$*, which is the length of the longest path between nodes in this graph, and that*

$$\mathcal{Y}(\Gamma_{\textit{3-chain}}) = \frac{1}{z}\begin{bmatrix} * & 0 & 0 \\ 0 & * & 0 \\ 0 & 0 & * \end{bmatrix} \oplus \frac{1}{z^2}\begin{bmatrix} * & * & 0 \\ * & * & * \\ 0 & * & * \end{bmatrix} \subset \mathcal{RH}_\infty^{\leq 2}.$$

■

Thus, given such a strongly connected adjacency matrix Γ, the distributed optimal controller $K^\star$ implemented using the graph specified by Γ can be obtained by solving the optimization problem (5.4) with subspace constraint $\mathcal{S}(\Gamma)$ – however, this optimization problem can only be reformulated as the convex programs (5.6) and (5.7) if the subspace $\mathcal{S}(\Gamma)$ is QI with respect to G_{22} [77].

5.4.2 Quadratically Invariant Communication Graphs

The discussion of §5.3 and §5.4.1 shows that communication graphs that are strongly connected and that generate a subspace (5.15) that is QI with respect to G_{22} allow for the distributed optimal control problem (5.4) to be solved via the finite dimensional convex program (5.7). In this subsection, we characterize a set of such communication graphs in terms of a *base QI* and a *maximal QI communication graph* corresponding to a plant G_{22}. The base QI communication graph defines a simple communication architecture that generates a QI subspace, whereas the maximal QI communication graph is the densest communication architecture that can be built given the physical constraints of the system.

We assume that the sub-controllers have disjoint measurement and actuation channels, i.e., that B_2 and C_2 are block-diagonal, and that the dynamics of the system are strongly connected, i.e., that $\text{bsupp}\,(A)$ corresponds to the adjacency matrix of a strongly connected graph. We discuss alternative approaches for when these assumptions do not hold in §5.7. For the sake of brevity, we often refer to a communication

graph by its adjacency matrix Γ.

The base QI communication graph

Our objective is to identify a simple communication graph, i.e., a graph defined by a sparse adjacency matrix Γ_{base}, such that the resulting subspace $\mathcal{S}(\Gamma_{\text{base}})$ is QI with respect to G_{22}. To that end, let the *base QI communication graph* of plant G_{22} with realization (5.2) be specified by the adjacency matrix

$$\Gamma_{\text{base}} := \text{bsupp}\,(A)\,. \tag{5.19}$$

Notice that under the block-diagonal assumptions imposed on the state-space parameters B_2 and C_2, this implies that Γ_{base} mimics or is a superset of the physical topology of the plant G_{22}, as $\text{bsupp}\left(G_{22}^{(t)}\right) = \text{bsupp}\,(C_2A^{t-1}B_2) \subseteq \text{bsupp}\,(A)^{t-1}$.

Define the *propagation delay* from sub-plant j to sub-plant i of a plant G_{22} to be the largest integer p_{ij} such that

$$(G_{22})_{ij} \in \frac{1}{z^{p_{ij}}}\mathcal{R}_p. \tag{5.20}$$

It is shown in [10] that if a subspace $\mathcal{S}$ constrains the blocks of the controller K to satisfy $K_{kl} \in \frac{1}{z^{c_{kl}+1}}\mathcal{R}_p$, and the communication delays[7] $\{c_{kl}\}$ satisfy the triangle inequality $c_{ki} + c_{ij} \geq c_{kj}$, then $\mathcal{S}$ is QI with respect to G_{22} if

$$c_{ij} \leq p_{ij} + 1 \tag{5.21}$$

for all $i, j \in \mathcal{N}$. An intuitive interpretation of this condition is that $\mathcal{S}$ is QI if it allows sub-controllers to communicate with each other as fast as their control actions propagate through the plant. Since we take the base QI communication graph Γ_{base} to mimic the topology of the plant G_{22}, we expect this condition to hold and for $\mathcal{S}(\Gamma_{\text{base}})$ to be QI with respect to G_{22}. We formalize this intuition in the following lemma.

[7] These are equivalent to the prior definition (5.13) of communication delays $\{c_{kl}\}$.

Lemma 5.1 *Let the plant G_{22} be specified by state-space parameters (A, B_2, C_2), and suppose that B_2 and C_2 are block diagonal. Let $\{p_{ij}\}$ denote the propagation delays of the plant G_{22} as defined in* (5.20)*. Assume that Γ_{base}, as specified as in equation* (5.19)*, is a strongly connected adjacency matrix, and let $\{b_{ij}\}$ denote the communication delays* (5.13) *imposed by the adjacency matrix Γ_{base}. The communication delays $\{b_{ij}\}$ then satisfy condition* (5.21) *and the subspace $\mathcal{S}(\Gamma_{base})$ is quadratically invariant with respect to G_{22}.*

Proof: The definition of the base QI communication graph Γ_{base} and the assumption that B_2 and C_2 are block-diagonal imply that $\text{bsupp}\left(G_{22}^{(t)}\right) \subseteq \text{bsupp}\left(A^{t-1}\right) \subseteq \text{supp}\left(\Gamma_{\text{base}}^{t-1}\right)$. This in turn can be verified to guarantee that (5.21) holds. Thus it suffices to show that the communication delays $\{b_{kl}\}$ satisfy the triangle inequality $b_{ki} + b_{ij} \geq b_{kj}$ for all $i, j, k \in \mathcal{N}$. First observe that (i) $b_{ii} + b_{ii} \geq b_{ii}$, and (ii) $b_{ii} + b_{ij} \geq b_{ij}$, as all $b_{ij} \geq 0$. Thus it remains to show that $b_{ki} + b_{ij} \geq b_{kj}$ for $i \neq j \neq k$. Suppose, seeking contradiction, that

$$b_{ki} + b_{ij} < b_{kj}. \tag{5.22}$$

Note that by definition (5.13) of the communication delays and Lemma 8.1.2 of [92], the inequality (5.22) is equivalent to

$$\begin{aligned}\min\{r \,|\, \exists \text{ path of length } r \text{ from } i \text{ to } k\} + \min\{r \,|\, \exists \text{ path of length } r \text{ from } j \text{ to } i\} \\ < \min\{r \,|\, \exists \text{ path of length } r \text{ from } j \text{ to } k\}.\end{aligned} \tag{5.23}$$

Notice however that we must have that

$$\begin{aligned}&\min\{r \,|\, \exists \text{ path of length } r \text{ from } j \text{ to } k\} \leq \\ &\min\{r \,|\, \exists \text{ path of length } r \text{ from } j \text{ to } i\} + \min\{r \,|\, \exists \text{ path of length } r \text{ from } i \text{ to } k\},\end{aligned} \tag{5.24}$$

as the concatenation of a path from j to i and a path from i to k yields a path from

j to k. Combining inequalities (5.22) and (5.24) yields the desired contradiction, proving the result. ■

Lemma 5.1 thus provides a simple means of constructing a base QI communication graph by taking a communication topology that mimics the physical topology of the plant G_{22}.

Augmenting the base QI communication graph

The delay condition (5.21) suggests that a natural way of constructing QI communication architectures given a base QI communication graph is to augment the base graph with additional communication links, as adding a link to a communication graph can only decrease its communication delays c_{ij}.

Proposition 5.1 *Let Γ_{base} be defined as in* (5.19)*, and let Γ be an adjacency matrix satisfying* $\operatorname{supp}(\Gamma_{base}) \subset \operatorname{supp}(\Gamma)$*. Then the generated subspace $\mathcal{S}(\Gamma)$, as defined in* (5.15)*, is quadratically invariant with respect to G_{22}.*

Proof: Let $\{b_{ij}\}$ and $\{c_{ij}\}$ denote the communication delays associated with the base QI communication graph Γ_{base} and the augmented communication graph Γ, respectively. It follows from the definition of the communication delays (5.13) that the support nesting condition $\operatorname{supp}(\Gamma_{\text{base}}) \subset \operatorname{supp}(\Gamma)$ implies that $b_{ij} \geq c_{ij}$ for all $i, j \in \mathcal{N}$. By Lemma 5.1 we have that $b_{ij} \leq p_{ij} + 1$, and therefore $c_{ij} \leq b_{ij} \leq p_{ij} + 1$. An identical argument to that used to prove Lemma 5.1 shows that the delays c_{ij} satisfy the required triangle inequality, implying that $\mathcal{S}(\Gamma)$ is QI with respect to G_{22}.

■

In words, the nesting condition $\operatorname{supp}(\Gamma_{\text{base}}) \subset \operatorname{supp}(\Gamma)$ simply means that the communication graph Γ can be constructed by adding communication links to the base QI communication graph Γ_{base}. It follows that any graph built by augmenting Γ_{base} with additional communication links generates a QI subspace (5.15).

Remark 5.4 *Although we have suggested a specific construction for Γ_{base}, Proposition 5.1 makes clear that any strongly connected graph that generates a subspace*

constraint that is QI with respect to G_{22} can be used as the base QI communication graph. We discuss the implications of this added flexibility in §5.7.

The maximal QI communication graph

In order to augment the base QI communication graph in a physically relevant way, one must first specify what additional communication links can be built given the physical constraints of the system. For example, if two sub-controllers are separated by a large physical distance, it may not be possible to build a direct communication link between them. The set of additional communication links that can be physically constructed is application dependent – we therefore assume that the controller designer has specified a collection $\mathscr{E}$ of directed edges that define what communication links can be built in addition to those already present in the base QI communication graph. In particular, we assume that it is possible to build a direct communication link from sub-controller j to sub-controller i, i.e., to build a communication graph $\Gamma_{\text{built}} = \Gamma_{\text{base}} + \Gamma$ with $\Gamma_{ij} = 1$, only if $(i, j) \in \mathscr{E}$.

Given a collection of directed edges $\mathscr{E}$, the *maximal QI communication graph* $\Gamma_{\max}$ is given by

$$\Gamma_{\max} := \Gamma_{\text{base}} + M, \tag{5.25}$$

where M is a $n \times n$ dimensional matrix with M_{ij} set to 1 if $(i, j) \in \mathscr{E}$ and 0 otherwise. In words, the maximal QI adjacency matrix $\Gamma_{\max}$ specifies a communication graph that uses all possible communication links listed in the set $\mathscr{E}$, in addition to those links already used by the base QI communication graph. Consequently, we say that a communication graph can be *physically built* if its adjacency matrix Γ satisfies

$$\operatorname{supp}(\Gamma) \subseteq \operatorname{supp}(\Gamma_{\max}), \tag{5.26}$$

i.e., if it can be built from communication links used by the base QI communication graph and/or those listed in the set $\mathscr{E}$.

The QI communication graph design set

We now define a set of strongly connected and physically realizable communication graphs that generate QI subspace constraints as specified in equation (5.15) – in particular, the base and maximal QI graphs correspond to the boundary points of this set.

Proposition 5.2 *Given a plant G_{22} and a set of directed edges $\mathscr{E}$, let the adjacency matrices Γ_{base} and $\Gamma_{\max}$ of the base and maximal QI communication graphs be defined as in* (5.19) *and* (5.25)*, respectively. Then an adjacency matrix Γ corresponds to a strongly connected communication graph that can be physically built and that generates a quadratically invariant subspace $\mathcal{S}(\Gamma)$ of the form* (5.15) *if*

$$\operatorname{supp}(\Gamma_{base}) \subseteq \operatorname{supp}(\Gamma) \subseteq \operatorname{supp}(\Gamma_{\max}). \tag{5.27}$$

Proof: Follows from Prop. 5.1 and definitions (5.25) and (5.26). ∎

The following corollary is then immediate.

Corollary 5.1 *Let Γ_1 and Γ_2 be adjacency matrices that satisfy the nesting condition* (5.27) *and suppose further that* $\operatorname{supp}(\Gamma_1) \subseteq \operatorname{supp}(\Gamma_2)$*. Let $\delta_\bullet$, with $\bullet \in \{base, 1, 2, \max\}$ be the closed loop norm achieved by the optimal distributed controller implemented using communication graph $\Gamma_\bullet$. Then*

$$d(\Gamma_{base}) \geq d(\Gamma_1) \geq d(\Gamma_2) \geq d(\Gamma_{\max}), \tag{5.28}$$

$$\mathcal{S}(\Gamma_{base}) \subseteq \mathcal{S}(\Gamma_1) \subseteq \mathcal{S}(\Gamma_2) \subseteq \mathcal{S}(\Gamma_{\max}), \tag{5.29}$$

and

$$\delta_{base} \geq \delta_1 \geq \delta_2 \geq \delta_{\max} \tag{5.30}$$

Proof: Relations (5.28) and (5.29) follow immediately from the hypotheses of the corollary and the definitions of the delays $d(\Gamma_\bullet)$ and the subspaces $\mathcal{S}(\Gamma_\bullet)$ as given in (5.14) and (5.15), respectively. The condition (5.30) on the norms $\delta_\bullet$ follows immediately from the subspace nesting condition (5.29) and the fact that the optimal norm $\delta_\bullet$ achievable by a distributed controller implemented using a communication graph with adjacency matrix $\Gamma_\bullet$ is specified by the optimal value of the objective function of the optimization problem (5.4) with distributed constraint $\mathcal{S}(\Gamma_\bullet)$. ∎

Corollary 5.1 states that as more edges are added to the base QI communication graph, the performance of the optimal distributed controller implemented on the resulting communication graph improves. Thus there is a quantifiable tradeoff between the communication complexity and the closed loop performance of the resulting distributed optimal controller. To fully explore this tradeoff, the controller designer would have to enumerate the *QI communication graph design set* which is composed of adjacency matrices satisfying the nesting condition (5.27). Denoting this set by $\mathscr{G}$, a simple computation shows that $|\mathscr{G}| = 2^{|\mathscr{E}|}$ – thus the controller designer has to consider a set of graphs of cardinality exponential in the number of possible additional communication links. This poor scaling motivates the need for a principled approach to exploring the design space of communication graphs via the regularized optimization problem (5.9).

5.5 The Communication Graph Co-Design Algorithm

In this section we leverage Propositions 5.1 and 5.2 as well as tools from approximation theory [20], [66] to construct a convex penalty function $\|\cdot\|_{\text{comm}}$, which we call the *communication link norm*, that allows the controller designer to explore the QI communication graph design set $\mathscr{G}$ in a principled manner via the regularized convex optimization problem (5.9). We then propose a communication architecture/control law co-design algorithm based on this optimization problem and show that it indeed does produce strongly connected communication graphs that generate quadratically invariant subspaces.

5.5.1 The Communication Link Norm

Recall that our approach to the co-design task is to induce suitable structure in the expression $\mathfrak{C}(V^\star)$, where $V^\star$ is the solution to the regularized convex optimization problem (5.9) employing the yet to be specified convex penalty function $\|\cdot\|_{\text{comm}}$. We argued that the structure induced in the expression $\mathfrak{C}(V^\star)$ should correspond to a strongly connected communication graph that generates a QI subspace of the form (5.5), and characterized a set of graphs satisfying these properties, namely the QI communication graph design set $\mathscr{G}$. To explore the QI communication graph design set $\mathscr{G}$, we begin with the base QI communication graph Γ_{base} and augment it with additional communication links drawn from the set $\mathscr{E}$. The convex penalty function $\|\cdot\|_{\text{comm}}$ used in the regularized optimization problem (5.9) should therefore penalize the use of such additional communication links – in this way the controller designer can tradeoff between communication complexity and closed loop performance by varying the regularization weight λ in optimization problem (5.9).

We view distributed controllers implemented using a dense communication graph as being composed of a superposition of simple *atomic* controllers that are implemented using simple communication graphs, i.e., using communication graphs obtained by adding a small number of edges to the base QI communication graph. This viewpoint suggests choosing the convex penalty function $\|\cdot\|_{\text{comm}}$ to be an atomic norm [20, 66, 90].

Indeed, if one seeks a solution $X^\star$ that can be composed as a linear combination of a small number of atoms drawn from a set $\mathscr{A}$, then a useful approach, as described in [20, 67, 69, 70, 93–95], to induce such structure in the solution of an optimization problem is to employ a convex penalty function that is given by the atomic norm induced by the atoms $\mathscr{A}$ [66, 90]. Examples of the types of structured solutions one may desire include sparse, group sparse and signed vectors, and low-rank, permutation and orthogonal matrices [20]. Specifically, if one desires a solution $X^\star$ that admits a

decomposition of the form

$$X^\star = \sum_{i=1}^{r} c_i A_i,\ A_i \in \mathscr{A},\ c_i \geq 0 \tag{5.31}$$

for a set of appropriately scaled and centered atoms $\mathscr{A}$, and a small number r relative to the ambient dimension, then solving

$$\underset{X}{\text{minimize}} \quad \|\mathfrak{A}(X)\|_{\mathcal{H}_2}^2 + \lambda \|X\|_{\mathscr{A}} \tag{5.32}$$

with $\mathfrak{A}(\cdot)$ an affine map, and the atomic norm $\|\cdot\|_{\mathscr{A}}$ given by[8]

$$\|X\|_{\mathscr{A}} := \inf \left\{ \textstyle\sum_{A \in \mathscr{A}} c_A \,\middle|\, X = \sum_{A \in \mathscr{A}} c_A A,\ c_A \geq 0 \right\} \tag{5.33}$$

results in solutions that are both consistent with the data as measured in terms of the cost function $\|\mathfrak{A}(X)\|_{\mathcal{H}_2}^2$, and that admit sparse atomic decompositions, i.e., that are a combination of a small number of elements from $\mathscr{A}$.

We can therefore fully characterize our desired convex penalty function $\|\cdot\|_{\text{comm}}$ by specifying its defining atomic set $\mathscr{A}_{\text{comm}}$ and then invoking definition (5.33). As alluded to earlier, we choose the atoms in $\mathscr{A}_{\text{comm}}$ to correspond to distributed controllers implemented on communication graphs that can be constructed by adding a small number of communication links from the set of allowed edges $\mathscr{E}$ to the base QI communication graph Γ_{base}. In order to avoid introducing additional notation we describe the atomic set specified by communication graphs that can be constructed by adding a single communication link from the set $\mathscr{E}$ to the base QI communication graph Γ_{base} – the presented concepts then extend to the general case in a natural way. We explain why a controller designer may wish to construct an atomic set specified by more complex communication graphs in §5.7.

[8] If no such decomposition exists, then $\|X\|_{\mathscr{A}} = \infty$.

The atomic set $\mathscr{A}_{\mathbf{comm}}$

To each communication link $(i,j) \in \mathscr{E}$ we associate the subspace $\mathcal{E}_{ij}$ given by

$$\mathcal{E}_{ij} := \mathcal{S}^{\perp}(\Gamma_{\text{base}}) \cap \mathcal{S}(\Gamma_{\text{base}} + E_{ij}). \tag{5.34}$$

Each subspace $\mathcal{E}_{ij}$ encodes the additional information available to the controller, relative to the base communication graph Γ_{base}, that is uniquely due to the added communication link (i,j) from sub-controller j to sub-controller i. Note that the subspaces $\mathcal{E}_{ij}$ are finite dimensional due to the strong connectedness assumption imposed on Γ_{base}, which leads to the equality $\mathcal{S}^{\perp}(\Gamma_{\text{base}}) = \mathcal{Y}^{\perp}(\Gamma_{\text{base}}) \cap \mathcal{RH}_{\infty}^{\leq d(\Gamma_{\text{base}})}$.

Example 5.2 *Consider the base QI communication graph Γ_{base} illustrated in Figure 5.2 and specified by* (5.17)*. This communication graph generates the subspace $\mathcal{S}(\Gamma_{base})$ shown in* (5.18)*. We consider choosing from two additional links to augment the base communication graph Γ_{base}: a directed link from node 1 to node 3, and a directed link from node 3 to node 1. Then $\mathscr{E} = \{(1,3),(3,1)\}$ and the corresponding subspaces $\mathcal{E}_{ij}$ are given by*

$$\mathcal{E}_{13} = \tfrac{1}{z^2}\begin{bmatrix} 0 & 0 & 0 \\ 0 & 0 & 0 \\ * & 0 & 0 \end{bmatrix}, \mathcal{E}_{31} = \tfrac{1}{z^2}\begin{bmatrix} 0 & 0 & * \\ 0 & 0 & 0 \\ 0 & 0 & 0 \end{bmatrix}.$$

■

The atomic set is then composed of suitably normalized elements of these subspaces:

$$\mathscr{A}_{\text{comm}} := \bigcup_{(i,j)\in\mathscr{E}} \left\{ A \in \mathcal{E}_{ij} \,\middle|\, \|A\|_{\mathcal{H}_2} = 1 \right\}. \tag{5.35}$$

Note that we normalize our atoms relative to the $\mathcal{H}_2$ norm as this norm is isotropic; hence this normalization ensures that no atom is preferred over another within the family of atoms defined by a subspace $\mathcal{E}_{ij}$. The resulting atomic norm, which we denote the *communication link norm*, is defined on elements $X \in \mathcal{RH}_{\infty}^{\leq d(\Gamma_{\text{base}})}$ and is

given by[9]

$$\begin{aligned} \|X\|_{\text{comm}} = \min_{A_{\text{base}},\{A_{ij}\}\in\mathcal{RH}_\infty^{\leq d(\Gamma_{\text{base}})}} \quad & \sum_{(i,j)\in\mathscr{E}} \|A_{ij}\|_{\mathcal{H}_2} \\ \text{s.t.} \quad & X = A_{\text{base}} + \sum_{(i,j)\in\mathscr{E}} A_{ij} \\ & A_{\text{base}} \in \mathcal{Y}(\Gamma_{\text{base}}) \\ & A_{ij} \in \mathcal{E}_{ij} \ \forall (i,j) \in \mathscr{E}, \end{aligned} \tag{5.36}$$

when this optimization problem is feasible – when it is not, we set $\|X\|_{\text{comm}} = \infty$. Applying definition (5.36) of the communication link norm to the regularized optimization problem (5.9) yields the convex optimization problem

$$\begin{aligned} \underset{V,A_{\text{base}},\{A_{ij}\}\in\mathcal{RH}_\infty^{\leq d(\Gamma_{\text{base}})}}{\text{minimize}} \quad & \|\mathfrak{L}(V)\|_{\mathcal{H}_2}^2 + \lambda \left(\sum_{(i,j)\in\mathscr{E}} \|A_{ij}\|_{\mathcal{H}_2} \right) \\ \text{s.t.} \quad & \mathfrak{C}(V) = A_{\text{base}} + \sum_{(i,j)\in\mathscr{E}} A_{ij} \\ & A_{\text{base}} \in \mathcal{Y}(\Gamma_{\text{base}}) \\ & A_{ij} \in \mathcal{E}_{ij} \ \forall (i,j) \in \mathscr{E}. \end{aligned} \tag{5.37}$$

Recall that in optimization problem (5.9) our approach to communication architecture design is to induce structure in the term $\mathfrak{C}(V)$ through the use of the communication link norm as a penalty function. Letting $\left(V^\star, \{A_{ij}^\star\}, A_{\text{base}}^\star\right)$ denote the solution to the optimization problem (5.37), we have that each nonzero $A_{ij}^\star$ in the atomic decomposition of $\mathfrak{C}(V)$ corresponds to an additional link from sub-controller j to sub-controller i being added to the base QI communication graph (in what follows we make precise how the structure of $\mathfrak{C}(V^\star)$ can be used to specify a communication graph). As desired, the communication link norm (5.36) penalizes the use of such additional links, and optimization problem (5.37) allows for a tradeoff between

[9] We apply definition (5.33) to the components of X that lie in $\mathcal{S}^\perp(\Gamma_{\text{base}})$ to obtain an atomic norm defined on elements of that space. We then introduce an unpenalized variable $A_{\text{base}} \in \mathcal{Y}(\Gamma_{\text{base}})$ to the atomic decomposition so that the resulting penalty function may be applied to elements $X \in \mathcal{RH}_\infty^{\leq d(\Gamma_{\text{base}})}$. The resulting penalty is actually a seminorm on $\mathcal{RH}_\infty^{\leq d(\Gamma_{\text{base}})}$ but we refer to it as a norm to maintain consistency with the terminology of [20].

communication complexity (as measured by $\sum_{(i,j)\in\mathscr{E}} \|A_{ij}\|_{\mathcal{H}_2}$) and closed loop performance (as measured by $\|\mathfrak{L}(V)\|^2_{\mathcal{H}_2}$) of the resulting distributed controller through the regularization weight λ. Note further that $A^\star_{\text{base}}$ is not penalized by the communication link norm, ensuring that the communication graph defined by the structure of $\mathfrak{C}(V^\star)$ has Γ_{base} as a subgraph.

Remark 5.5 *Optimization problem* (5.37) *is finite dimensional, and hence can be formulated as a second order cone program by associating the finite impulse response transfer matrices* $(V, A_{base}, \{A_{ij}\})$, $\mathfrak{C}(V)$ *and* $\mathfrak{L}(V)$ *with their matrix representations. To see this, note that* $\mathcal{Y}(\Gamma_{base}) \subseteq \mathcal{RH}_\infty^{\leq d(\Gamma_{base})}$, *and that by the discussion after the definition* (5.34) *of the subspaces* $\mathcal{E}_{ij}$, *they too satisfy* $\mathcal{E}_{ij} \subseteq \mathcal{RH}_\infty^{\leq d(\Gamma_{base})}$. *Thus the horizon* $d(\Gamma_{base})$ *over which the optimization problem* (5.37) *is solved is finite.*

5.5.2 Co-Design Algorithm and Solution Properties

In this section we formally define the communication architecture/control law co-design algorithm in terms of the optimization problem (5.37), and show that it can be used to co-design a strongly connected communication graph Γ that generates a QI subspace $\mathcal{S}(\Gamma)$ as defined in (5.15).

The co-design procedure is described in Algorithm 1. The algorithm consists of first solving the regularized optimization problem (5.37) to obtain solutions $\left(V^\star, \{A^\star_{ij}\}, A^\star_{\text{base}}\right)$. Using these solutions, we produce the designed communication graph Γ_{des} by augmenting the base QI communication graph Γ_{base} with all edges (i,j) such that $A^\star_{ij} \neq 0$. In particular, each non-zero term $A^\star_{ij}$ corresponds to an additional edge $(i,j) \in \mathscr{E}$ that the co-designed distributed control law will use – thus by varying the regularization weight λ the controller designer can control how much the use of an additional link is penalized by the optimization problem (5.37). As $\text{supp}\,(\Gamma_{\text{base}}) \subseteq \text{supp}\,(\Gamma_{\text{des}}) \subseteq \text{supp}\,(\Gamma_{\max})$ by construction, the designed communication graph Γ_{des} satisfies the assumptions of Proposition 5.2 – it is therefore strongly connected, can be physically built, and generates a subspace $\mathcal{S}(\Gamma_{\text{des}})$, according to (5.15), that is QI with respect to G_{22} and that admits a decomposition of the form (5.5). The subspace

input : regularization weight λ, generalized plant G, base QI communication graph Γ_{base}, edge set $\mathscr{E}$;
output : designed communication graph adjacency matrix Γ_{des}, optimal Youla parameter $Q^\star_{\text{des}} \in \mathcal{S}(\Gamma_{\text{des}})$;
initialize:: $\Gamma_{\text{des}} \leftarrow \Gamma_{\text{base}}$, $Q^\star_{\text{des}} \leftarrow 0$;
co-design communication graph
  $\left(V^\star, \{A^\star_{ij}\}, A^\star_{\text{base}}\right) \leftarrow$ solution to optimization problem (5.37) with regularization weight λ;
  foreach $(i,j) \in \mathscr{E}$ *s.t.* $A^\star_{ij} \neq 0$ **do**
    $\Gamma_{\text{des}} \leftarrow \Gamma_{\text{des}} + E_{ij}$;
  end
end
refine optimal controller
  $Q^\star_{\text{des}} \leftarrow$ solution to optimization problem (5.7) with distributed constraint $\mathcal{Y}(\Gamma_{\text{des}})$, as specified by Theorem 5.1;
end
return : Γ_{des}, $Q^\star_{\text{des}}$;

Algorithm 1: Communication Architecture Co-Design

$\mathcal{S}(\Gamma_{\text{des}})$ thus satisfies the assumptions of Theorem 5.1, meaning that the distributed optimal controller $K^\star_{\text{des}}$ restricted to the designed subspace $\mathcal{S}(\Gamma_{\text{des}})$ is specified in terms of the solution $Q^\star_{\text{des}}$ to the convex quadratic program (5.7). In this way the optimal distributed controller restricted to the designed communication architecture, as well as the performance that it achieves, can be computed exactly.

Although the solution $V^\star$ to optimization problem (5.37) could be used to generate a distributed controller that can be implemented on the designed communication graph Γ_{des}, we claim that it is preferable to use the solution $Q^\star_{\text{des}}$ to the non-regularized optimization problem (5.7). First, the use of the communication link norm penalty in the optimization problem (5.7) has the effect of shrinking the solution towards the origin. This means that the resulting controller specified by $V^\star$ is less aggressive, i.e., has smaller control gains, than the controller specified by the solution to the optimization problem (5.7) with subspace constraint $\mathcal{Y}(\Gamma_{\text{des}})$.

Second, notice that for two graphs Γ_{ij} and Γ_{kl} obtained by augmenting the base QI communication graph Γ_{base} with the communication links (i,j) and (k,l), respectively, it holds that $\mathcal{S}(\Gamma_{ij}) + \mathcal{S}(\Gamma_{kl}) \subseteq \mathcal{S}(\text{supp}\,(\Gamma_{ij} + \Gamma_{kl}))$, with the inclusion being strict in

general. In words, the linear superposition of the subspaces (5.15) generated by the two communications graphs Γ_{ij} and Γ_{kl} is in general a strict subset of the subspace generated by the single communication graph $\text{supp}\,(\Gamma_{ij} + \Gamma_{kl})$. Suppose now that the corresponding solutions $A^\star_{ij}$ and $A^\star_{kl}$ to optimization problem (5.37) are non-zero: then $\Gamma_{\text{des}} = \Gamma_{\text{base}} + E_{ij} + E_{kl}$, but the expression $\mathfrak{C}(V^\star)$ lies in the subspace given by $\mathcal{S}(\Gamma_{ij}) + \mathcal{S}(\Gamma_{kl})$. By the previous discussion $\mathcal{S}(\Gamma_{ij}) + \mathcal{S}(\Gamma_{kl}) \subset \mathcal{S}(\Gamma_{\text{des}})$, and thus we are imposing additional structure on the the expression $\mathfrak{C}(V^\star)$ relative to that imposed on the solution to the non-regularized optimization problem (5.7) with subspace constraint $\mathcal{Y}(\Gamma_{\text{des}})$. This can be interpreted as the controller specified by the structure of $\mathfrak{C}(V^\star)$ not utilizing paths in the communication graph that contain both links (i, j) and (k, l). These sources of conservatism in the control law are however completely removed if one uses the solution $Q^\star_{\text{des}}$ to the non-regularized optimization problem (5.7).

Thus we have met our objective of developing a convex optimization based procedure for co-designing a distributed optimal controller and the communication architecture upon which it is implemented. In the next section we discuss the computational complexity of the proposed method and illustrate its efficacy on numerical examples.

5.6 Computational Examples

We show that the number of scalar optimization variables needed to formulate the regularized optimization problem (5.37) scales, up to constant factors, in a manner identical to the number of variables needed to formulate the non-regularized optimization problem (5.7). We then illustrate the usefulness of our approach via two examples.

Computational Complexity

We assume that the number of control inputs p_2 and the number of measurements q_2 scale as $O(n)$, where n is the number of sub-controllers in the system, i.e., we assume that there is an order constant number of actuators and sensors at each sub-controller.

For an element $V \in \mathcal{RH}_\infty^{\leq d}$, each term $V^{(t)}$ in its power-series expansion is a real matrix of dimension $O(n) \times O(n)$, and thus V is defined by $O(n^2 d)$ scalar variables. The convex quadratic program (5.7) is therefore specified in terms of $O(n^2 d)$ variables.

To describe the number of scalar optimization variables in the regularized optimization problem (5.37), we need to take into account the contributions from V, A_{base} and $\{A_{ij}\}$. As per the discussion in the previous paragraph, V and A_{base} are composed of at most $O(n^2 d)$ scalar optimization variables. It can be checked that each A_{ij} has $O(d)$ optimization variables, and hence the collection $\{A_{ij}\}$ contributes $O(d|\mathscr{E}|)$ scalar optimization variables. Each sub-controller can have at most $O(n)$ additional links originating from it, and thus $|\mathscr{E}|$ scales, at worst, as $O(n^2)$. It follows that the regularized optimization problem (5.37) can also be specified in terms of $O(n^2 d)$ scalar optimization variables.

Finally, we note that the regularized optimization problem (5.37) is a second order cone program (SOCP) with at most $O(n^2 d)$ second order constraints. It therefore enjoys favorable iteration complexity that scales as $O(\sqrt{d}n)$ [96], and its per-iteration complexity is at worst $O(d^3 n^6)$ [97], but is typically much less when structure is exploited. In particular it is not atypical to solve a SOCP with tens to hundreds of thousands of variables [98]: noting that d scales at worst as $O(n)$, we therefore expect our method to be applicable to problems with hundreds of sub-controllers. Further, as we illustrate in the 20 sub-controller ring example below, the computational benefits of our approach compared to a brute force search are already tangible for systems with tens of sub-controllers.

6 sub-controller chain system

Consider a generalized plant (5.2) specified by a tridiagonal matrix $A_{\text{6-chain}} \in \mathbb{R}^{6\times 6}$ with randomly generated nonzero entries, $B_2 = C_2 = I_6$, $B_1 = C_1^\top = \begin{bmatrix} I_6 & 0_6 \end{bmatrix}$ and $D_{21} = D_{12}^\top = \begin{bmatrix} 0_6 & I_6 \end{bmatrix}$. The physical topology of the plant G_{22} is that of a 6 subsystem chain (a 3 subsystem chain is illustrated in Figure 5.2), and therefore the base QI communication graph $\Gamma_{\text{6-chain}} = \text{bsupp}\,(A_{\text{6-chain}})$ also defines a 6 sub-controller chain.

We define the set of edges that can be added to the base graph to be

$$\mathscr{E} = \{(i,j) \in \mathcal{N} \times \mathcal{N} \,\big|\, |i-j| = 2\}, \tag{5.38}$$

i.e., the communication graph/control law co-design task consists of determining which additional directed communication links between second neighbors should be added to the base QI communication graph $\Gamma_{\text{6-chain}}$ to best improve the performance of the distributed optimal controller implemented on the resulting augmented communication graph.

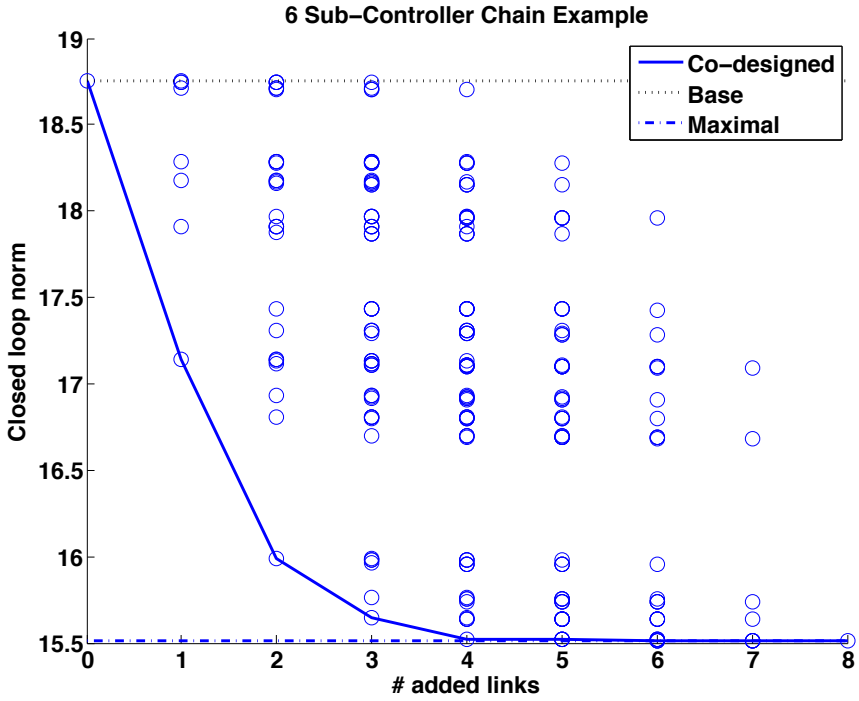

Figure 5.3: The closed loop norms achieved by distributed optimal controllers implemented on communication graphs constructed by adding $k = 1, \ldots, |\mathscr{E}|$ links to the base QI communication graph $\Gamma_{\text{6-chain}}$ are plotted as circles. The solid line denotes the performance achieved by distributed optimal controllers implemented on the communication graphs identified by the co-design procedure described in Algorithm 1. The dotted/dashed lines indicate the closed loop norm achieved by the distributed optimal controllers implemented on the base and maximal QI communication graphs, respectively.

In order to assess the efficacy of the proposed method in uncovering communication topologies that are well suited to distributed optimal control, we first computed

the optimal closed loop performance achievable by a distributed controller implemented on every possible communication graph that can be constructed by augmenting the base QI communicating graph $\Gamma_{\text{6-chain}}$ with $k = 1, \ldots, |\mathscr{E}|$ additional links drawn from the set $\mathscr{E}$. In particular, we exhaustively explored the QI communication graph set $\mathscr{G}$ and computed the achievable closed loop norms – these closed loop norms are plotted as blue circles in Figure 5.3. We then performed the co-design procedure described in Algorithm 1 for different values of regularization weight $\lambda \in [0, 50]$. The resulting closed loop norms achieved by the co-designed communication architecture/control law are plotted as a solid blue line in Figure 5.3. We also plot the closed loop norms achieved by controllers implemented using the base and maximal QI communication graphs.

We observe that as the regularization weight λ is increased, simpler communication topologies are generated by the co-design procedure. Further, our algorithm is able to successfully identify the optimal communication topology and the corresponding distributed optimal control law for every fixed number of additional links.

20 sub-controller ring system

Consider a generalized plant (5.2) specified by a matrix $A_{\text{20-ring}} \in \mathbb{R}^{20\times 20}$ with (i,j)th entry set to a nonzero randomly generated number if $|i-j| \leq 1$ where the subtraction is modulo 20 (e.g., 1-20 = 1), and 0 otherwise. The additional state-space parameters are given by $B_2 = C_2 = I_{20}$, $B_1 = C_1^\top = \begin{bmatrix} I_{20} & 0_{20} \end{bmatrix}$ and $D_{21} = D_{12}^\top = \begin{bmatrix} 0_{20} & I_{20} \end{bmatrix}$. For the example considered below, $|\lambda_{\max}(A_{\text{20-ring}})| = 2.91$. The physical topology of the plant G_{22} is that of a 20 subsystem ring, i.e., a chain topology with first and last nodes connected, and therefore the base QI communication graph $\Gamma_{\text{20-ring}} = \text{bsupp}\,(A_{\text{20-ring}})$ also defines a 20 sub-controller ring. We again define the set of edges $\mathscr{E}$ that can be added to the base graph to be those between second neighbors as in (5.38). In this case, the QI communication graph set $\mathscr{G}$ is too large to exhaustively explore: in particular $|\mathscr{G}| = 2^{40} \approx 10^{12}$. We performed the co-design procedure described in Algorithm 1 for different values of regularization weight $\lambda \in [0, 1000]$. The resulting closed loop norms achieved by the co-designed communication architecture/control

law are plotted as a solid blue line in Figure 5.4. We also plot the closed loop norms achieved by controllers implemented using the base and maximal QI communication graphs. We observe again that as the regularization weight λ is increased, simpler and simpler communication topologies are designed. Notice that our method selected 10 carefully placed communication links to add to the base QI communication graph, leading to a closed loop performance only 2% higher than that achieved by the optimal controller implemented using the maximal QI communication graph.

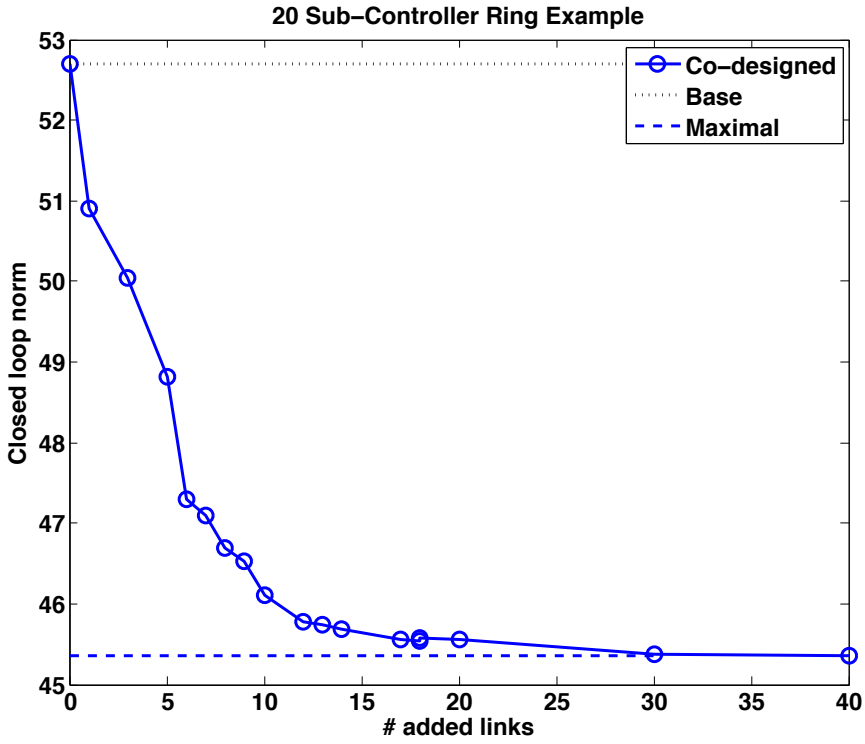

Figure 5.4: The solid line denotes the performance achieved by distributed optimal controllers implemented on the communication graphs identified by the co-design procedure described in Algorithm 1. The dotted and dashed lines indicate the closed loop norm achieved by the distributed optimal controllers implemented on the base and maximal QI communication graphs, respectively.

5.7 Discussion

Optimal structural recovery: We showed in the previous chapter (and in [22]) that the variational solution to an $\mathcal{H}_2$ optimal control problem augmented with an

atomic norm that penalizes the use of actuators can succeed in identifying an optimal actuation architecture when the dynamics of the plant satisfy certain conditions. The numerical experiments of §5.6 provide empirical evidence that our approach to communication architecture design identifies optimally structured controllers as well – it is of interest to see whether conditions analogous to those of the previous chapter (and of [22]) can provide theoretical support to the empirical success of our approach.

The k-communication link norm: The communication link norm was defined in terms of atoms corresponding to communication graphs constructed by adding a single link to the base QI communication graph. However it is possible to include atoms corresponding to communication graphs augmented with at most k-links instead, for any positive integer k; denote the resulting k-communication link norm by $\|\cdot\|_{k-\text{comm}}$. If the atoms are suitably normalized,[10] for all positive integers k_1 and k_2 satisfying $k_1 \leq k_2$ it then holds that $\|G\|_{k_1-\text{comm}} \leq \|G\|_{k_2-\text{comm}}$ for all transfer matrices G satisfying $\|G\|_{k_1-\text{comm}} < \infty$. Geometrically, restricted to the domain of $\|\cdot\|_{k_1-\text{comm}}$, the unit ball of $\|\cdot\|_{k_2-\text{comm}}$ is an inner approximation to that of $\|\cdot\|_{k_1-\text{comm}}$, and may therefore lead to simpler communication graphs when used as a penalty function in the regularized optimization problem (5.9). How to choose k will likely be informed by the aforementioned conditions on optimal structure recovery, and by computational considerations, as the number of elements $\{A_{ij}\}$ required to implement the k-communication link norm scales as $O(n^{2k})$.

Constructing base QI communication graphs: The structural assumptions made on (A, B_2, C_2) in §5.4 are needed to ensure that the base QI communication graph as specified in (5.19) is strongly connected and generates a QI subspace. However, as we note in Remark 5.4, any strongly connected communication topology leading to a QI subspace can be used as the base QI communication graph. Exploring how to construct base QI communication graphs in a principled way when the structural assumptions on (A, B_2, C_2) are relaxed, perhaps utilizing the methods in [99], is an interesting direction for future work. We emphasize however that the

[10] In particular, elements $A \in \mathscr{A}_{\text{k-comm}}$ constrained to lie in a subspace $\mathcal{E}$ should be normalized as $\|A\|_{\mathcal{H}_2} = (\text{card}\,(\mathcal{E}) + \kappa)^{-\frac{1}{2}}$, where $\kappa > 0$ is a positive constant that controls how much a single atom of larger cardinality is preferred over several atoms of lower cardinality.

rest of the discussion in §5.4 remains valid once a base QI communication graph is identified even if the structural assumptions on (A, B_2, C_2) are relaxed . We also note that these issues are a consequence of the communication protocol imposed between sub-controllers – determining alternative communication protocols that allow the structural assumptions to be relaxed is also an interesting direction for future work.

Scalability: Although we expect the methods presented to be applicable to systems composed of hundreds of sub-controllers, it is important that the general approach of the RFD framework be applicable to truly large-scale systems composed of heterogeneous subsystems. The limits on the scalability of our proposed method are due to the underlying controller synthesis method [16], as opposed to being inherent to the communication link norm. To that end we have been pursuing *localized optimal control* [37] as a scalable distributed optimal controller synthesis method – a direction for future work is to see if communication architecture co-design can be incorporated into the localized optimal control framework.

Chapter 6

Low-Rank and Low-Order Decompositions for Local System Identification

6.1 Introduction

Thus far this thesis has presented tractable algorithms for the synthesis of distributed optimal controllers, as well as computational tools for exploring the tradeoff between controller architecture complexity and closed-loop performance. Of course, none of these algorithms can be applied without first identifying the state-space parameters of the underlying large-scale distributed system. However, traditional system identification techniques such as subspace identification or prediction error are not computationally scalable – furthermore, the former technique also destroys, rather than leverages, any *a priori* information about the system's interconnection structure.

Related work: We are not the first to make this observation, and indeed [100] presents a local, structure preserving subspace identification algorithm for large scale (multi) banded systems (such as those that arise from the linearization of 2D and 3D partial differential equations), based on identifying local subsystem dynamics. Their approach is to approximate neighboring subsystems' states with linear combinations of inputs and outputs collected from a local neighborhood of subsystems, and they show that the size of this neighborhood is dependent on the conditioning of the so-called structured observability matrix of the global system.

In this chapter, we focus on the local identification problem, and leave the task of identifying the dynamics of the interconnection between these subsystems to future work, although we are able to solve this problem in what we term the "full interconnection measurement" setting (to be formally defined in Section 6.2). Our method is different from the approach suggested in [100] in three respects: (1) we focus on identifying impulse response elements, rather than reconstructing state sequences, and (2) our methods are purely local, in that we do not require the exchange of information with any neighboring subsystems, and finally, (3) we do not need to assume a (multi) banded structure. In light of this, we view our contribution as complementary to those presented in [100], and it will be interesting to to see if the two approaches can be combined in future work.

Our approach is based on two simple observations. First, if all of the signals connecting the local subsystem to the global system, or *interconnection signals*, can be measured, then under mild technical assumptions, the local observations are sufficient to identify both the local dynamics, and the coupling with the global system. In effect, measuring the interconnection signals isolates the local subsystem, reducing the problem to a classical system identification problem. Second, if an interconnection signal is not measured, then we have that the transfer function from local inputs and observed interconnection signals to local measurements naturally decomposes as the sum of two elements: one corresponding to local dynamics, which in general we expect to have *full-rank, but low order*, and one corresponding to global dynamics, which will be of *low-rank, but high order* (see Figure 6.1 for a pictorial representation of both settings).

Chapter contributions: Inspired by convex approaches to rank [72] and atomic norm minimization [101] in system identification, and to matrix decomposition in latent variable identification in graphical models [102], we conjecture that this difference in structure provides sufficient *incoherence* (c.f. [103] and [104] for examples of incoherence conditions) to allow the two signals to be separated through convex methods, in particular using nuclear norm minimization techniques. Indeed a similar idea has been applied successfully to blind source separation problems [105]. The

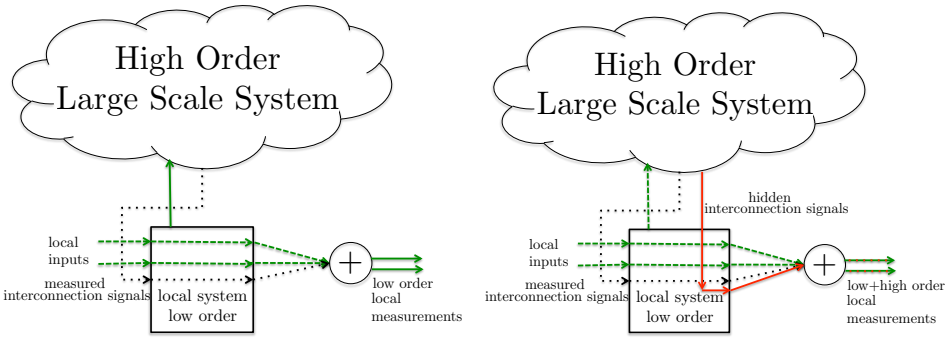

(a) Full interconnection measurements.

(b) Hidden interconnection measurements.

Figure 6.1: Illustrated in Figures 6.1 (a) and (b) are the full and hidden interconnection measurement cases, respectively. Dashed green lines correspond to low-order signals, and dotted/solid black/red lines correspond to measured/hidden high-order interconnection signals. In the full measurement case, the high order dynamics of the large scale system are isolated from the local measurements, as the interconnection signals can simply be treated as inputs to the system. In the hidden interconnection measurement setting, high order global signals "leak" into our local measurements via the hidden interconnection signal (solid red), but do so through a low-rank transfer function.

results of this chapter were originally published in [24].

Chapter organization: This chapter is organized as follows: in Section 6.2, we establish notation, and formally define the two variants of the problem to be solved, namely full and hidden interconnection measurement problems. In Sections 6.3 and 6.4, we provide nuclear norm minimization based algorithms for identifying local subsystem dynamics in both the full and hidden interconnection measurement settings, respectively. We present numerical experiments supporting our approach in Section 6.5, and end with conclusions and directions for future work in Section 6.6.

6.2 Problem Formulation

6.2.1 Notation

For a matrix

$$X = \begin{bmatrix} X_0 & X_1 \dots & X_{2N} \end{bmatrix} \tag{6.1}$$

we define the Hankel operator $\mathcal{H}(X)$ to be

$$\mathcal{H}(X) := \begin{bmatrix} X_1 & X_2 & \dots & X_N \\ X_2 & X_3 & \iddots & X_X \\ \vdots & \iddots & \ddots & \vdots \\ X_N & X_{N+1} & \dots & X_{2N} \end{bmatrix}, \tag{6.2}$$

and its Fourier transform to be given by

$$\mathcal{F}(X)(e^{j\omega_k}) = \sum_{t=0}^{2N-1} X_t e^{-j\omega_k t} \tag{6.3}$$

for $\omega_k = \frac{\pi k}{N}$, $k \in \{0, \dots, 2N-1\}$.

For a set of measurements $\{m_t^i\}_{t=0}^N$, $m_t^i \in R^C$, and natural numbers, N, M and r, with N even, we define $M_{N,M,r}^i \in \mathbb{R}^{C(r+1)\times(M+1)}$ by

$$M_{N,M,r}^i := \begin{bmatrix} m_{N-M}^i & m_{N-(M-1)}^i & \dots & m_N^i \\ m_{N-(M+1)}^i & m_{N-M}^i & \dots & m_{N-1}^i \\ \vdots & \vdots & \ddots & \vdots \\ m_{N-(M+r)}^i & m_{N-(M-1+r)}^i & \dots & m_{N-r}^i \end{bmatrix}, \tag{6.4}$$

where we adopt the convention that $m_t^i = 0$ for all $t < 0$. When N, M and r are clear from context, we drop the subscripts and simply denote the matrix by M^i.

For a general matrix M, we let $\|M\|_F$ denote its Froebenius norm, i.e. $\|M\|_F^2 = \text{trace} M^\top M$, and $\|M\|_*$ denote its nuclear norm, i.e. $\|M\|_* = \sum_i \sigma_i$, where σ_i are the singular values of M.

For a subspace $\mathcal{S}$, we denote by $\mathbb{P}_{\mathcal{S}}(\cdot)$ the orthogonal projection operator onto $\mathcal{S}$ with respect to the euclidean inner-product, and by $\mathcal{S}^\perp$ the orthogonal complement of the subspace, once again with respect to the euclidean inner-product.

6.2.2 Distributed systems with sparse interconnections

We consider a distributed system comprised of n linear time invariant (LTI) subsystems, which interact with each other according to a physical interaction graph $\mathcal{G} = (\mathcal{X}, E)$. We denote by $i \in \mathcal{X}$ the i^{th} node in the graph, and by x^i the state of the corresponding subsystem. We assume that each subsystem $i \in \mathcal{X}$ has its own control input u^i and centered white noise process noise w^i (satisfying $\mathbb{E}[w_t^i w_t^{j\top}] = W^{ij}$, $\mathbb{E}[w_s^i w_t^{j\top}] = 0 \ \forall s \neq t$), and that plants physically interact with each other according to E. In particular, an edge $e_{ij} \in E$ is non-zero if and only if subsystem j directly affects the dynamics of subsystem i. Defining the neighbor set of node i as $\mathcal{N}_i = \{j \in \mathcal{X} \,:\, e_{ij} \neq 0\}$, we can then write the dynamics of each subsystem as

$$x_{t+1}^i = A^{ii} x_t^i + \sum_{j \in \mathcal{N}_i} A^{ij} x_t^j + B^i u_t^i + w_t^i, \tag{6.5}$$

with initial conditions $x_i(0) = 0$, subsystem state $x^i \in \mathbb{R}^{n_i}$, neighboring subsystem states $x_t^j \in \mathbb{R}^{n_j}$, subsystem input $u^i \in \mathbb{R}^{p_i}$ and subsystem process noise $w_t^i \in \mathbb{R}^{n_i}$. For reasons that will become apparent, we will refer to the signals $(A^{ij} x_t^j)_{t=0}^N$ as the interconnection signals at node i over a horizon $N \geq 0$.

6.2.3 Local and interconnection observations

In the following we distinguish between two types of observations that can be collected at node i. The first, which we call local observations, correspond to standard measurements of the local state, i.e. we call $y_t^i \in \mathbb{R}^{q_i}$, as given by

$$y_t^i = C^i x_t^i + D^i u_t^i + \delta_t^i, \tag{6.6}$$

the local state observations at time t, with $\delta_t^i \in \mathbb{R}^{q^i}$ a centered white noise process.

The second, which we term interconnection observations, correspond to measurements of incoming signals from neighboring nodes, i.e. we call $z_t^i \in \mathbb{R}^{m_i}$, as given

by

$$z_t^i \;=\; \bar{C}^i \bar{x}_t^i + \bar{\delta}_t^i, \tag{6.7}$$

the interconnection observations at time t, where $\bar{x}_t^i = (x_t^j)_{j\in\mathcal{N}_i} \in \mathbb{R}^{\sum_{j\in\mathcal{N}_i} n_j}$, and $\bar{\delta}_t^i \in \mathbb{R}^{\sum_{j\in\mathcal{N}_i} n_j}$ is a centered white noise process.

6.2.4 Local system identification

Our system identification goal is to identify, up to a similarity transformation, the the tuple (A^{ii}, B^i, C^i, D^i) given only the time history of (u^i, y^i, z^i) – that is to say we seek a local estimation procedure for the subsystem dynamics. This task is non-trivial as the subsystem is connected to the remaining full system, and thus even identifying the true order of the local subsystem can be challenging.

In the sequel, we assume that the full system is Hurwitz, that (A^{ii}, C^i) is observable, and without loss that each C^i has full row rank, and once again distinguish between two cases. The first is when we have that all interconnection signals are contained within the linear span of the interconnection observations – we refer to this case as the *full interconnection measurement* case. Formally, this can be stated as

$$A^{ij} x_t^j \in \operatorname{lin}\left(\bar{C}^i \bar{x}_t^i\right), \; \forall t \geq 0, \; \forall j \in \mathcal{N}_i, \tag{6.8}$$

or more succinctly, that there exists a linear transformation $\mathcal{L}_{ij}$ such that

$$A^{ij} = \mathcal{L}_{ij}(\bar{C}^i), \; \forall j \in \mathcal{N}_i. \tag{6.9}$$

We also define $\mathcal{L}_i$ as the linear operator

$$\mathcal{L}_i := [\mathcal{L}_{ij_1}, \ldots, \mathcal{L}_{ij_{|\mathcal{N}_i|}}] \tag{6.10}$$

such that

$$\sum_{j\in\mathcal{N}_i} A^{ij} x_t^j = \mathcal{L}_i(\bar{C}) \bar{x}_t^i, \;\; \forall t \geq 0. \tag{6.11}$$

We will show that under mild coordination with neighboring subsystems, we are able to identify (A^{ii}, B^i, C^i, D^i) (to within the accuracy allowable by the noise) using only local information. Intuitively, by measuring these connecting signals, they can be treated as inputs to the subsystem, effectively isolating node i from the global dynamics (see Figure 6.1(a)) – however, in order to ensure persistence of excitation under this setting, non-local elements of randomness need to be injected into the system, hence the need for coordination.

The second case, which we call the *hidden interconnection measurement* setting, occurs when not all interconnection signals are observed, i.e. when conditions (6.8) or (6.9) do not hold. The local dynamics can no longer be isolated from the global dynamics due to these unobserved interconnection signals – as such, our full interconnection measurement method would lead to the identification of a high order local model due to the "hidden" connection to the full system (see Figure 6.1(b)). Inspired by the success of convex methods for sparse and low-rank decomposition techniques in identifying latent variables in graphical models [102], and for blind source separation [105], we propose a convex programming method for identifying and separating out the local low-order dynamics from the global high-order dynamics, which are due to the hidden connection with the full system.

6.3 Full interconnection measurements

We begin by assuming that (6.8) and (6.9) hold, and consider the case when all noise terms are identically zero. A robust variant of our solution will be presented at the end of this section when noise is present in the system.

For any $t \geq 0$, we may then write

$$y_t^i = \sum_{k=0}^{t} s_k^i \begin{bmatrix} u_{t-k}^i \\ z_{t-k}^i \end{bmatrix}, \tag{6.12}$$

with $s_0^i = [D^i, 0]$, $s_t^i = C^i(A^{ii})^{t-1}[B^i, \mathcal{L}(\bar{C}^i)]$ the subsystem's impulse response elements.

With this in mind, fix natural numbers N, M and r, with N even, and let $v_t^i = [{u_t^i}^\top, {z_t^i}^\top]^\top$, $V^i_{N,M,r}$ be given by (6.4), and

$$Y^i = \begin{bmatrix} y^i_{N-M} & y^i_{N-(M-1)} & \cdots & y^i_N \end{bmatrix} \tag{6.13}$$

$$S^i = \begin{bmatrix} s^i_0 & s^i_1 & \ldots & s^i_r \end{bmatrix}. \tag{6.14}$$

Choosing $r = N$, we may then write

$$Y^i = S^i V^i. \tag{6.15}$$

Thus we seek conditions under which (6.15) has a unique solution – i.e. we seek conditions under which

$$V^i \in \mathbb{R}^{(N+1)(p_i+m_i)\times(M+1)}$$

has a right inverse, yielding the solution

$$S^i = Y^i (V^i)^\dagger, \tag{6.16}$$

where $X^\dagger$ denotes the pseudo-inverse of X.

A necessary condition, that we assume holds in the sequel, is that M is sufficiently large such that $M + 1 \geq (N + 1)(p_i + m_i)$.

Remark 6.1 *One may choose to approximate outputs as coming from a finite impulse response system of order r by choosing $r < N$; as the system is assumed to be stable, picking a sufficiently large r then allows for a computational gain without sacrificing accuracy. In this case, the aforementioned necessary condition then becomes $M+1 \geq (r + 1)(p_i + m_i)$.*

Next we characterize necessary and sufficient conditions for V^i to have full row-rank. In order to make the analysis more transparent, introduce the auxiliary matrices

U^i and Z^i, constructed from $\{u_t^i\}_{t=0}^N$ and $\{z_t^i\}_{t=0}^N$, respectively, and note that

$$\text{rank}(V^i) = \text{rank}\left(\begin{bmatrix} U^i \\ Z^i \end{bmatrix}\right).$$

Therefore, necessary and sufficient conditions are that each of (i) U^i and (ii) $\mathbb{P}_{U^{i\perp}}(Z^i)$ (the projection of Z^i onto the orthogonal complement of the row space of U^i) have full row rank. Condition (i) is easily satisfied (with probability one) by choosing u_t^i to be a white random process – we therefore assume this holds and focus on condition (ii).

It should be immediate to see that if no other inputs are administered to the system then $\mathbb{P}_{U^{i\perp}}(Z^i) = 0$, as the system's trajectory lies entirely in the span of the row space of U^i. Therefore, let $\mathcal{A}_i := \{j \in \mathcal{X} : u^j \not\equiv 0\}$ denote the set of "active" inputs in the rest of the system, and let $u_t^{-i} = \left(u_t^j\right)_{j \neq i \in \mathcal{A}_i}$.

Then $Z^i \in \text{lin}(U^i, U^{-i})$, where U^{-i} is generated by $\{u_t^{-i}\}_{t=0}^N$. If (i) the transfer function from u^{-i} to z^i has full row rank, and (ii) sufficiently many active inputs are present (specifically, a number greater than or equal to m_i), and chosen to be such that U^{-i} is full row rank (which, again, is generically true for white input processes), then indeed $\mathbb{P}_{U^{i\perp}}(Z^i)$ will have full row rank.

Thus we see that through a marginal amount of coordination (signaling other subsystems to inject exciting inputs into the system), a purely local estimation procedure can be used to exactly recover the first N impulse response elements $s_0, \ldots, s_N$ of the local subsystem, to which standard realization procedures can then be applied to extract (up to a similarity transformation), the tuple $(A^{ii}, [B^i, \mathcal{L}(\bar{C}^i)], C^i, D^i)$.

6.3.1 A robust variant

Following [72], we can formulate a robust variant of our previous approach when the noise terms are non-zero. Defining

$$\Delta^i := Y^i - S^i V^i \tag{6.17}$$

we then solve the following nuclear norm minimization

$$\begin{aligned} \text{minimize}_{S^i} \quad & \|\mathcal{H}(S^i)\|_* \\ \text{s.t.} \quad & \|\Delta^i\|_F \leq \delta \end{aligned} \tag{6.18}$$

where δ is a tuning parameter that ensures consistency of the estimated impulse response elements with the observed data. Note that this approach can also be suitably modified to accommodate bounded noise [72], or unbounded noise with known covariance [73], or to handle missing time points in the output signal data as described in [106].

6.4 Hidden interconnection measurements

When condition (6.8) does not hold, the local identification task becomes much more difficult – by not measuring all of the connecting signals, global high-order dynamics "leak" into our local estimation procedure (see Figure 6.1(b)). Inspired by sparse and low-rank decomposition methods used to identify latent variables in graphical models [102], and by Hankel rank minimization techniques used in blind source separation problems [105], this section proposes a regularized variant of program (6.18) that has shown promise in numerical experiments.

Formal results proving the success of this technique (analogous to those found in [70, 102]) are the subject of current work. This subsection aims rather to provide some intuition and justification for the method. In particular, define the number of hidden signals at node i to be

$$k_i = \sum_{j \in \mathcal{N}_i} \dim \left(\mathbb{P}_{\text{lin}\left(\bar{C}\right)^\perp} \left(\text{lin} \left(A^{ij} \right) \right) \right) \tag{6.19}$$

that is to say, the dimension of the subspace of the hidden interconnection signals.

We may then write, analogous to (6.12)

$$y_t^i = \sum_{k=0}^{t} s_k^i \begin{bmatrix} u_{t-k}^i \\ z_{t-k}^i \end{bmatrix} + \sum_{k=0}^{t} h_k^i \begin{bmatrix} u_{t-k}^i \\ z_{t-k}^i \\ u_{t-k}^{-i} \end{bmatrix}. \tag{6.20}$$

where the s^i are once again the impulse response elements of the local-subsystem, whereas $h_0^i = 0$, and (h_t^i) are the impulse response elements describing the global dynamics that are "leaking" in to our subsystem via the hidden interconnection signals. Let $w_t^i = [{v_t^i}^\top, {u_t^{-i}}^\top]^\top$, and W^i be as in (6.4), and

$$H^i = \begin{bmatrix} H_{N-M}^i & H_{N-(M-1)}^i & \dots & H_N^i \end{bmatrix}, \tag{6.21}$$

allowing us to write

$$Y^i = \begin{bmatrix} S^i & H^i \end{bmatrix} \begin{bmatrix} V^i \\ W^i \end{bmatrix}. \tag{6.22}$$

We now make the key observation that the transfer function $H(e^{j\omega_k}) = \mathcal{F}(H^i)$ can have rank at most k_i, the number of hidden interconnection signals. In all of the following, we assume that the transfer function from (u^i, z^i) to y^i is full rank, and that

$$\min\left(p_i + m_i,\, q_i\right) > k_i \tag{6.23}$$

holds. Specifically, we ask that both the dimension q_i of the subspace spanned by our local observations, and the dimension $p_i + m_i$ of the subspace spanned by the "inputs" u^i and z^i, be larger than the dimension k_i of the subspace spanned by the hidden interconnection signals. Interpreted in terms of the rank of transfer functions, we ask that the rank of the local component of transfer function from (u^i, z^i) to y^i, given by $\min\left(p_i + m_i,\, q_i\right)$ under our full rank assumption, be larger than the rank k_i of the global component of the transfer function from (u^i, z^i) to y_i.

If these conditions hold, we then have a *structural* means of distinguishing between the two components of the impulse response of the local subsystem. First, we expect $\mathcal{H}(S^i)$ to have low rank, as it describes the low-order dynamics of the local model, whereas $\mathcal{H}(H^i)$ will not, as it corresponds to the high-order global dynamics

that leak in via the hidden connecting signals. Secondly, by our local full rank assumption, we will have that $S\left(e^{j\omega_k}\right)$ is full rank (with rank $\min\left(p_i + m_i,\, q_i\right)$), whereas $\operatorname{rank}\left(H\left(e^{j\omega_k}\right)\right) \leq k_i$; as mentioned above, the hidden interconnection signals act as a structural "choke" point, limiting the rank of the interconnecting transfer function.

This suggests a natural decomposition of the impulse response elements of y^i into a local full rank but low-order component with simple dynamics, and a hidden high-order but low-rank component. Using the nuclear-norm heuristic for low-rank approximations [70], we may then modify program (6.18) to control the rank of $H\left(e^{j\omega_k}\right)$:

$$\begin{aligned} \text{minimize}_{S^i,\, H^i} \quad & \|\mathcal{H}(S^i)\|_* \\ \text{s.t.} \quad & \Delta^i = 0 \\ & \|H\left(e^{j\omega_k}\right)\|_* \leq \delta_h,\ \omega_k = \tfrac{2\pi k}{M},\ k = 0,\, 1, \ldots, M-1 \end{aligned} \tag{6.24}$$

where now

$$\Delta^i = Y^i - \left(\begin{bmatrix} S^i & H^i \end{bmatrix} \begin{bmatrix} V^i \\ W^i \end{bmatrix}\right), \tag{6.25}$$

and δ_h is an additional tuning parameter used to control the rank of $H\left(e^{j\omega_k}\right)$ across frequencies. When noise is present, we relax the constraint on Δ^i to $\|\Delta^i\|_F \leq \delta$, as in the robust variant of the full interconnection measurement case.

This method is, however, non-local in that it requires the communication of U^{-i} to node i in order to implement it. In light of this, we also suggest the following local approximation to (6.24). In particular, we define

$$\tilde{\Delta}_i = Y^i - \left(\begin{bmatrix} S^i & H^i \end{bmatrix} \begin{bmatrix} V^i \\ V^i \end{bmatrix}\right) \tag{6.26}$$

and propose solving

$$\begin{aligned} \text{minimize}_{S^i,\, H^i} \quad & \|\mathcal{H}(S^i)\|_* \\ \text{s.t.} \quad & \|\tilde{\Delta}^i\|_F \leq \delta \\ & \|H\left(e^{j\omega_k}\right)\|_* \leq \delta_h,\ \omega_k = \tfrac{2\pi k}{M},\ k = 0,\, 1, \ldots, M-1. \end{aligned} \tag{6.27}$$

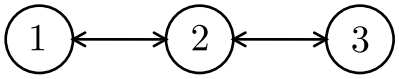

Figure 6.2: The graph depicts the physical interconnection structure of the three-subsystem chain.

Essentially, we treat the unknown active inputs U^{-i} as disturbances entering the system through $H^i(e^{j\omega_k})$, and therefore allow $\tilde{\Delta}_i$ to deviate from 0, but still insist on consistency with the observed data.

6.5 Numerical Experiments

We consider the following three subsystem chain (as illustrated in Figure 6.2), with x_t, $w_t \in \mathbb{R}^9$ and $u \in \mathbb{R}^5$,

$$x_t = Ax_t + Bu_t + w_t \tag{6.28}$$

with A and B given as in equations (6.35) and (6.36) (found at the end of the paper), and identically and independently distributed $w_t \sim \mathcal{N}(0, .01^2 I)$. Each node has a state $x_t^i \in \mathbb{R}^3$, which we assume are ordered such that

$$x_t = \begin{bmatrix} x_t^1 \\ x_t^2 \\ x_t^3 \end{bmatrix}.$$

We will consider the task of identifying node 1's system parameters, namely we seek to identify the tuple (A^{11}, B^1, C^1, D^1) where

$$A^{11} = \begin{bmatrix} 0.2839 & 0.2125 & -0.3097 \\ 0.1528 & -0.3525 & 0.2400 \\ 0.0183 & -0.1709 & -0.0109 \end{bmatrix}, \tag{6.29}$$

$$B^1 = \begin{bmatrix} 0.6394 & -0.3201 \\ 0.8742 & -0.1374 \\ 1.7524 & 0.6158 \end{bmatrix} \tag{6.30}$$

$$C^1 = \begin{bmatrix} 0.6348 & -0.1760 & -0.1274 \\ 0.8204 & 0.5625 & 0.5542 \end{bmatrix} \tag{6.31}$$

$$D^1 = \begin{bmatrix} -1.0973 & 1.4047 \\ -0.7313 & -0.6202 \end{bmatrix} \tag{6.32}$$

given local observations $y_t^1 = C^1 x_t^1 + \delta_t^1$, with $\delta_t^1 \sim \mathcal{N}(0, .01^2 I)$ and varying amounts of interconnection measurements. Note that in this system $\bar{x}_t^i = x_t^2$, and that indeed this fact remains true regardless of the number of subsystems in the chain.

We begin with the full interconnection measurement setting, with measurement noise $\bar{\delta}_t^1 \sim \mathcal{N}(0, .01^2 I)$ and

$$z_t^1 = \begin{bmatrix} 0.4895 & 0.6449 & 0.4762 \\ -1.5874 & 0.1367 & 0.6874 \\ 0.8908 & 0.1401 & 0.9721 \end{bmatrix} x_t^2 + \bar{\delta}_t^1 =: \bar{C}^i x_t^2 + \bar{\delta}_t^1. \tag{6.33}$$

It is easily verified that $\bar{C}^i$ is invertible, and thus satisfies (6.8) and (6.9). Solving program (6.18) with $N = 600$, $M = 300$, $r = 21$ and $\delta = 0.5$, we obtain an estimation error of $\|\hat{S}^i - S^i\|_F = .008$, relative to $\|S\|_F = 2.871$; i.e. we recover the impulse response elements to within the limits set by the noise. Additionally, rank $(\mathcal{H}(S^i)) = 3$, the true order of the system.

Next we consider the case where we have hidden interconnection signals. In particular, we let

$$z_t^1 = \begin{bmatrix} 0.4895 & 0.6449 & 0.4762 \\ -1.5874 & 0.1367 & 0.6874 \end{bmatrix} x_t^2 =: \bar{C}^i x_t^2. \tag{6.34}$$

Once again, we easily verify that $\bar{C}^i$ has full row-rank of 2, and therefore conclude that the dimension of the hidden interconnection subspace is 1, which is less than

$p_1 + m_1 = 4$ and $q_1 = 2$. We solve program (6.27) with $N = 600$, $M = 300$, $r = 21$, $\delta_h = .05$ and $\delta = 4.5$, and obtain an estimation error of $\|\hat{S}^i - S^i\|_F = .093$, relative to $\|S\|_F = 2.871$; although our error is above the noise level, it is still a reasonable estimate of the local dynamics. Most importantly we believe, however, is that (i) the top three singular values of $\mathcal{H}(S^i)$ were at least an order of magnitude larger than the remaining singular values for a fairly broad range of δ and δ_h (see Figure 6.3), and that (ii) the rank of each $H(e^{j\omega_k})$ term was correctly identified as 1 for all values of $\delta_h \in [0, 0.15]$ across a broad range of values of δ. Indeed, numerical experiments seem to suggest that the method is well suited to identifying the true order of the local dynamics, and the dimension of the hidden interconnection subspace, opening up the possibility of further refining results using parametric methods.

6.6 Conclusion

We presented a nuclear norm minimization based approach to separating local and global dynamics from local observations, and argued that this method can be used as part of a distributed system identification algorithm. In particular, we noted that when all interconnection signals can be measured, the problem essentially reduces to a classical system identification problem. When some interconnection signals are not measured, we exploit the fact that the transfer function from (u^i, z^i) to y^i naturally decomposes into a local contribution that is low-order, but full rank, and a global contribution that is high-order, but low rank to formulate the local system identification problem as a matrix decomposition problem amenable to convex programming.

In future work, we will look to develop non-asymptotic consistency results for our estimation procedure, analogous to those found in [70, 101, 102]. It is also of importance to develop a principled method for interconnecting our local subsystems properly to ultimately yield an accurate global model, analogous to the algorithm presented in [100]. Finally, more numerical experiments need to be conducted to further validate the efficacy of this method, especially on real world, as opposed to synthetic, data.

$$A = \begin{bmatrix} 0.2839 & 0.2125 & -0.3097 & 0.1843 & 0.0775 & -0.1358 & 0 & 0 & 0 \\ 0.1528 & -0.3525 & 0.2400 & 0.0976 & -0.1246 & -0.0821 & 0 & 0 & 0 \\ 0.0183 & -0.1709 & -0.0109 & -0.3269 & -0.0005 & 0.1012 & 0 & 0 & 0 \\ 0.0857 & 0.3037 & -0.1947 & 0.0914 & 0.3916 & 0.3797 & 0.0774 & -0.0510 & 0.2253 \\ -0.1698 & -0.1557 & -0.1865 & 0.2742 & 0.2066 & -0.5958 & 0.3695 & 0.1370 & -0.4422 \\ 0.4134 & 0.1407 & 0.2100 & 0.1776 & 0.0653 & -0.2677 & 0.1827 & -0.2593 & 0.0085 \\ 0 & 0 & 0 & -0.5795 & -0.2251 & 0.2736 & -0.1237 & 0.0857 & -0.4406 \\ 0 & 0 & 0 & -0.0667 & -0.0172 & 0.1418 & 0.2158 & 0.2762 & 0.2506 \\ 0 & 0 & 0 & -0.0787 & 0.0360 & -0.0661 & -0.0605 & 0.0366 & 0.0962 \end{bmatrix} \tag{6.35}$$

$$B^1 = \begin{bmatrix} 0.6394 & -0.3201 \\ 0.8742 & -0.1374 \\ 1.7524 & 0.6158 \end{bmatrix}, \; B^2 = \begin{bmatrix} 0.9779 & 0.0399 \\ -1.1153 & -2.4828 \\ -0.5500 & 1.1587 \end{bmatrix}, \; B^3 = \begin{bmatrix} -1.0263 \\ 1.1535 \\ -0.7865 \end{bmatrix}, \; B = \begin{bmatrix} B^1 & 0 & 0 \\ 0 & B^2 & 0 \\ 0 & 0 & B^3 \end{bmatrix} \tag{6.36}$$

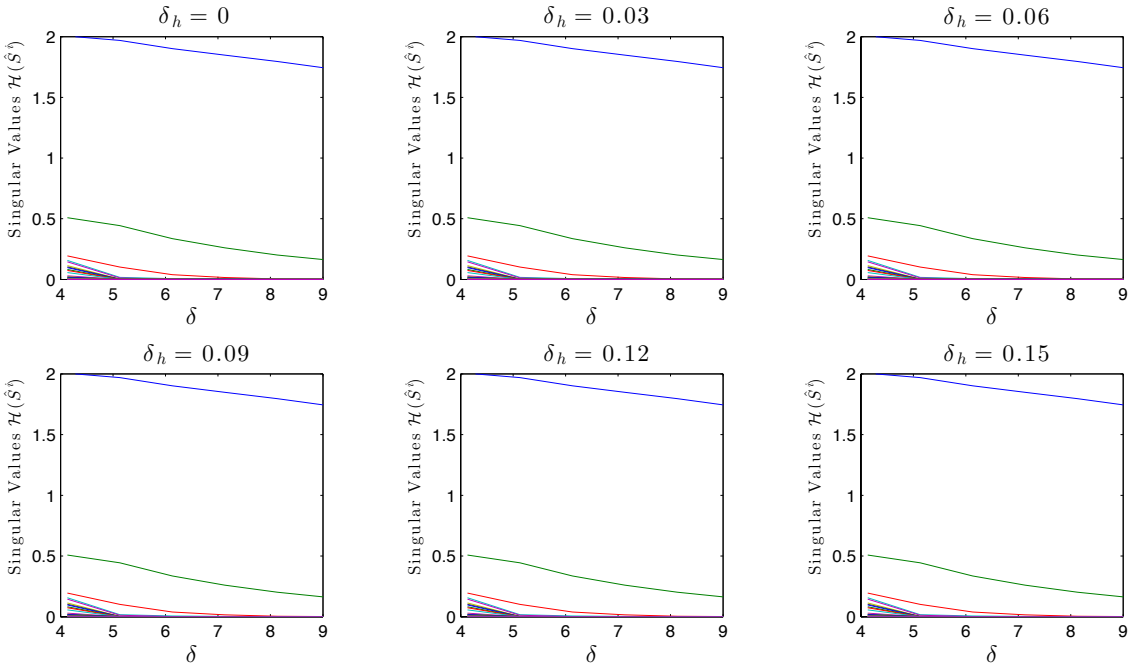

Figure 6.3: By examining how the values of the singular values of $\mathcal{H}(\hat{S}^i)$ vary across different values of δ and δ_h, the order of the local subsystem is correctly identified as three.

Chapter 7

Conclusions and Future Work

This thesis has focussed on the feedback control laws of distributed large-scale cyber-physical systems. It is important to recognize however that feedback control, as discussed in this thesis, is but one element of the overall control scheme of a cyber-physical system. As we preview in the following section, integrating distributed optimal control into a general theory of layered architectures for cyber-physical systems is an exciting and important direction for future work.

7.1 Future Work: A theory of dynamics, control and optimization in layered architectures

While layered control architectures have become ubiquitous and arguably necessary in achieving predictable and desirable behavior in complex cyber-physical systems, there is no general theory that offers a principled approach to designing and reverse-engineering layered architectures. Future work will aim to address this gap by integrating the results of this thesis (and those that it builds on) into such a broad theory.

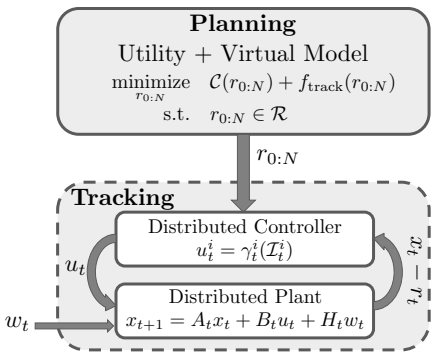

Figure 7.1: A functional schematic of the layered architecture derived in [1].

The starting point for this theory is the observation that there are two complementary tasks that must be addressed by the

controller of a cyber-physical system: (i) identifying an optimal trajectory with respect to a functional or economic utility function, and (ii) efficiently making the state of the system follow this optimal trajectory despite model uncertainty, disturbances, sensor noise, and distributed information sharing constraints. While traditional approaches to layered architectures treat these two tasks in a fairly independent manner (i.e., static set-point planning is done using little to no modeling of the dynamics of the underlying system), we argue that in order to develop a truly integrated theory, these two tasks must be considered together. To that end, in recent work [1] we generalized the Layering as Optimization (LAO) framework [107, 108] to incorporate not only optimization, but dynamics and control as well. We show that by suitably relaxing an optimal control problem that jointly addresses determining and following an optimal trajectory, one can naturally recover a layered architecture composed of a low-level tracking layer and a top-level planning layer (cf. Fig 7.1). The tracking layer consists of a distributed optimal controller that takes as an input a reference trajectory generated by the top-level layer, where this top-level layer consists of a trajectory planning problem that optimizes the weighted sum of a utility function and a "tracking penalty" regularizer. This latter term can be viewed as the planning layer's "virtual model" of the underlying physics of the system, and serves as a balance between the two by ensuring that the planned trajectory can indeed be efficiently followed by the tracking layer. These results form the foundation of a new theoretical framework, firmly rooted in distributed optimization and control, that informs when and how to use layering in the design of a dynamical cyber-physical system.

An important benefit of integrating distributed optimal control theory into such a theory of layered architectures is that it makes immediate the usefulness of these ideas in the context of timely application areas such as software defined networking. We briefly comment on some of our current and future work in this area.

7.1.1 Software Defined Networking

Software defined networking (SDN) is a huge paradigm shift in the networking community. A defining feature of SDN is the abstraction introduced between the traditional forwarding (data) plane and the control plane. This abstraction allows for an explicit separation between data forwarding and data control, and provides an interface through which network applications (such as traffic engineering, congestion control and caching) can programmatically control the network. This in turn allows for diverse, distributed application software to be run using diverse, distributed hardware in a seamless way: in essence, SDN enables the implementation of a *network operating system*. This added flexibility leads to new architectural and algorithmic design challenges, such as deciding which aspects of network functionality should be implemented in a centralized fashion in the application plane, which components of network structure should be virtualized by the control plane, and which elements of network control should remain in the data plane. In principle any combination of centralized, virtualized and decentralized functionality can be implemented via SDN.

The Layering as Optimization (LAO) decomposition approach to Network Utility Maximization (NUM) [107] problems is widely regarded as *the* "theory of architecture" for networking. However it is important to note that the LAO/NUM approach to architecture design was developed in the pre-SDN era, and hence does not incorporate the added flexibility and elasticity that SDN affords to network control applications. In particular, LAO/NUM problems focus exclusively on solving *static* network resource allocation problems that do not explicitly incorporate transient performance or fast-time scale dynamics. In [109], we use traditional ideas from distributed optimal control theory to study the effect of delay in admission control problems by comparing the performance of centralized, decentralized and distributed controllers. In [110], we incorporated these ideas into our new dynamic theory of layered architectures [1] and developed a theory that combines the LAO/NUM framework with distributed optimal control. We argued argued that this approach should be viewed as a natural generalization of NUM to the SDN paradigm, and applied this novel

framework to a novel joint traffic engineering/admission control problem. We showed that a *hybrid SDN* approach in which a modified traffic engineering problem is solved in the application plane and a distributed admission controller is implemented in the data plane leads to robust and efficient network behavior that outperforms both traditional distributed and fully centralized SDN approaches.

7.2 Concluding Remarks

This thesis presented contributions to three aspects of the foundational theory of distributed optimal control: controller synthesis, controller architecture design and distributed system identification. However, as we argued in this final chapter, there is a need for a principled and unified theory for the analysis and design of cyber-physical systems. We believe that the results of this thesis, as well as those outlined in §7.1, will be important pieces of this broader theory.

Bibliography

[1] N. Matni and J. C. Doyle, "A theory of dynamics, control and optimization in layered architectures," in *The IEEE American Control Conference (ACC), 2016. To appear.*, 2016.

[2] K. Zhou, J. C. Doyle, and K. Glover, *Robust and Optimal Control*. Upper Saddle River, NJ, USA: Prentice-Hall, Inc., 1996.

[3] G. E. Dullerud and F. G. Paganini, *A course in robust control theory : a convex approach*, ser. Texts in applied mathematics. New York: Springer, 2000.

[4] A. Mahajan, N. Martins, M. Rotkowitz, and S. Yuksel, "Information structures in optimal decentralized control," in *Decision and Control (CDC), IEEE 51st Annual Conference on*, Dec 2012, pp. 1291–1306.

[5] H. S. Witsenhausen, "A counterexample in stochastic optimum control," *SIAM Journal on Control*, vol. 6, no. 1, pp. 131–147, 1968.

[6] P. Grover and A. Sahai, "Is witsenhausen's counterexample a relevant toy?" in *Decision and Control (CDC), 2010 49th IEEE Conference on*. IEEE, 2010, pp. 585–590.

[7] ——, "Implicit and explicit communication in decentralized control," in *Communication, Control, and Computing (Allerton), 2010 48th Annual Allerton Conference on*. IEEE, 2010, pp. 278–285.

[8] Y.-C. Ho and K.-C. Chu, "Team decision theory and information structures in optimal control problems–part i," *Automatic Control, IEEE Transactions on*, vol. 17, no. 1, pp. 15–22, 1972.

[9] M. Rotkowitz and S. Lall, "A characterization of convex problems in decentralized control," *Automatic Control, IEEE Transactions on*, vol. 51, no. 2, pp. 274–286, 2006.

[10] M. Rotkowitz, R. Cogill, and S. Lall, "Convexity of optimal control over networks with delays and arbitrary topology," *International Journal of Systems, Control and Communications*, vol. 2, no. 1-3, pp. 30–54, 2010.

[11] J. Doyle, K. Glover, P. Khargonekar, and B. Francis, "State-space solutions to standard h2 and h infin; control problems," *Automatic Control, IEEE Transactions on*, vol. 34, no. 8, pp. 831–847, Aug 1989.

[12] L. Lessard and S. Lall, "A state-space solution to the two-player decentralized optimal control problem," in *49th Annual Allerton Conference on Communication, Control, and Computing*. IEEE, 2011, pp. 1559–1564.

[13] C. W. Scherer, "Structured $\mathcal{H}_\infty$-optimal control for nested interconnections: A state-space solution," *arXiv:1305.1746*, 2013.

[14] P. Shah and P. A. Parrilo, "$\mathcal{H}_2$-optimal decentralized control over posets: A state space solution for state-feedback," in *Decision and Control (CDC), 2010 49th IEEE Conference on*, 2010, pp. 6722–6727.

[15] A. Lamperski and L. Lessard, "Optimal state-feedback control under sparsity and delay constraints," in *3rd IFAC Workshop on Distributed Estimation and Control in Networked Systems*, 2012, pp. 204–209.

[16] A. Lamperski and J. C. Doyle, "The $\mathcal{H}_2$ control problem for quadratically invariant systems with delays," *Automatic Control, IEEE Transactions on. To appear.*, 2015.

[17] N. Matni, "Distributed control subject to delays satisfying an $\mathcal{H}_\infty$ norm bound," in *Decision and Control (CDC), 2014 IEEE Annual Conference on*, Dec 2014, pp. 4006–4013.

[18] N. Matni and J. Doyle, "Optimal distributed lqg state feedback with varying communication delay," in *Decision and Control (CDC), 2013 IEEE 52nd Annual Conference on*, Dec 2013, pp. 5890–5896.

[19] N. Matni, A. Lamperski, and J. C. Doyle, "Optimal two player LQR state feedback with varying delay," in *IFAC World Congress*, vol. 19, no. 1, 2014, pp. 2854–2859.

[20] V. Chandrasekaran, B. Recht, P. Parrilo, and A. Willsky, "The convex geometry of linear inverse problems," *Foundations of Computational Mathematics*, vol. 12, pp. 805–849, 2012.

[21] N. Matni and V. Chandrasekaran, "Regularization for design," in *Decision and Control (CDC), 2014 IEEE 53rd Annual Conference on*, Dec 2014, pp. 1111–1118.

[22] ——, "Regularization for design," *IEEE Transactions on Automatic Control, Conditionally Accepted*, 2015. [Online]. Available: http://arxiv.org/abs/1404.1972

[23] N. Matni, "Communication delay co-design in $\mathcal{H}_2$ distributed control using atomic norm minimization," *IEEE Transactions on Control of Network Systems, Accepted*, vol. arXiv:1404.4911, 2015.

[24] N. Matni and A. Rantzer, "Low-rank and low-order decompositions for local system identification," *CoRR*, vol. arXiv:1403.7175, 2014.

[25] B. Bamieh and P. G. Voulgaris, "A convex characterization of distributed control problems in spatially invariant systems with communication constraints," *Sys. & Control Letters*, vol. 54, no. 6, pp. 575 – 583, 2005.

[26] M. Fardad, F. Lin, and M. Jovanovic, "Sparsity-promoting optimal control for a class of distributed systems," in *American Control Conference (ACC), 2011*, June 2011, pp. 2050–2055.

[27] F. Lin, M. Fardad, and M. R. Jovanovic, "Design of optimal sparse feedback gains via the alternating direction method of multipliers," *Automatic Control, IEEE Transactions on*, vol. 58, no. 9, pp. 2426–2431, 2013.

[28] G. Fazelnia, R. Madani, and J. Lavaei, "Convex relaxation for optimal distributed control problem," in *Decision and Control (CDC), 2014 IEEE 53rd Annual Conference on*, Dec 2014.

[29] A. Kalbat, R. Madani, G. Fazelnia, and J. Lavaei, "Efficient convex relaxation for stochastic optimal distributed control problem," in *Communication, Control, and Computing, IEEE 52nd Annual Allerton Conference on*, 2014.

[30] K. Dvijotham, E. Theodorou, E. Todorov, and M. Fazel, "Convexity of optimal linear controller design," in *Decision and Control (CDC), 2013 IEEE 52nd Annual Conference on*, Dec 2013, pp. 2477–2482.

[31] K. Dvijotham, E. Todorov, and M. Fazel, "Convex structured controller design," *arXiv preprint arXiv:1309.7731*, 2013.

[32] N. Motee and A. Jadbabaie, "Approximation methods and spatial interpolation in distributed control systems," in *American Control Conference, 2009. ACC '09.*, June 2009, pp. 860–865.

[33] N. Motee and Q. Sun, "Sparsity measures for spatially decaying systems," in *American Control Conference (ACC)*, June 2014, pp. 5459–5464.

[34] A. Rantzer, "Distributed control of positive systems," *arXiv preprint arXiv:1203.0047*, 2012.

[35] T. Tanaka and C. Langbort, "The bounded real lemma for internally positive systems and h-infinity structured static state feedback," *IEEE transactions on automatic control*, vol. 56, no. 9, pp. 2218–2223, 2011.

[36] Y.-S. Wang, N. Matni, S. You, and J. C. Doyle, "Localized distributed state feedback control with communication delays," in *The IEEE American Control Conference (ACC), 2014*. IEEE, 2014, pp. 5748–5755.

[37] Y.-S. Wang, N. Matni, and J. Doyle, "Localized LQR optimal control," in *Decision and Control (CDC), 2014 IEEE 53rd Annual Conference on*, Dec 2014, pp. 1661–1668.

[38] Y.-S. Wang and N. Matni, "Localized distributed optimal control with output feedback and communication delays," in *Communication, Control, and Computing (Allerton), 2014 52nd Annual Allerton Conference on*, Sept 2014, pp. 605–612.

[39] A. Lamperski and J. Doyle, "Dynamic programming solutions for decentralized state-feedback lqg problems with communication delays," in *American Control Conference (ACC)*, June 2012, pp. 6322–6327.

[40] J. Swigart and S. Lall, "An explicit state-space solution for a decentralized two-player optimal linear-quadratic regulator," in *American Control Conference (ACC), 2010*. IEEE, 2010, pp. 6385–6390.

[41] A. Lamperski and L. Lessard, "Optimal decentralized state-feedback control with sparsity and delays," *arXiv preprint arXiv:1306.0036*, 2013.

[42] J. Sandell, N. and M. Athans, "Solution of some nonclassical LQG stochastic decision problems," *Automatic Control, IEEE Transactions on*, vol. 19, no. 2, pp. 108 – 116, apr 1974.

[43] B.-Z. Kurtaran and R. Sivan, "Linear-quadratic-gaussian control with one-step-delay sharing pattern," *Automatic Control, IEEE Transactions on*, vol. 19, no. 5, pp. 571 – 574, oct 1974.

[44] T. Yoshikawa, "Dynamic programming approach to decentralized stochastic control problems," *Automatic Control, IEEE Transactions on*, vol. 20, no. 6, pp. 796 – 797, dec 1975.

[45] T. Tanaka and P. A. Parrilo, "Optimal output feedback architecture for triangular LQG problems," *arXiv preprint arXiv:1403.4330*, 2014.

[46] A. Rantzer, "A separation principle for distributed control," in *Decision and Control, 2006 45th IEEE Conference on*, dec. 2006, pp. 3609 –3613.

[47] A. Gattami, "Generalized linear quadratic control theory," in *Decision and Control, 2006 45th IEEE Conference on*, dec. 2006, pp. 1510 –1514.

[48] H. R. Feyzmahdavian, A. Gattami, and M. Johansson, "Distributed output-feedback LQG control with delayed information sharing," in *IFAC Worskhop on Distributed Estimation and Control of Networked Systems*, vol. 3, no. 1, 2012, pp. 192–197.

[49] A. Nayyar, A. Mahajan, and D. Teneketzis, "Optimal control strategies in delayed sharing information structures," *Automatic Control, IEEE Transactions on*, vol. 56, no. 7, pp. 1606 –1620, july 2011.

[50] ——, "Decentralized stochastic control with partial history sharing: A common information approach," *Automatic Control, IEEE Transactions on*, vol. 58, no. 7, pp. 1644–1658, 2013.

[51] L. Lessard, "State-space solution to a minimum-entropy $\mathcal{H}_\infty$-optimal control problem with a nested information constraint," *arXiv preprint arXiv:1403.5020*, 2014.

[52] A. Alavian and M. C. Rotkowitz, "Q-parametrization and an sdp for $\mathcal{H}_\infty$-optimal decentralized control," *4th IFAC Workshop on Distributed Estimation and Control in Networked Systems (2013)*, pp. 301 – 308, 2013.

[53] B. A. Francis, "A course in $\mathcal{H}_\infty$ control theory," 1987.

[54] S. Sabau and N. C. Martins, "Necessary and sufficient conditions for stabilizability subject to quadratic invariance," in *Decision and Control and European*

Control Conference (CDC-ECC), 2011 50th IEEE Conference on. IEEE, 2011, pp. 2459–2466.

[55] S. P. Boyd, *Linear matrix inequalities in system and control theory*. Siam, 1994, vol. 15.

[56] N. Matni, "Communication delay co-design in $\mathcal{H}_2$ decentralized control using atomic norm minimization," in *Decision and Control (CDC), 2013 IEEE 52nd Annual Conference on*, Dec 2013, pp. 6522–6529.

[57] N. Matni and J. C. Doyle, "A dual problem in $\mathcal{H}_2$ decentralized control subject to delays," in *The IEEE American Control Conference (ACC), 2013*. IEEE, 2013, pp. 5772–5777.

[58] H. P. Rotstein, "Constrained $\mathcal{H}_\infty$-optimization for discrete-time control systems," Ph.D. dissertation, California Institute of Technology, Pasadena, CA, USA, 1993.

[59] J. Hespanha, P. Naghshtabrizi, and Y. Xu, "A survey of recent results in networked control systems," *Proceedings of the IEEE*, vol. 95, no. 1, pp. 138–162, 2007.

[60] V. Gupta, D. Spanos, B. Hassibi, and R. Murray, "On LQG control across a stochastic packet-dropping link," in *American Control Conference, 2005. Proceedings of the 2005*, 2005,, pp. 360–365.

[61] E. Garone, B. Sinopoli, and A. Casavola, "LQG control over lossy TCP-like networks with probabilistic packet acknowledgements," *International Journal of Systems, Control and Communications*, vol. 2, no. 1, pp. 55–81, 2010.

[62] C.-C. Chang and S. Lall, "Synthesis for optimal two-player decentralized control over tcp erasure channels with state feedback," in *Decision and Control and European Control Conference (CDC-ECC), 2011 50th IEEE Conference on*. IEEE, 2011, pp. 3824–3829.

[63] Y. Nakahira, N. Matni, and J. C. Doyle, "Hard limits on robust control over delayed and quantized communication channels with applications to sensorimotor control," in *Decision and Control, 2015 IEEE Annual Conference on, To appear*, 2015.

[64] A. Lamperski and J. C. Doyle, "On the structure of state-feedback LQG controllers for distributed systems with communication delays," in *Decision and Control and European Control Conference (CDC-ECC), 2011 50th IEEE Conference on*, Dec. 2011, pp. 6901 –6906.

[65] D. Leong and T. Ho, "Erasure coding for real-time streaming," in *Information Theory Proceedings (ISIT), 2012 IEEE International Symposium on*, 2012, pp. 289–293.

[66] F. Bonsall, "A general atomic decomposition theorem and Banach's closed range theorem," *The Quarterly Journal of Mathematics*, vol. 42, no. 1, pp. 9–14, 1991.

[67] E. Candes, J. Romberg, and T. Tao, "Robust uncertainty principles: exact signal reconstruction from highly incomplete frequency information," *Info. Theory, IEEE Trans. on*, vol. 52, no. 2, pp. 489–509, Feb. 2006.

[68] D. L. Donoho, "Compressed sensing," *IEEE Trans. Inform. Theory*, vol. 52, pp. 1289–1306, 2006.

[69] M. Fazel, "Matrix rank minimization with applications," Ph.D. dissertation, PhD thesis, Stanford University, 2002.

[70] B. Recht, M. Fazel, and P. A. Parrilo, "Guaranteed minimum-rank solutions of linear matrix equations via nuclear norm minimization," *SIAM Rev.*, vol. 52, no. 3, pp. 471–501, Aug. 2010.

[71] P. Shah, B. N. Bhaskar, G. Tang, and B. Recht, "Linear system identification via atomic norm regularization," in *Decision and Control (CDC), 2012 IEEE 51st Annual Conference on*, 2012, pp. 6265–6270.

[72] M. Fazel, H. Hindi, and S. Boyd, "A rank minimization heuristic with application to minimum order system approximation," in *American Control Conference (ACC), 2001*, June 2001, pp. 4734–4739.

[73] L. Ljung, "Some classical and some new ideas for identification of linear systems," *Journal of Control, Automation and Electrical Systems*, vol. 24, no. 1-2, pp. 3–10, 2013.

[74] V. Jonsson, A. Rantzer, and R. Murray, "A scalable formulation for engineering combination therapies for evolutionary dynamics of disease," in *American Control Conference (ACC), 2014*, June 2014, pp. 2771–2778.

[75] M. Fardad, F. Lin, and M. Jovanovic, "Design of optimal sparse interconnection graphs for synchronization of oscillator networks," *Automatic Control, IEEE Transactions on*, vol. 59, no. 9, pp. 2457–2462, Sept 2014.

[76] N. Dhingra, M. Jovanovic, and Z.-Q. Luo, "An ADMM algorithm for optimal sensor and actuator selection," in *Decision and Control (CDC), 2014 IEEE 53rd Annual Conference on*, Dec 2014, pp. 4039–4044.

[77] L. Lessard and S. Lall, "Quadratic invariance is necessary and sufficient for convexity," in *American Control Conference (ACC), 2011*, June 2011, pp. 5360–5362.

[78] M. A. Dahleh and I. J. Diaz-Bobillo, *Control of uncertain systems: a linear programming approach*. Prentice-Hall, Inc., 1994.

[79] S. Sabau and N. C. Martins, "Stabilizability and norm-optimal control design subject to sparsity constraints," *arXiv:1209.1123*, 2012.

[80] L. Lessard, M. Kristalny, and A. Rantzer, "On structured realizability and stabilizability of linear systems," in *American Control Conference (ACC), 2013*. IEEE, 2013, pp. 5784–5790.

[81] A. E. Hoerl and R. W. Kennard, "Ridge regression: Biased estimation for nonorthogonal problems," *Technometrics*, vol. 12, no. 1, pp. 55–67, 1970.

[82] M. Yuan and Y. Lin, "Model selection and estimation in regression with grouped variables," *Journal of the Royal Statistical Society: Series B (Statistical Methodology)*, vol. 68, no. 1, pp. 49–67, 2006.

[83] H. Zou and T. Hastie, "Regularization and variable selection via the elastic net," *Journal of the Royal Statistical Society: Series B (Statistical Methodology)*, vol. 67, no. 2, pp. 301–320, 2005.

[84] G. Obozinski, L. Jacob, and J.-P. Vert, "Group lasso with overlaps: the latent group lasso approach," *arXiv preprint arXiv:1110.0413*, 2011.

[85] G. Raskutti, M. J. Wainwright, and B. Yu, "Restricted eigenvalue properties for correlated gaussian designs," *The Journal of Machine Learning Research*, vol. 11, pp. 2241–2259, 2010.

[86] E. J. Candes and T. Tao, "Decoding by linear programming," *Information Theory, IEEE Transactions on*, vol. 51, no. 12, pp. 4203–4215, 2005.

[87] S. You and N. Matni, "A convex approach to sparse H-infinity analysis and synthesis," in *Decision and Control, 2015 IEEE Annual Conference on, To appear*, 2015.

[88] Y.-S. Wang and N. Matni, "Localized LQG optimal control for large-scale systems," in *IEEE American Control Conference, To appear.*, 2016.

[89] Y.-S. Wang, N. Matni, and J. C. Doyle, "Localized LQR control with actuator regularization," in *The IEEE American Control Conference, To appear.*, 2016.

[90] G. Pisier, *Probabilistic methods in the geometry of Banach spaces*. Springer, 1986.

[91] A. Lamperski and J. Doyle, "Output feedback $\mathcal{H}_2$ model matching for decentralized systems with delays," in *American Control Conference (ACC), 2013*, June 2013, pp. 5778–5783.

[92] C. D. Godsil, G. Royle, and C. Godsil, *Algebraic Graph Theory*. Springer New York, 2001, vol. 207.

[93] S. S. Chen, D. L. Donoho, and M. A. Saunders, "Atomic decomposition by basis pursuit," *SIAM Rev.*, vol. 43, no. 1, pp. 129–159, Jan. 2001.

[94] D. L. Donoho, "For most large underdetermined systems of linear equations the minimal ℓ_1-norm solution is also the sparsest solution," *Comm. Pure Appl. Math*, vol. 59, pp. 797–829, 2004.

[95] E. J. Candes and B. Recht, "Exact matrix completion via convex optimization," *Found. Comp. Math.*, vol. 9, no. 6, pp. 717–772, Dec. 2009.

[96] F. Alizadeh and D. Goldfarb, "Second-order cone programming," *Mathematical programming*, vol. 95, no. 1, pp. 3–51, 2003.

[97] M. S. Lobo, L. Vandenberghe, S. Boyd, and H. Lebret, "Applications of second-order cone programming," *Linear Algebra and its Applications*, vol. 284, no. 1–3, pp. 193 – 228, 1998.

[98] H. D. Mittelmann. (2014) MISOCP and large SOCP benchmark. [Online]. Available: http://plato.asu.edu/ftp/socp.html

[99] M. Rotkowitz and N. Martins, "On the nearest quadratically invariant information constraint," *Automatic Control, IEEE Transactions on*, vol. 57, no. 5, pp. 1314–1319, May 2012.

[100] A. Haber and M. Verhaegen, "Subspace identification of large-scale interconnected systems," *arXiv preprint arXiv:1309.5105*, 2013.

[101] P. Shah, B. N. Bhaskar, G. Tang, and B. Recht, "Linear system identification via atomic norm regularization," in *Decision and Control (CDC), 2012 IEEE 51st Annual Conference on*, Dec 2012, pp. 6265–6270.

[102] V. Chandrasekaran, P. A. Parrilo, and A. S. Willsky, "Latent variable graphical model selection via convex optimization," in *Communication, Control, and Computing (Allerton), 2010 48th Annual Allerton Conference on*. IEEE, 2010, pp. 1610–1613.

[103] V. Chandrasekaran, S. Sanghavi, P. A. Parrilo, and A. S. Willsky, "Rank-sparsity incoherence for matrix decomposition," *SIAM Journal on Optimization*, vol. 21, no. 2, pp. 572–596, 2011.

[104] J. A. Tropp, "Greed is good: Algorithmic results for sparse approximation," *Information Theory, IEEE Transactions on*, vol. 50, no. 10, pp. 2231–2242, 2004.

[105] T. Tanaka, C. Langbort, L. Mestha, and A. Gil, "Blind source separation by nuclear norm minimization and local recoverability analysis," *Signal Processing Letters, IEEE*, vol. 20, no. 8, pp. 827–830, Aug 2013.

[106] Z. Liu, A. Hansson, and L. Vandenberghe, "Nuclear norm system identification with missing inputs and outputs," *Systems & Control Letters*, vol. 62, no. 8, pp. 605–612, 2013.

[107] M. Chiang, S. Low, A. Calderbank, and J. Doyle, "Layering as optimization decomposition: A mathematical theory of network architectures," *Proc. of the IEEE*, vol. 95, no. 1, pp. 255–312, Jan 2007.

[108] D. Palomar and M. Chiang, "A tutorial on decomposition methods for network utility maximization," *Selected Areas in Communications, IEEE Journal on*, vol. 24, no. 8, pp. 1439–1451, Aug 2006.

[109] N. Matni, A. Tang, and J. C. Doyle, "A case study in network architecture tradeoffs," in *Proceedings of the 1st ACM SIGCOMM Symposium on Software*

Defined Networking Research, ser. SOSR '15. New York, NY, USA: ACM, 2015, pp. 18:1–18:7.

[110] N. Matni, D. Ho, A. Tang, D. Meyer, and J. C. Doyle, "Dynamics, control and optimization in layered network architectures," in *Technical report.*, 2016.